Title

The Intestinal Visceral Musculature: A Dynamic Niche for Metamorphosing Midgut and Hindgut of Drosophila melanogaster

Author

Aghajanian, Patrick

Publication Date

2014

Peer reviewed|Thesis/dissertation

UNIVERSITY OF CALIFORNIA

Los Angeles

The Intestinal Visceral Musculature: A Dynamic Niche for Metamorphosing Midgut and Hindgut of *Drosophila melanogaster*

A dissertation submitted in partial satisfaction of the

requirements for the degree Doctor of Philosophy

in Molecular, Cell, and Developmental Biology

by

Patrick Aghajanian

2014

ABSTRACT OF THE DISSERTATION

The Intestinal Visceral Musculature: A Dynamic Niche for Metamorphosing Midgut and Hindgut of *Drosophila melanogaster*

by

Patrick Aghajanian

Doctor of Philosophy in Molecular, Cell, and Developmental Biology

University of California, Los Angeles, 2014

Professor Volker Hartenstein, Chair

Stem cell maintenance in the small intestine in vertebrates has been well studied, though many factors involved in that process are still unknown. This study focuses on the development of the visceral muscle and intestinal tissues of *Drosophila melanogaster* during metamorphosis in order to further explain the intestinal stem cell/niche environment. Through stage wise dissection and immunohistochemical assays we were able to determine, (1) the adult posterior midgut is formed by cells of the anterior hindgut. (2) The visceral muscle de-differentiates and re-differentiates in a step wise manner during metamorphosis. (3) The presumptive intestinal stem cells (pISCs) of the midgut undergo many waves of division, are motile, and differentiate to endocrine cell fates at late pupal stages under the control of prospero and notch signaling. (4) A population of pISCs in the posterior midgut migrate past the midgut/hindgut boundary to form the renal stem cells of the adult Malpighian tubules. (5) The development of the midgut and hindgut epithelium during metamorphosis. These findings, taken together provide new understanding of these specific environments that may be applied to their homologous counterparts.

The dissertation of Patrick Aghajanian is approved.

Frank A. Laski

Ming Guo

William Lowry

Volker Hartenstein, Committee Chair

University of California, Los Angeles

2014

Table of Contents

Acknowledgements

Chapter 2 is a published article which has been contributed by these authors in order of authorship: Shigeo Takashima, Manash Paul, Patrick Aghajanian, Amelia Younossi-Hartenstein, and Volker Hartenstein

Chapter 3 is an article prepared for publication which has been contributed by these authors in order of authorship: Shigeo Takashima, Patrick Aghajanian, Amelia Younossi-Hartenstein, Paola Ortiz, Manash Paul, and Volker Hartenstein

Chapter 4 is an article prepared for publication which has been contributed by these authors in order of authorship: Patrick Aghajanian, Shigeo Takashima, Paola Ortiz, Amelia Younossi-Hartenstein, and Volker Hartenstein

Curriculum Vitae

Education

2007 University Of California Los Angeles
B.S. Molecular, Cell, and Developmental Biology

Employment

June 2009 – March 2014 University of California Los Angeles
Westwood, CA
Graduate Researcher (Laboratory of Dr. Volker Hartenstein)

- Research on *Drosophila* Midgut and Hindgut development during metamorphosis.

March 2006 – August 2007 University of California Los Angeles
Westwood, CA
Undergraduate Researcher (Laboratory of Dr. Anna Wu)

- *In vitro* experiments in cell death and proliferation assays using prostate cancer cell lines, maintaining cell lines and producing different constructs of various proteins for mammalian and bacterial expression.

June 2005 – August 2005 Glendale Community College
Glendale, CA
***Drosophila* Lab Assistant**

- Duties consisted of teaching students how to anesthetize fruit flies, sex them, and determine a limited number of other phenotypes. Students were then taught how to write in a scientific research format to describe their summer research experience.

September 2004 - June 2005 Glendale Community College
Glendale, CA
Supplemental Instruction Leader (Chemistry/Calculus)

- My duties consisted of aiding students who had difficulty understanding material from their chemistry or Calculus courses and providing them with supplementary materials with which to learn from.

Rotations

Dr. Caius Radu: Worked with B16 mouse melanoma cell line and looked for transport proteins that were overexpressed as targets for small molecule imaging and therapeutics.

Dr. John Colicelli: Worked on cloning a constitutively active form of RIN1 which is an enhancer of ABL tyrosine kinase activity in order to assay for inhibitors of their interaction.

Dr. Austin Nakano: Established cardiomyocyte colonies for flow cytometry analysis of cell markers.

Publications

Takashima S, Paul M, Aghajanian P, Younossi-Hartenstein A, Hartenstein V., *Migration of Drosophila intestinal stem cells across organ boundaries*. Development. 2013 May;140(9):1903-11.

Leyton JV, Olafsen T, Sherman MA, Bauer KB, Aghajanian P, Reiter RE, Wu AM., *Engineered humanized diabodies for microPET imaging of prostate stem cell antigen-expressing tumors*. Protein Eng Des Sel. 2009 Mar;22(3):209-16

Posters

The Development of the Drosophila Midgut: Enterocytes, Endocrine Cells, Stem Cells (Presented at the MCDB Research Conference at the Lake Arrowhead Conference Center, November 2009)

Development of the Drosophila Intestinal Tract During Metamorphosis (Presented at the MCDB Research Conference at the Lake Arrowhead Conference Center, November 2010)

Chapter 1: Introduction

Vertebrate Gastrointestinal System

The vertebrate small and large intestines originate from the Cdx2 positive posterior endoderm post gastrulation. In mouse, at embryonic day 8 (E8) to E9.5, the posterior endoderm folds over itself and forms the gut tubes (Noah et al., 2011). The visceral mesoderm, derived from the splanchnopleura of the early embryo, has been implicated to be involved in the development of the gastro-intestinal systems in vertebrates. After gastrulation, the visceral mesoderm surrounds the forming endodermal gut tube. The visceral mesoderm is thought to aide in the endodermal tube closure and its connection to the dorsal body wall. From E10.5 to E14.5 the endodermal epithelium of the intestines form villi in an anterior to posterior pattern. Villus formation is the product of both the condensation/growth of the surrounding mesenchyme and the formation of intraepithelial cavities. The visceral mesoderm starts differentiating into smooth muscle, following an anterior to posterior wave, at E11. The circular muscle layer differentiates first, followed after around 48 hours by the longitudinal muscles (McHugh, 1995).

Reciprocal signals exchanged between endoderm and visceral mesoderm orchestrate vertebrate gut development. The endoderm signals to the visceral mesoderm via Sonic hedgehog (Shh). This in turn activates the expression of FoxF1/F2 transcription factors and BMP-4 in the surrounding visceral mesoderm (Roberts et al., 1995; Mahlapuu et al., 2001-1; Mahlapuu et al., 2001-2). The FoxF proteins regulate the expression of Wnt and BMP, which have been shown to be heavily involved in gut epithelial progenitor and intestinal stem cell (ISC) development (He et al., 2005; Ormestad et al., 2006). Contrastingly, BMP-4 has also been shown, in *Xenopus*, to regulate the expression of FoxF1. FoxF1 has been implicated as a master regulator for the visceral mesoderm, which, when downregulated results in disorganized and undifferentiated

smooth muscle cells around the gut during embryonic development (Tseng et al., 2004; Mahlapuu et al., 2001-1; Mahlapuu et al., 2001-2).

In mature organisms the villi of the small intestine are composed of a heterogeneous community of cells. The epithelium is made up of enterocytes, goblet cells, endocrine cells, paneth cells and intestinal stem cells (ISCs). Among other cell types, the surrounding mesenchyme contains myofibroblasts, lymphatic cells and smooth muscle. Cavities within the villi, called crypts, are where the ISCs and Paneth cells are localized. As the small intestine produces a large amount of cell turnover, ISCs are necessary to continually replenish the epithelial lining of the gut. As mature intestinal epithelium is shed at the top of the villi, the ISCs divide and self-renew producing transient amplifying cells that rapidly proliferate and differentiate into the many cell type of the gut lining.

Self-renewal and differentiation are controlled by signals originating from Paneth cells (Sato et al., 2011), though it has been continually suggested that the surrounding myofibroblasts and visceral muscle play a role in the ISC regulation as well (Jiang et al., 2012; Takashima et al., 2012). Wnt, which is expressed by both the myofibroblasts (Gregorieff et al., 2005) and Paneth cells provides signals for proliferation and self-renewal (Haegbarth et al., 2009). It is expressed in an activity gradient beginning from the bottom of the crypts to the tops of the villi (Carulli et al., 2014). Additionally, Notch signaling is heaving involved in ISC maintenance and fate decisions. While blocking Notch leads to mitotic quiescence and secratory cell fate decisions, increasing Notch activity has been shown to increase proliferative behavior and differentiation to goblet fates (van der Flier et al., 2008). Bone morphogenic protein (BMP) plays the role of the

differentiation signal and arrests the cell cycle as the gut epithelial cells migrate to the top of the villi. The expression of BMP and its antagonists (GREM1 and 2) have been detected in the surrounding mesenchyme, including smooth muscle and myofibroblasts (Kosinski et al., 2007). BMP expression is increased as the cells progress to the top of the villi, while GREM expression is localized in the bottoms of the crypts.

Vertebrate Muscle

As the muscle is an important regulator of the ISC niche, it is also important understand its maintenance. In vertebrate skeletal muscle, tissue is regenerated via the use of satellite cells, which represent the stem cells of the muscle. Satellite cells are located in the basal lamina under the muscle fibers and are maintained by the surrounding extracellular matrix which serves as their niche. In chick embryos, it has been shown that satellite cells, just like the regular muscle fibers, derive from the embryonic dermomyotome. Myoblasts derived from this embryonic structure spread out and assemble into the muscles attached to the axial and appendicular skeleton.

Pax3 and Pax 7 are important for the determination of myogenic fate decisions and have redundant functionality, but recent observations have shown that they play a role in early satellite cell distinction in the dermomyotome (Relaix et al. 2005). At E10.5 the this $Pax3^{+}/Pax7^{+}$ population halts expression of multiple markers for muscle differentiation and programming such as myosin heavy chain (MyHC), MyoD, desmin, and Myf5. In addition, these cells display a high proliferative capacity and contribute to muscle growth during development as the main proliferating cell population. By E18.5, the $Pax3^{+}/Pax7^{+}$ cells become embedded in the basal

lamina where they will contribute to post-natal muscle growth and repair (Relaix et al. 2005). In the adult animal, satellite cells respond in a regenerative capacity to muscle damage in the form of necrosis (Lepper et al. 2011), and to stress caused by increased physical activity (Kadi et al. 2004). However, in cases of muscle degenerative diseases such as amyotrophic lateral sclerosis, satellite cells lose their regenerative capabilities and are unable to fully differentiate (Pradat et al. 2011).

Aside from a pool of undifferentiated stem cells, myocytes themselves can also proliferate to produce new muscle fibers. Thus, skeletal myocytes have the capacity to dedifferentiate into single celled myocytes and redeifferentiate in reaction to myotube damage. In once case Mu et al. tested this hypothesis by inducing lacerations to muscle in mice which had muscle derived cells (MDCs) either expressing ubiquitous Cre-recombinase or LoxP sites flanking a stop codon followed by a β-galactosidase gene. Muscle fibers formed by a fusion of these two MDC types were identified by their expression of B-galactosidase. After muscle injury, single celled β-gal positive myocytes are formed from the fibers. The β-gal expression was coupled with Pax7, Sca-1 and CD34, the former of which we have indicated to be a marker for satellite cells and the latter proteins to be markers of undifferentiated stem cells. These same cells were isolated and able to proliferate form myotubes *in vitro* (Mu et al., 2011).

Few stem cells have been described for smooth muscle. Newly identified multipotent vascular stem cells, described later below, and a subset of cells in the vertebrate myometrium are the only currently known smooth muscle stem like cells. In the myometrium, a group of BrdU label retaining cells exists at the periphery of smooth muscle bundles. Though their origins are not

well defined, these cells are hypothesized to be the regenerative satellite cells for repairing myometrial wall damage (Szotek et al., 2007; Arango et al., 2005). It has long been thought that also some types of smooth muscle, in particular vascular smooth muscle cells, dedifferentiate, proliferate, and redifferentiate in response to disease and damage. There have, indeed, been studies to show the potential for these cells to be induced into dedifferentiation *in vitro* (Lehti et al., 2009) as well as identified in *in vivo* studies (Layne et al., 2002).

Recently, however, these results have been contested in a paper published by Tang et al. through the identification of possible multipotent vascular stem cells (MVSCs) which are located in the media layer of the blood vessel wall. The presence of these MVSCs were confirmed via lineage trace analysis using smooth muscle myosin. Unlike differentiated vascular smooth muscle cells, MVSCs, negative for smooth muscle myosin heavy chain (SM-MHC) and mitotically competent (Ki67+), were able to proliferate and differentiate to contribute to tissue remodeling in response to vascular injury. SM-MHC-/Ki67+ cells isolated from the tunica media and left in culture after a 30 day period showed morphological changes as well as increased expression of smooth muscle actin (SMA) and calponin-1 (CNN-1) which are highly expressed in mature smooth muscle cells.

Using cells derived from SM-MHC-Cre/LoxP-EGFP mice, the authors were able to show, through lineage tracing analysis, that the MVSCs were not derived from de-differentiation of the mature vascular smooth muscle. Additionally, MVSCs have high telomerase activity when compared to surrounding tissue and are able to self-renew while continuing to express neural crest (Sox10) and endodermal (Sox17) markers, which are normally expressed in SM-MHC-

cells, when subjected dilutional cloning assay (Tang et al., 2012). All of these data taken together support the role of MVSCs as a renewable source for vascular smooth muscle repair.

Drosophila Gut and Intestinal Stem Cells (ISCs)

The Drosophila gut consists of three major compartments, the foregut, midgut and hindgut. The Drosophila midgut consists of two different tissues, an endodermally derived epithelium and a mesodermally derived visceral muscle layer. At the *Drosophila* embryonic stage 11, the endoderm forms mesenchymal masses at the anterior and posterior ends called the anterior and posterior midgut rudiments. During early stage 12, the presumptive midgut endoderm begins the formation of the midgut epithelium, undergoing a mesenchymal-to-epithelial transition which requires the presence of visceral mesoderm (Tepass and Hartenstein, 1994). At this time, both the anterior and posterior midgut rudiments extend processes along the visceral mesoderm and fuse to one another. After fusion (stage 13), the presumptive midgut forms a rectangular midgut epithelium. At stage 17 the midgut compartmentalizes and forms a confluent tube with the foregut and the hindgut (Tepass and Hartenstein, 1994).

All of the adult midgut tissue (enterocytes, endocrine cells, stem cells) are derived from a subset of cells called adult midgut progenitors (AMPs) that are present in the *Drosophila* embryo and larva. These AMPs do not integrate into the embryonic or larval epithelium, but are instead localized basal to the epithelium. AMPs divide in 8 parasynchronous waves during larval development. During the first three divisions, AMPs spread out; after that, they form clusters ("islands") scattered evenly over the midgut. Clusters grow from 2-4 cells per cluster (second instar) to 10-12 cells per cluster (wandering larva).

Within each cluster, a transient niche for developing AMPs has been described. Thus, 2-3 cells at the periphery of each cluster ("peripheral cells") flatten and form a sheath that surrounds the central AMPs ("central cells"). Peripheral cells are Stat positive and provide central AMPs with growth and self-renewal signals (Mathur et al., 2010). With the onset of metamorphosis, the peripheral cells become an intermediate layer (the "transient pupal midgut") between the AMPs and the dying larval gut (Takashima et al., 2011). Central AMPs differentiate as the adult gut (enterocytes); some cells maintain their undifferentiated, proliferative mode (presumptive intestinal stem cells or pISCs); these cells eventually give rise to the population of stem cells (ISCs) that persist throughout adult life. The Hartenstein lab revealed that the pISCs under go a "maturation phase" in which their lineages differ from the one described in the literature for the adult (Takashima et al., 2010).

Many major signaling pathways modulate midgut ISC fate in the adult. ISCs can be observed in the adult via Delta, escargot (Esg) a member of the snail/slug transcription factor family, and Stat. High levels of Delta signal coupled with low levels of Notch are expressed in the ISCs. An increase in Notch signaling and a decrease in Delta leads to the formation of and intermediate undifferentiated cell type called an enteroblast (EB). Prospero activation in the EBs leads to an enteroendocrine fate, whereas a continued expression of Notch causes an enterocyte fate. Notch and Delta additionally regulate ISC mitotic activity, to the point that a Notch or Delta knock out leads to tumor formation (Ohlstein et al., 2007; Micchelli et al., 2006). Jak/Stat signaling has been implied for multiple functions. Stat is expressed in adult ISCs and EBs and is required for, but not sufficient for differentiation to an enteroendocrine cell fate. Stat is not required for ISC self-renewal, though an increase in Stat leads to higher ISC mitotic activity (Beebe et al., 2010).

The ISCs are also under the control of wingless (Wg) and EGFR signaling (EGFR ligand Vein), originating from the visceral muscle, both of which are necessary for self-renewal and proliferation (Jiang et al., 2009; Lin et al., 2008; Xu et al., 2011). While Wg is important for self-renewal, Notch activity is epistatically dominant to Wg.

The hindgut is a part of the intestinal tube that reabsorbs water and electrolytes and consists of large cuboidal cells and a smaller, proliferative ISC population. It originates from a group of cells called the proctodeal primordium during the blastoderm stage (stage 5). After the posterior midgut primordium is internalized, the proctodeal ring is involuted. At stage 10/11 of development, the Malpighian tubules, the kidney homologue of *Drosophila*, evaginate from the proctodeal primordium. This is coupled by the migration of the hindgut visceral mesoderm, which begins to surround the hindgut epithelium. At stage 13, 2 ureters connect the Malpighian tubules to the hindgut epithelium concurrently with the complete extension of the hindgut visceral mesoderm (Lengyel et al., 2002). Embryonic hindgut development is concluded at stage 17 with the connection to the midgut tube.

The hindgut proliferation zone (HPZ), located in the anterior-most region of the hindgut by the midgut-hindgut boundary, provides a second population of stem cells. In the larva, this zone forms a coherent zone of proliferating cells. Similar to the AMPs of the midgut described above, the larval HPZ forms the adult hindgut enterocytes, as well as group of hindgut intestinal stem cells (hISCs) in the adult. The Wg and Hedgehog (Hh) signals control the balance of cells that, during larval development, differentiates (high Hh levels) or remains mitotically active (high Wg levels). Furthermore, during pupal development, the larval gut apoptosis and is replaced by a

newly developed adult hindgut (Takashima et al., 2008). Few studies of hindgut maturation during metamorphosis have been conducted however, which necessitates an investigation of what processes and tissues may influence the elongation of the hindgut during this period. Hindgut ISCs proliferate at a low rate in the normal adult animal; recent studies have shown, however, that these stem cells become strongly mitotically active following tissue damage (Fox et al., 2009).

Structure and development of Drosophila VM

Very much like vertebrates, the visceral mesoderm in *Drosophila* forms a layer of circular muscle around the gastrointestinal tract which is surrounded by a layer of longitudinal smooth muscle fibers. Also similar to vertebrate visceral muscle is their expression of various factors that control the mitotic activity and fate determination of the ISCs in the gut (Jiang et al., 2009; Xu et al., 2011; Lin et al., 2008).The visceral muscles of the *Drosophila melanogaster* midgut form an orthogonal layout of longitudinal and circular fibers, with longitudinal fibers located basally to the circular fibers. The visceral muscle develops in the embryo as a product of myoblasts in the trunk and caudal visceral mesoderm. B*iniou*, similar to its vertebrate homologue (FoxF1) is required for the development of visceral muscle. *Biniou* is activated by the BMP-4 homologue DPP (Decapentaplegic) which induces the formation of the visceral musculature from the dorsal mesoderm via it's induction of *tinman* (a transcription factor and homeobox gene) (Mclin et al. 2009). Two populations of myoblasts (founder myoblasts and fusion myoblasts) migrate to the midgut endoderm and then fuse to form a syncytium. (2-3 nuclei circular muscle, 3-5 nuclei longitudinal muscle.) This process is very similar to the formation of the body wall muscle in *Drosophila* larvae (San-Martin et al., 2001). Longitudinal visceral

muscles arise from the posterior mesoderm, the ventral most part of early Brachyenteron (Byn) expression.

Circular Visceral muscle persists from the larva through metamorphosis to the adult. Embryonic visceral muscle progenitors express dumbfounded (DUF) and Sticks and stones (SNS) (Klapper et al., 2002). Using a Gal4/UAS transplant system, Klapper et al. were able to detect the presence of a syncytium in both circular muscle of the hindgut during metamorphosis, but also confirmed muscle syncytia in the longitudinal muscles of the embryonic, larval, and adult midguts. Furthermore, they also confirmed the persistence of larval syncytial circular muscles to adult muscle using Gal4/UAS single celled clones. (Klapper et al., 2001). GFP+ cells from daughterless-Gal4 UAS-GFP flies were injected into the posterior mesoderm of *Drosophila* embryos. With this it was determined that longitudinal muscles were maintained through metamorphosis as cell nuclei counts remain the same.

Klapper et al. (2000) directly followed longitudinal visceral muscle fibers during pupal stages. They observed that at about 4 hr APF the longitudinal muscles begin to contract to the anterior and posterior regions of the midgut, starting from the central midgut. At around 40 hrs muscles extend again over the middle parts of the midgut. 70 hrs APF is when the muscles reach a state similar to adult maturation. They seem to suggest that muscle cells become dedifferentiated and then redifferentiated. As opposed to the longitudinal fibers, little information is available about the origin and pupal development of the circular fibers, which constitute the majority of visceral muscle. The objective of this study is to characterize the changes in the visceral muscle and its influence on gut development in a periodic manner during metamorphosis. In this study, we will

examine the changes in visceral muscle morphology in the pupa. (Klapper et al., 2000) Unlike in vertebrates, there has never been a population of regenerative tissue described for the visceral muscle in *Drosophila*. This may possibly be due an alternate mechanistic explanation for muscle regeneration than satellite like cells which hasn't yet been elucidated. Though other invertebrates may have applicable answers to these questions.

Intestinal phenotypes in other invertebrates

Similar to *Drosophila*, in most other insects, a tri-compartmental digestive system with a foregut, midgut, and hindgut and attached Malpighian tubules can be observed. Additionally, midgut regenerative cells have been characterized for many of these organisms with species specific functional differences. They may function like *Drosophila* as a regularly dividing and differentiating population (*Tenbrio molitor*), purely for damage repair (Culicidae mosquitoes) or may be absent altogether (*Glossina morsitans morsitans*) (Lehane, 1998). Many insects also have a similar visceral muscle pattern to that of *Drosophila*, consisting of a circular muscle layer surrounded by a longitudinal muscle layer. Among them, the *Aedes aegypti* midgut additionally seems to have a mechanism for muscle fibril degeneration during metamorphosis similar to what has been described in *Drosophila*. From P6-P21 the muscle fibers seem to weaken/flatten in comparison to earlier pupa stages. Muscle atrophy forms earlier in the posterior midgut that the anterior. The authors hypothesize that proteosomes are responsible for fiber degradation as they noted structures the size and shape of proteosomes adjacent to myofilaments. Though the muscle fibers themselves seem to have been degraded, the neuromuscular junctions and synapses remain intact. What remains of the degenerated tissue are incomplete bands of muscle fibers, mitochondria, and nuclei. (Bernick et al. 2007)

The sea cucumber, *Holothuria glaberrima*, also has an orthogonally arranged set of syncitial muscles surrounding its intestines. Multiple studies have suggested that due to visceral muscle injury, *H. glaberrima* muscles dedifferentiate and form single nucleus myoblasts that are negative for the F-actin binding toxin phalloidin, which binds to myofilaments in mature muscle(Murray et al., 2004; Candelaria et al., 2006). The myofilaments depolymerize to form spindle like structures within the myoblasts. After reforming mature muscle syncitia, the myofilaments repolymerize (García-Arrarás et al., 2011; Candelaria et al., 2006).

In this study we will investigate multiple morphological changes that take place in tissues derived from all three germ layers that contribute to the structure of the gut. Most importantly, these investigations will examine changes during pupal development, a period that has had little observational study when pertaining to gut metamorphosis. Paramount among our observations will be the development of *de novo* adult hindgut and midgut and the morphological changes of the visceral muscle. Secondarily, we will examine the maintenance of adult progenitor and ISC populations during metamorphosis. This will be done in part by examining signaling pathways involved and subsequently by elucidating the role of the visceral muscle in gut epithelial remodeling.

References

Arango NA, Szotek PP, Manganaro TF, Oliva E, Donahoe PK, Teixeira J. (2005) Conditional deletion of beta-catenin in the mesenchyme of the developing mouse uterus results in a switch to adipogenesis in the myometrium. *Dev Biol*. 288(1):276-83

Beebe K, Lee WC, Micchelli CA. (2010) JAK/STAT signaling coordinates stem cell proliferation and multilineage differentiation in the Drosophila intestinal stem cell lineage. *Dev Biol*. 338(1):28-37

Bernick EP, Moffett SB, Moffett DF. (2007) Organization, ultrastructure, and development of midgut visceral muscle in larval *Aedes aegypti*. *Tissue Cell*. 39(4):277-92

Candelaria AG, Murray G, File SK, García-Arrarás JE. (2006) Contribution of mesenterial muscle dedifferentiation to intestine regeneration in the sea cucumber *Holothuria glaberrima*. *Cell Tissue Res*. 325(1):55-65

Carulli AJ, Samuelson LC, Schnell S. (2014) Unraveling intestinal stem cell behavior with models of crypt dynamics. *Integr Biol (Camb)*. [Epub ahead of print]

Fox DT, Spradling AC. (2009) The Drosophila hindgut lacks constitutively active adult stem cells but proliferates in response to tissue damage. *Cell Stem Cell*. 5(3):290-7

García-Arrarás JE, Dolmatov IY. (2010) Echinoderms: potential model systems for studies on muscle regeneration. *Curr Pharm Des*. 16(8):942-55.

Gregorieff A, Pinto D, Begthel H, Destrée O, Kielman M, Clevers H. (2005) Expression pattern of Wnt signaling components in the adult intestine. *Gastroenterology*. 129(2):626-38

Haegebarth A, Clevers H. (2009) Wnt signaling, lgr5, and stem cells in the intestine and skin. *Am J Pathol*. 174(3):715-21

He XC, Zhang J, Li L. (2005) Cellular and molecular regulation of hematopoietic and intestinal stem cell behavior. *Ann N Y Acad Sci*. 1049:28-38

Jiang H, Edgar BA. (2009) EGFR signaling regulates the proliferation of Drosophila adult midgut progenitors. *Development*. 136(3):483-93

Jiang H, Edgar BA. (2012) Intestinal stem cell function in Drosophila and mice. *Curr Opin Genet Dev*. 22(4):354-60

Kadi F, Schjerling P, Andersen LL, Charifi N, Madsen JL, Christensen LR, Andersen JL. (2004) The effects of heavy resistance training and detraining on satellite cells in human skeletal muscles. *J Physiol*. 558(Pt 3):1005-12

Klapper R. (2000) The longitudinal visceral musculature of Drosophila melanogaster persists through metamorphosis. *Mech Dev*. 95(1-2):47-54

Klapper R, Heuser S, Strasser T, Janning W. (2001) A new approach reveals syncytia within the visceral musculature of Drosophila melanogaster. *Development*. 128(13):2517-24.

Klapper R, Stute C, Schomaker O, Strasser T, Janning W, Renkawitz-Pohl R, Holz A. (2002) The formation of syncytia within the visceral musculature of the Drosophila midgut is dependent on duf, sns and mbc. *Mech Dev*. 110(1-2):85-96

Kosinski C, Li VS, Chan AS, Zhang J, Ho C, Tsui WY, Chan TL, Mifflin RC, Powell DW, Yuen ST, Leung SY, Chen X. (2007) Gene expression patterns of human colon tops and basal crypts and BMP antagonists as intestinal stem cell niche factors. *Proc Natl Acad Sci U S A*. 104(39):15418-23

Layne MD, Yet SF, Maemura K, Hsieh CM, Liu X, Ith B, Lee ME, Perrella MA. (2002) Characterization of the mouse aortic carboxypeptidase-like protein promoter reveals activity in differentiated and dedifferentiated vascular smooth muscle cells. *Circ Res*. 90(6):728-36

Lehane MJ. (1998) The Midgut. *Microscopic Anatomy of Invertebrates Part B*. Chapter 30 725-747.

Lehti K, Rose NF, Valavaara S, Weiss SJ, Keski-Oja J. (2009) MT1-MMP promotes vascular smooth muscle dedifferentiation through LRP1 processing. *J Cell Sci*. 122(Pt 1):126-35

Lengyel JA, Iwaki DD. (2002) It takes guts: the Drosophila hindgut as a model system for organogenesis. *Dev Biol*. 243(1):1-19

Lepper C, Partridge TA, Fan CM. (2011) An absolute requirement for Pax7-positive satellite cells in acute injury-induced skeletal muscle regeneration. *Development*. 138(17):3639-46

Lin G, Xu N, Xi R. (2008) Paracrine Wingless signalling controls self-renewal of Drosophila intestinal stem cells. *Nature*. 455(7216):1119-23.

Mahlapuu M, Enerbäck S, Carlsson P. (2001) Haploinsufficiency of the forkhead gene Foxf1, a target for sonic hedgehog signaling, causes lung and foregut malformations. *Development*. 128(12):2397-406

Mahlapuu M, Ormestad M, Enerbäck S, Carlsson P. The forkhead transcription factor Foxf1 is required for differentiation of extra-embryonic and lateral plate mesoderm. *Development*. 128(2):155-66

Martin BS, Ruiz-Gómez M, Landgraf M, Bate M. (2001) A distinct set of founders and fusion-competent myoblasts make visceral muscles in the Drosophila embryo. *Development*. 128(17):3331-8

Mathur D, Bost A, Driver I, Ohlstein B. (2010) A transient niche regulates the specification of Drosophila intestinal stem cells. *Science*. 327(5962):210-3.

McHugh KM. (1995) Molecular analysis of smooth muscle development in the mouse. *Dev Dyn*. 204(3):278-90

McLin VA, Henning SJ, Jamrich M. (2009) The role of the visceral mesoderm in the development of the gastrointestinal tract. *Gastroenterology*. 136(7):2074-91

Micchelli CA, Perrimon N. (2006) Evidence that stem cells reside in the adult Drosophila midgut epithelium. *Nature*. 439(7075):475-9

Mu X, Peng H, Pan H, Huard J, Li Y. (2011) Study of muscle cell dedifferentiation after skeletal muscle injury of mice with a Cre-Lox system. *PLoS One*. 6(2):e16699

Murray G, García-Arrarás JE. (2004) Myogenesis during holothurian intestinal regeneration. *Cell Tissue Res*. 318(3):515-24.

Noah TK, Donahue B, Shroyer NF. (2011) Intestinal development and differentiation. *Exp Cell Res*. 317(19):2702-10

Ohlstein B, Spradling A. (2007) Multipotent Drosophila intestinal stem cells specify daughter cell fates by differential notch signaling. *Science*. 315(5814):988-92

Ormestad M, Astorga J, Landgren H, Wang T, Johansson BR, Miura N, Carlsson P. (2006) Foxf1 and Foxf2 control murine gut development by limiting mesenchymal Wnt signaling and promoting extracellular matrix production. *Development*. 133(5):833-43

Pradat PF, Barani A, Wanschitz J, Dubourg O, Lombès A, Bigot A, Mouly V, Bruneteau G, Salachas F, Lenglet T, Meininger V, Butler-Browne G. (2011) Abnormalities of satellite cells function in amyotrophic lateral sclerosis. *Amyotroph Lateral Scler*. 12(4):264-71

Relaix F, Rocancourt D, Mansouri A, Buckingham M. (2005) A Pax3/Pax7-dependent population of skeletal muscle progenitor cells. *Nature*. 35(7044):948-53

Roberts DJ, Johnson RL, Burke AC, Nelson CE, Morgan BA, Tabin C. (1995) Sonic hedgehog is an endodermal signal inducing Bmp-4 and Hox genes during induction and regionalization of the chick hindgut. *Development*. 121(10):3163-74

Sato T, van Es JH, Snippert HJ, Stange DE, Vries RG, van den Born M, Barker N, Shroyer NF, van de Wetering M, Clevers H. (2011) Paneth cells constitute the niche for Lgr5 stem cells in intestinal crypts. *Nature*. 469(7330):415-8

Szotek PP, Chang HL, Zhang L, Preffer F, Dombkowski D, Donahoe PK, Teixeira J. (2007) Adult mouse myometrial label-retaining cells divide in response to gonadotropin stimulation. *Stem Cells*. 25(5):1317-25

Takashima S, Adams KL, Ortiz PA, Ying CT, Moridzadeh R, Younossi-Hartenstein A, Hartenstein V. (2010) Development of the Drosophila entero-endocrine lineage and its specification by the Notch signaling pathway. *Dev Biol.* 353(2):161-72

Takashima S, Gold D, Hartenstein V. (2012) Stem cells and lineages of the intestine: a developmental and evolutionary perspective. *Dev Genes Evol*. 223(1-2):85-102

Takashima S, Mkrtchyan M, Younossi-Hartenstein A, Merriam JR, Hartenstein V. (2008) The behaviour of Drosophila adult hindgut stem cells is controlled by Wnt and Hh signalling. *Nature*. 454(7204):651-5.

Tang Z, Wang A, Yuan F, Yan Z, Liu B, Chu JS, Helms JA, Li S. (2012) Differentiation of multipotent vascular stem cells contributes to vascular diseases. *Nat Commun*. 3:875

Tepass U, Hartenstein V. (1994) Epithelium formation in the Drosophila midgut depends on the interaction of endoderm and mesoderm. *Development*. 120(3):579-90

Tseng HT, Shah R, Jamrich M. (2004) Function and regulation of FoxF1 during Xenopus gut development. *Development*. 131(15):3637-47

van der Flier LG, Clevers H. (2009) Stem cells, self-renewal, and differentiation in the intestinal epithelium. *Annu Rev Physiol.* 71:241-60

Xu N, Wang SQ, Tan D, Gao Y, Lin G, Xi R. (2011) EGFR, Wingless and JAK/STAT signaling cooperatively maintain Drosophila intestinal stem cells. *Dev Biol*. 354(1):31-43

Chapter 2: Migration of *Drosophila* Intestinal Stem Cells Across Organ Boundaries

Development 140, 1903-1911 (2013) doi:10.1242/dev.082933

Migration of *Drosophila* intestinal stem cells across organ boundaries

Shigeo Takashima, Manash Paul, Patrick Aghajanian, Amelia Younossi-Hartenstein and Volker Hartenstein*

SUMMARY

All components of the *Drosophila* intestinal tract, including the endodermal midgut and ectodermal hindgut/Malpighian tubules, maintain populations of dividing stem cells. In the midgut and hindgut, these stem cells originate from within larger populations of intestinal progenitors that proliferate during the larval stage and form the adult intestine during metamorphosis. The origin of stem cells found in the excretory Malpighian tubules ('renal stem cells') has not been established. In this paper, we investigate the migration patterns of intestinal progenitors that take place during metamorphosis. Our data demonstrate that a subset of adult midgut progenitors (AMPs) move posteriorly to form the adult ureters and, consecutively, the renal stem cells. Inhibiting cell migration by AMP-directed expression of a dominant-negative form of Rac1 protein results in the absence of stem cells in the Malpighian tubules. As the majority of the hindgut progenitor cells migrate posteriorly and differentiate into hindgut enterocytes, a group of the progenitor cells, unexpectedly, invades anteriorly into the midgut territory. Consequently, these progenitor cells differentiate into midgut enterocytes. The midgut determinant *GATAe* is required for the differentiation of midgut enterocytes derived from hindgut progenitors. Wingless signaling acts to balance the proportion of hindgut progenitors that differentiate as midgut versus hindgut enterocytes. Our findings indicate that a stable boundary between midgut and hindgut/Malpighian tubules is not established during early embryonic development; instead, pluripotent progenitor populations cross in between these organs in both directions, and are able to adopt the fate of the organ in which they come to reside.

KEY WORDS: Stem cell, Migration, Intestine, Malpighian tubule, Metamorphosis, *Drosophila*

INTRODUCTION

To compensate for cell loss, most animal tissues maintain slowly proliferating populations of stem cells that are able to differentiate on demand. Given the great potential of stem cells for the management of many human diseases, it is important to understand in detail the molecular pathways that control the biology of stem cells, including their origin, pattern of proliferation and migration during development. In this paper, we focus on the development of intestinal stem cells (ISCs) that form part of the gut and excretory system of the fruit fly *Drosophila melanogaster*. Stem cells have been described for the *Drosophila* endodermal midgut, as well as for the ectodermal Malpighian tubules and hindgut. In the midgut and Malpighian tubules, stem cells are scattered more or less evenly over the outer (basal) surface of the epithelium (Ohlstein and Spradling, 2006; Micchelli and Perrimon, 2006; Singh et al., 2007). In the hindgut, proliferating cells are confined to a narrow segment that forms the hindgut-midgut boundary (hindgut proliferation zone, HPZ) (Takashima et al., 2008). A similar ring of proliferating cells also exists in the adult foregut (Singh et al., 2011). Stem cells develop as part of the adult gut progenitors that can be already distinguished in the embryonic and larval gut (Jiang and Edgar, 2009; Mathur et al., 2010; Takashima et al., 2011a; Takashima et al., 2011b). Small clusters ('nests') of dividing adult midgut progenitors (AMPs) are distributed over the larval midgut. Two ring-shaped domains of proliferating cells flanking the midgut anteriorly and posteriorly, form the primordia of the adult foregut and hindgut, respectively. During pupal development, most of the larval gut undergoes programmed cell death, similar to what has been described for some vertebrate systems undergoing metamorphosis (Ishizuya-Oka and Shi, 2007; Hasebe et al., 2011). The adult gut primordia spread, fuse together and differentiate as the adult foregut, midgut and hindgut. Only the larval Malpighian tubules, according to previous reports, survive metamorphosis and become the adult tubules.

Recent genetic studies have elucidated several of the signaling pathways that control the proliferation and differentiation of gut progenitors in the larva, and ISCs in the adult. Among these are: the Notch and Wnt/Wingless pathways, which keep gut progenitors and ISCs in a dividing non-differentiated state (Ohlstein and Spradling, 2006; Ohlstein and Spradling, 2007; Micchelli and Perrimon, 2006; Lin et al., 2008; Lee et al., 2009; Xu et al., 2011); EGFR and JAK/STAT, which act upstream of Notch to trigger proliferation and promote enterocyte survival in the midgut (Jiang et al., 2009; Jiang et al., 2011; Liu et al., 2010; Xu et al., 2011); and Hedgehog, which promotes enterocyte differentiation in the hindgut (Takashima et al., 2008). However, many of the mechanisms that specify ISCs, in particular the signaling events that, during metamorphosis, select these cells from among the adult gut progenitors and keep them undifferentiated, are still unknown. It is also not clear how the ISCs, once determined, migrate to their final position. Notably, the site of origin of ISCs populating the adult Malpighian tubules has remained unknown so far.

In this paper, we have investigated the origin of stem cells that form near the boundary between midgut, hindgut and Malpighian tubules. Our findings show that, during early stages of metamorphosis, two unsuspected, major movements of gut progenitors take place. First, adult midgut progenitors (AMPs) give rise not only to the adult midgut epithelium, but also move posteriorly to form the adult ureters. During later pupal stages, subsets of AMPs migrate from the ureters onto the Malpighian

Department of Molecular Cell and Developmental Biology, University of California Los Angeles, Los Angeles, CA 90095, USA.

*Author for correspondence (volkerh@mcdb.ucla.edu)

Accepted 26 February 2013

tubules to establish the population of renal stem cells associated with these structures in the adult. Blocking cell migration by directed expression of a Rac dominant-negative form results in the lack of the stem cells in the Malpighian tubules. A second major movement of presumptive stem cells takes place during early pupal development when cells of the hindgut proliferation zone, instead of extending posteriorly to generate the adult hindgut, move anteriorly to form the posterior segment of the adult midgut. Our findings indicate that the boundary between the endodermal midgut and ectodermal hindgut/Malpighian tubules that appears in the embryo is not maintained during metamorphosis: pluripotent progenitor populations cross between these domains in both directions and are able to adopt the fate of the domain they come to reside in.

MATERIALS AND METHODS

Fly stocks

Flies used in this study were (sources in parentheses): *byn-Gal4* (Dr J. Lengyel, University of California, Los Angeles, USA); *esg-Gal4, pros-Gal4* (National Institute of Genetics, Japan); *OregonR*^{w1118}, *tub-Gal80*^{ts}*7*, *tub-Gal80*^{ts}*20*, *UAS-mCD8GFP*, *UAS-flp*, *UAS-GFP, UAS-myr-mRFP*, *UAS-mitoGFP, UAS-Rac1*^{N17} (a dominant-negative form of *Rac1*), and *Act5C >Stop >lacZ* (*Act5C promoter-FRT-phl[+]-FRT-lacZ.nls*) (Bloomington Stock Center); *10XStat92E-GFP* (Dr E. Bach, New York University School of Medicine, NY, USA); *UAS-dGATAeRNAi* (VDRC, Austria; #10418, #10420); and *UAS-wg* (Dr H. Krause, University of Toronto, Ontario, Canada). All flies were reared with normal fly food at room temperature or in incubators at 18°C, 25°C or 29°C.

Lineage trace experiments

Flies carrying genotypes of *tub-Gal80*^{ts}/+; *esg-Gal4 UAS-myr-mRFP/UAS-flp*; *Act5C >Stop >lacZ/+* or *tub-Gal80*^{ts}*/UAS-flp*, *byn-Gal4 UAS-GFP/Act5C >Stop >lacZ* were used for tracing the lineage of adult midgut progenitors (*esg+*) or HPZ cells (*byn+*), respectively. Animals raised at 18°C were transferred to at 29°C to inactivate Gal80^{ts} repressor enabling flip-out 'Stop cassette' of *Act5C >Stop >lacZ* transgene to label permanently the cells of given lineages. To trace the lineages during metamorphosis, third instar larvae were transferred to 29°C and then dissected at the desired pupal stages. In some experiments, the temperature shift was applied as a 6-hour pulse to restrict the labeled lineage, resulting in labeling of subsets of progeny (e.g. Fig. 5C). Without a temperature shift, we observed no or a very limited number of labeled cells (supplementary material Fig. S2). When overexpressing *GATAe* combined with the lineage tracing, animals with genotype of *tub-Gal80*^{ts}*/UAS-GATAe*; *byn-Gal4 UAS-GFP/UAS-flp Act5C >Stop >lacZ* were used.

In situ hybridization

Gut samples were fixed with 4% formaldehyde for 45 minutes at room temperature and stored in 100% methanol at –20°C until use. Hybridization was performed with a digoxigenin-labeled RNA probe prepared against *GATAe* cDNA following standard protocols (Takashima et al., 2011a).

Immunohistochemistry

Antibodies used in this study were: mouse anti-Arm (1:10), mouse anti-Cut (1:10) and mouse anti-Prospero (1:50) (all purchased from Developmental Studies Hybridoma Bank, University of Iowa); mouse anti-β-galactosidase (1:100, Promega); rabbit anti-phoshorylated-histone H3 (1:1000, Cell Signaling Technology, Danvers, MA); rabbit anti-Pdm1/nubbin (1:1000, Yeo et al., 1995); goat anti-mouse IgG Alexa488 (1:100); goat anti-mouse IgG Alexa546 (1:300); goat anti-rabbit IgG Alexa488 (1:100) (Invitrogen, Carlsbad, CA); and goat anti-rabbit IgG Cy3 (1:200) (Jackson ImmunoResearch, West Grove, PA). Antibody staining was performed as described previously (Takashima et al., 2011a). TOTO-3 or TOPRO-3 nuclear dye (Invitrogen) was added to the mounting medium when necessary.

Transmission electron microscopy

Guts were dissected in PBS and fixed with 2.5% glutaraldehyde and then with 1% osmium tetroxide. Samples were dehydrated with ascending ethanol series and acetone, embedded in Epon resin, and sectioned with a Leica ultramicrotome at a thickness of ~50-70 nm. The specimens were stained with uranyl acetate and lead citrate. Images were observed and photographed with a JEOL 100CX transmission electron microscope (JEOL, Peabody, MA).

RESULTS

Adult gut progenitors migrate across organ boundaries during metamorphosis

To trace the origin of adult gut tissues, we used a lineage-tracing construct (*Act5C >Stop >lacZ*; see Materials and methods), driven by either *esg-Gal4* [expressed in adult midgut progenitors (AMPs; supplementary material Fig. S1A)] or *byn-Gal4* (expressed in the hindgut; supplementary material Fig. S1B). Flies with the genotype of *esg-Gal4/UAS-flp*; *tub-Gal80*^{ts}*/Act5C >Stop >*lacZ or *tub-Gal80*^{ts}*/UAS-flp*; *byn-Gal4, UAS-GFP/Act5C >Stop >lacZ* were heat treated from the first instar larva resulting in the stable expression of *lacZ* reporter in cells expressing *esg-Gal4* or *byn-Gal4*, respectively. In preparations fixed at the adult stage, we observed that, after activating the construct in AMPs by *esg-Gal4*, the entire midgut was labeled, with the exception of a short midgut segment (termed 'posterior terminal midgut' in the following) located right in front of the hindgut. To our surprise, labeling also extended to the ureters and the stem cells of the Malpighian tubules (renal stem cells) (Fig. 1A), neither of which expresses *esg* in the larva (supplementary material Fig. S1A) or embryo (data not shown). Expression of *lacZ* by *byn-Gal4* in the larval HPZ was not only confined to the adult hindgut, but also extended anteriorly to the adjacent posterior terminal midgut (Fig. 1B). These findings suggest that during metamorphosis, adult gut progenitors migrate and cross the boundaries between midgut,

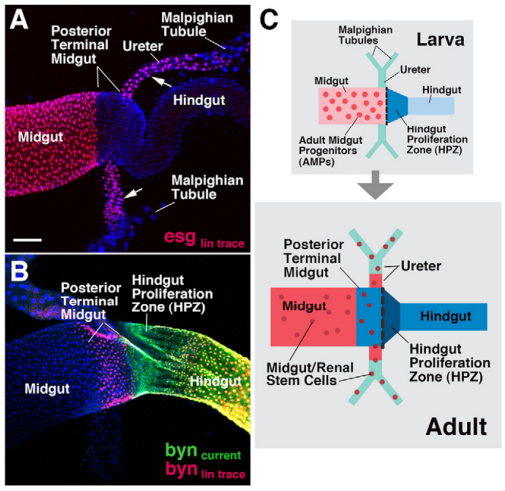

Fig. 1. Lineage tracing of adult midgut and hindgut progenitors. (**A**,**B**) Gut progenitor lineages labeled by *lacZ*. Progenitors were labeled from early larval stage by a lineage-reporter gene (*lacZ*, red) activated by *esg-Gal4* (A; esg $_{lin\ trace}$) or *byn-Gal4* (B; byn $_{lin\ trace}$), respectively. Labeled progeny of progenitors in adult gut are depicted. Arrows in A indicate labeled renal stem cells on Malpighian tubules. Current expression of *byn-Gal4 >UAS-GFP* in adult hindgut is shown in green (byn $_{current}$). Nuclei are stained with TOTO-3 or TOPRO-3 dye (shown in blue) in all confocal pictures of all figures hereafter. (**C**) Schematic depiction of larval and adult hindgut-midgut boundary region, illustrating the movement of gut progenitors that is inferred from lineage-tracing experiments. Scale bar: 50 μm.

hindgut and Malpighian tubules. AMPs, which are located in the larval midgut, form the ureters and the renal stem cell population of the Malpighian tubules; the HPZ, part of the larval hindgut, crosses anteriorly and gives rise to the posterior terminal midgut (Fig. 1C).

Origin of renal stem cells from migrating midgut progenitor cells

To reconstruct in detail when and how the migration of gut progenitors takes place, we used the lineage-tracing approach introduced above, but in this case lineage labeling was performed within restricted time window such as from first to third instar, or from third instar to different stages of metamorphosis up to 72 hours after puparium formation (APF; Fig. 2). In the late third instar larva right before metamorphosis, *esg*-positive AMPs formed clusters of 8-12 cells each scattered throughout the midgut. No AMPs were seen in the larval ureters or Malpighian tubules (Fig. 2A). In the 6-hour pupa, the *esg*-positive AMPs formed a complete outer epithelial layer: the presumptive adult midgut (Fig. 2B). This layer enclosed the *esg*-negative larval midgut layer. A third tissue layer, the transient pupal midgut (tPMG), which derives from the peripheral cells of the AMP clusters, was sandwiched in between the adult and larval midgut (Takashima et al., 2011a; Takashima et al., 2011b; Fig. 2B′). We found that the tPMG layer projects into the base of the larval ureters, engulfing cells of the proximal segment of the larval ureter (Fig. 2E). The *esg*-positive outer epithelium also reached posteriorly, forming a new proximal segment of the ureter (Fig. 2B-D,F-H). This *esg*-positive, AMP-derived ureter segment, which (aside from *esg* expression) can be distinguished from the distal (larval) ureter by its small cell size, lengthened until it acquired its full extension, covering approximately half of the length of the ureter (Fig. 2H), by 72 hours APF.

During the time between 6 and 24 hours APF, the majority of the AMP-derived cells of the midgut and ureters expressed specific differentiation markers, such as Pdm1 and Cut (Fig. 3A-C), respectively, and lost the expression of *esg* (Fig. 3D). However, a subset of cells maintained high *esg* levels. Most of them were found on the midgut epithelium and are presumptive adult intestinal stem cells (pISCs) of the midgut (Jiang et al., 2009). Interestingly, we also found some of the *esg*-positive cells on ureters and Malpighian tubules. Initially at 16 hours APF they were found at the bases of the ureters (supplementary material Fig. S1A); at 24 hours APF, they distributed among the cells of ureters (Fig. 3E). At 48 and 72 hours APF, increasing numbers of *esg*-positive cells were found on the proximal tubules (Fig. 3F-H; supplementary material Fig. S1A). Based on their small size and pattern of distribution on the Malpighian tubules and ureters, we find that they are renal stem cells (Singh et al., 2007) developing from pISCs.

Rac1 is a small GTPase that mediates actin filament reorganization and its disruption has been shown to interfere with cell motility in *Drosophila* (Paladi and Tepass, 2004). We used *esg-Gal4* driver line to express a dominant-negative construct of *Drosophila Rac1* ($Rac1^{N17}$) during the pupal period, and assayed for the distribution of pISCs in the adult gut and pISC-derived presumptive renal stem cells (pRSCs) on the Malpighian tubules (Fig. 3H-J). Flies with the genotype of *esg-Gal4*, *UAS-mRFP*/+; $tub\text{-}Gal80^{ts}$/*UAS-*$Rac1^{N17}$ were heat treated from late third instar and their phenotype was observed after adult eclosion. The overexpression of $Rac1^{N17}$ caused loss of renal stem cells on the adult ureter and Malpighian tubules (Fig. 3I). By contrast, when $Rac1^{N17}$ was overexpressed starting at 24 hours APF, by which time the adult ureter is partially formed and some pRSCs already reside in it (see Fig. 3E), we found *esg*-positive renal stem cells on the

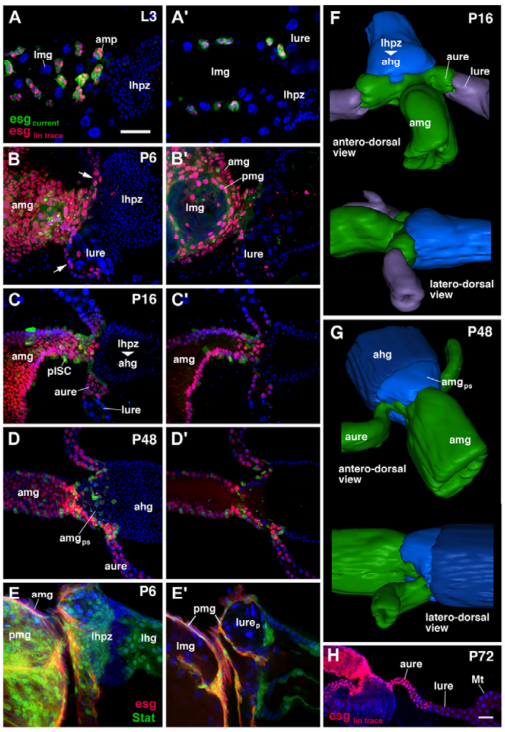

Fig. 2. Movement of midgut progenitors during metamorphosis. (**A-D′**,**H**) *Z*-projections of confocal sections of the hindgut-midgut boundary at different developmental stages. *esg-Gal4* driven lineage tracing at the stages of (A,A′) wandering third instar larva (L3), (B,B′) prepupa at 6 hours APF (P6), (C,C′) early pupa at 16 hours APF (P16), (D,D′) middle pupa at 48 hours APF (P48) and (H) late pupa at 72 hours APF. (**E**) Expression of *esg* (red) and *10XStat92E-GFP* (green) at 6 hours APF prepupa (P6). (A-E,H) Sections tangentially through gut wall ('surface view'); (A′-E′) sections through gut midline ('sagittal view'). AMPs and their progeny were labeled by *lacZ* reporter (red) using *esg-Gal4* driver from first instar stage onwards (A) or from third instar stage (B-D,H), respectively. Current expression of *esg-Gal4* is visualized by *UAS-myr-mRFP* (shown in green). (E,E′) *10XStat92E-GFP* (green) highlights the transient pupal midgut (pmg) (Takashima et al., 2011b). At the larval stage (A,A′), midgut progenitors (amp) form clusters throughout the larval midgut (lmg). Shortly after the onset of metamorphosis (B,B′,E,E′), AMP-derived cells constitute the adult midgut epithelium (amg), the transient pupal midgut (pmg), which engulfs the larval midgut, and the base of the ureter (lmg and $lure_p$ in E′). From 16 hours APF onwards, AMP-derived cells also populate the proximal ureter (aure) and form intestinal stem cells (pISCs) upregulating the expression of *esg* (C,D,H). (**F**,**G**) Three-dimensional digital models of the hindgut-midgut boundary region in laterodorsal view and anterodorsal view at 16 hours APF (P16) (F) and at 48 hours APF (P48) (G), respectively. Tissues descended from midgut progenitors are rendered green; the adult hindgut (ahg) and posterior terminal midgut (amg_{ps}), produced by the hindgut proliferation zone (hpz), are rendered in blue. ahg, adult hindgut; amg, adult midgut; amg_{ps}, posterior terminal midgut; amp, adult midgut progenitor; aure, adult ureter; lhg, larval hindgut; lhpz, larval hindgut proliferation zone; lmg, larval midgut; lure, larval ureter; $lure_p$, proximal larval ureter; Mt, Malpighian tubule; pISC, presumptive intestinal stem cell; pmg, transient pupal midgut. Scale bars: 50 µm.

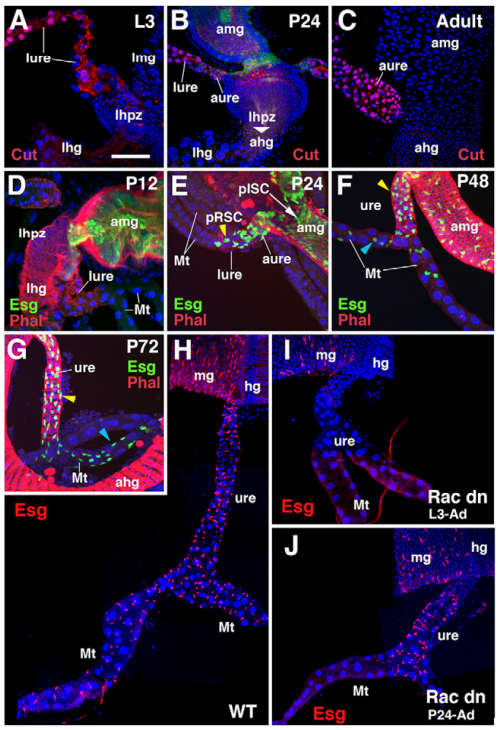

Fig. 3. Origin and migration of renal stem cells. (**A-C**) Expression of Cut protein (red) at the hindgut-midgut boundary in wandering larvae (A), 24 hour pupa (B) and adult (C). In the larva, Cut is confined to the Malpighian tubules and ureter (A). In the early pupa, AMP-derived adult ureter cells (aure; distinguishable from larval ureter cells by their much smaller size) turn on Cut expression (B) and maintain it in the adult (C). (**D-G**) *Z*-projections of confocal sections of the ureter and Malpighian tubules at different pupal stages. Prepupa at 12 hours APF (D; P12), pupa at 24 hours (E; P24), 48 hours (F; P48) and 72 hours APF (G; P72). Visceral muscle is stained with Rhodamine-Phalloidin (red). *esg*-positive presumptive intestinal stem cells (pISCs) and renal stem cells (pRSCs) are shown in green (*esg-Gal4 >UAS-mCD8GFP*). pRSCs populate the proximal ureter by P24 (E) and spread on to the Malpighian tubules (F,G; yellow arrowheads indicate pRSCs on ureters; cyan arrowheads indicate pRSCs on Malpighian tubules). (**H-J**) *Z*-projections of the ureter and Malpighian tubules in which midgut pISCs and pRSCs are labeled with *esg-Gal4 >UAS-mRFP* (red). (H) Wild-type control. (I,J) $Rac1^{N17}$ is overexpressed by *esg-Gal4* from third instar larva (I) or from 24 hours APF (J) to adult. ahg, adult hindgut; amg, adult midgut; aurc, adult ureter; hg, hindgut; lhg, larval hindgut; lhpz, larval hindgut proliferation zone; lmg, larval midgut; lure, larval ureter; mg, midgut; Mt, Malpighian tubule; pISC, presumptive intestinal stem cell; pRSC, presumptive renal stem cell; ure, ureter. Scale bar: 50 μm.

ureter but not in the Malpighian tubules (Fig. 3J). The results show that early Rac1 inhibition interferes with the extension of the adult ureter, as well as subsequent distal migration of pRSCs on to the tubules, whereas later treatment does not interfere with the formation of the proximal ureter, but with only the further migration of pRSC.

The hindgut proliferation zone forms the posterior terminal midgut of the adult

Lineage-tracing experiments using *byn-Gal4* driver temperature-activated from third instar larvae allowed us to follow the fate of the hindgut proliferation zone (HPZ) (Fig. 4A,D-F) during metamorphosis. Throughout the embryonic and larval stages, *byn* expression was confined to the hindgut, including the HPZ, which is set apart from the differentiated larval hindgut as a ring-shaped domain of small, columnar cells (Fig. 4A,B; supplementary material Fig. S1B). During the pupal stage, around 24-30 hours APF, the HPZ telescoped posteriorly and replaced the degenerating larval hindgut (data not shown) (Takashima et al., 2008). A subset of cells of the HPZ delaminated around 6 hours APF and formed an interior 'plug' that occluded the lumen at the hindgut-midgut boundary (Fig. 4C,D′-E′). At 48 hours APF, the plug had expanded anteriorly, reaching a level anterior to the ureter (Fig. 4F). Up until 16 hours APF, these cells maintained expression of *byn* (green and red cells in Fig. 4E). Subsequently, by 48 hours APF, they lost *byn* expression (red cells in Fig. 4F; supplementary material Fig. S1B). At this stage, cells of the plug (trans)differentiated into midgut enterocytes, expressing molecular markers (e.g. Pdm1; Fig. 5A,C) and structural markers of midgut enterocytes. Before delamination, all cells of the HPZ showed hallmarks of ectoderm/hindgut: they had an apical junctional complex consisting of a zonula adherens and pleated septate junctions, and secreted a cuticle layer (Fig. 5G-I). After transitioning into posterior midgut enterocytes (48 hours APF), plug-derived cells exhibited an apical brush border (long microvilli without cuticle; Fig. 5J) and smooth septate junctions, characteristic of midgut/endoderm (Fig. 5J′). The change in junctional complex was accompanied by the relocalization of structural proteins, such as Fasciclin 3 (Fas3) (Fig. 5B). Cells of the hindgut, including the HPZ, express high levels of Fas3 around their basolateral membrane, as described for ectodermal epithelia in general. By contrast, enterocytes of the midgut, including the plug-derived posterior terminal midgut, showed strongly reduced levels of Fas3, localized around their apical membrane (Fig. 5B,B′).

Interestingly, endocrine cells, which can be labeled by *prospero* (*pros*), settling in the posterior terminal midgut were negative for the *byn*-lineage marker (Fig. 5D). Likewise, ISCs (labeled by *10XStat92E-GFP*) also did not co-label with the *byn*-lineage marker in the posterior terminal midgut (Fig. 5E); instead, they were descended from the AMPs (Fig. 5F). These findings indicate that pISCs migrate into the posterior terminal midgut from anteriorly adjacent midgut regions.

The HPZ-midgut transformation requires the function of *GATAe*

As *byn* expression is gradually lost from the plug when the plug transforms into midgut enterocytes, we hypothesized that its downregulation is accompanied by upregulation of a gene that instructs midgut cell differentiation. GATAe is a C2H2 type zinc-finger protein that is required for cell differentiation of embryonic endoderm in the late embryo and its action antagonizes *byn* (Okumura et al. 2005). In the embryo, the expression of *GATAe* was detected in the midgut and Malpighian tubules (Fig. 6A,B; Okumura et al., 2005). In the larva, we found that *GATAe* appears not only in the midgut cells, including AMPs, but also in the anterior part of the HPZ, where it overlaps with the expression of *byn* (Fig. 6C,D). We speculated that *GATAe* expression may enable cells of the anterior HPZ to be transformed into midgut cells. We tested this idea by downregulating *GATAe* using RNAi-mediated gene knockdown directed by the *byn-Gal4* driver. Animals with the

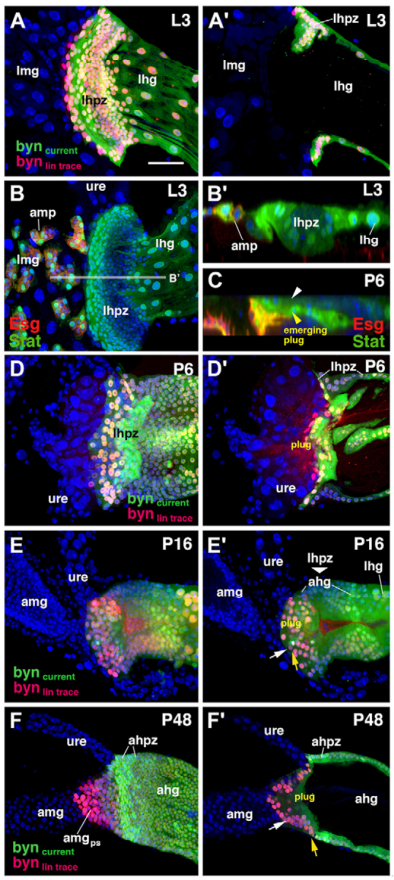

Fig. 4. Movement of hindgut progenitors during metamorphosis. (**A-F'**) *Z*-projections of confocal sections of the hindgut-midgut boundary at different developmental stages. (A-B') Wandering larva (L3); (C-D') prepupa at 6 hours APF (P6); (E,E') early pupa at 16 hours APF (P16); (F,F') middle pupa at 48 hours APF (P48). Surface views (left column) and sagittal views (right column) are shown. The lineage of the adult hindgut progenitors detected by a lineage-tracing *lacZ* reporter (red), activated by *byn-Gal4* from early third instar (A) or from late third instar (D-F) to the time of the observation. Current expression of *byn-Gal4* is visualized by *UAS-GFP* (green). (B,C) Green label visualizes the expression of *10XStat92E-GFP*. At the larval stage (A-B'), adult hindgut progenitors are confined to the larval hindgut proliferation zone (lhpz) at the boundary between larval midgut (lmg) and hindgut (lhg). Hindgut progenitors are cylindrical epithelial cells integrated in the gut epithelium (B'). In the prepupa (C,D), a subset of cells of the HPZ delaminate, resulting in an outer layer (white arrowhead in C) and an inner layer (yellow arrowhead), which goes on to form a solid 'plug' that occludes the gut lumen at the hindgut-midgut boundary (D',E'). Beyond 24 hours APF, cells of the former plug have moved anteriorly, re-epithelialized and become the posterior terminal midgut (amg_{ps} in F; outlined by white and yellow arrows in F'). ahg, adult hindgut; ahpz, adult hindgut proliferation zone; amg, adult midgut; amg_{ps}, posterior terminal midgut; amp, adult midgut progenitor; lhpz, larval hindgut proliferation zone; lhg, larval hindgut; lmg, larval midgut; ure, ureter. Scale bar: 50 μm.

genotype of *tub-Gal80^{ts}/UAS-GATAeRNAi*; *byn-Gal4*, *UAS-GFP/+* were reared at 18°C and transferred to 29°C from late third instar in order to ablate *GATAe* specifically in hindgut cells, including the anterior part of the HPZ, and the phenotype was examined after adult eclosion. In these animals, the anterior HPZ was able to form a plug, but subsequent anterior extension and transition into the posterior terminal midgut were disrupted, remaining within the lumen at the anterior hindgut (Fig. 6E-H). These findings demonstrate that *GATAe* is indeed required for both the forward expansion and epithelialization of the HPZ-derived plug, as well as their subsequent differentiation into endodermal midgut enterocytes.

Balanced Wingless activity is required to adjust the appropriate forward-versus-backward expansion of the HPZ

In a previous study (Takashima et al., 2008) we had shown that the activity of Wingless (Wg) signal promotes the continued proliferation of the HPZ, and inhibits the differentiation of hindgut enterocytes. *wg* is normally expressed in the anterior HPZ during the larval and early pupal stages, and is required for maintaining the stem/progenitor state of hindgut cells (Takashima et al., 2008). Overexpressing *wg* in the HPZ during metamorphosis results in an expansion of stem/progenitor cells and a lack of cell differentiation (Takashima et al., 2008). When we overexpressed *wg* in earlier time points from the early larval period onwards (*tub-Gal80^{ts}/UAS-wg*; *byn-GAL4 UAS-GFP/+*) and animals were fixed as late larvae, pupae or adults, an additional phenotype became apparent. In late larvae, the posterior part of the HPZ, which in wild-type larvae becomes sculpted into several longitudinal folds or columns (Fig. 7B), remained flat and undifferentiated (Fig. 7A). At pupal stages, this was followed by a dramatic change in HPZ morphogenesis. First, the size of the plug that forms from the HPZ was strongly increased. Second, at around 52 hours APF, most of the cells of the HPZ formed a plug that extended abnormally far anteriorly (Fig. 7C). At the same time, the larval hindgut epithelium (which in wild-type control pupae 52 hours APF or younger had been completely replaced by the HPZ; Fig. 7D), persists in the *wg*-overexpressed animals (Fig. 7C). In consequence, a massively increased posterior terminal midgut was observed in the adult (Fig. 7E). At that stage, the enlarged plug had adopted an epithelial phenotype, but the cells remained immature in terms of reduced size and absence of Pdm1 expression (Fig. 7F). However, in other respects, the cells showed clear attributes of midgut rather than of hindgut; for example, expression of Fas3 was low and apically polarized, as in midgut cells (Fig. 7G-I). As in wild-type posterior terminal midgut, *esg*-positive pISCs and *pros*-positive enteroendocrine cells were present in the enlarged posterior terminal midgut of *wg*-activated flies (Fig. 7J-L). We conclude that the level of Wg expression, aside from its basic role in maintaining proliferating cells, forms part of the mechanism that determines what part of the HPZ gives rise to midgut versus hindgut.

DISCUSSION

Drosophila midgut progenitors give rise to renal stem cells

Our current study revealed that the intestinal progenitor cells of the *Drosophila* midgut (AMPs) show a dynamic behavior that is unparalleled among adult progenitor cell populations described thus far. Even though they appear to originate from a single, endodermal cell population in the embryo and remain confined to the midgut during the larval period, AMPs spread out in the pupa and intermingle with cells of different germ layer origin. They reconstitute part of the ureter of the adult, and from there migrate

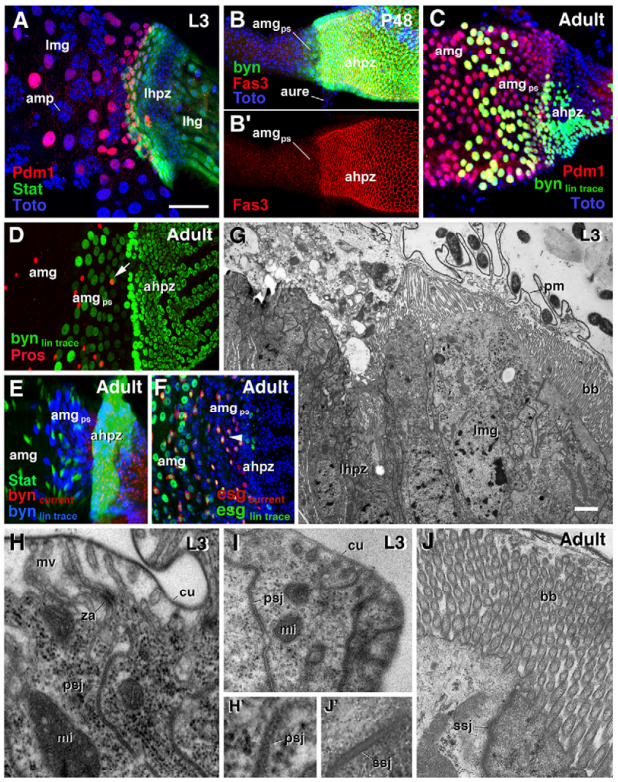

Fig. 5. Differentiation of HPZ-derived ectodermal cells into midgut. (**A**) In late third instar larva (L3), Pdm1 (red) marks differentiated midgut enterocytes (large polyploid cells), whereas undifferentiated adult midgut progenitors (amp; recognizable by their small cell size) are not Pdm1 positive. (**B**,**B'**) At 48 hours APF (P48), posterior terminal midgut (amg_{ps}) derived from HPZ (marked by faint green; *byn-Gal4 >UAS-GFP*) loses high Fas3 expression. (**C**) A 6-hour heat pulse with *byn-GAL4* at third instar labels a subset of HPZ-derived cells in the posterior terminal midgut, which are positive for Pdm1. (**D**) The posterior terminal midgut is not *pros* positive, indicating that endocrine cells (e.g. white arrow) in this region are derived from midgut pISCs (the lineage was traced from third instar to adult with *byn-GAL4*). (**E**) *10XStat92E-GFP*-positive ISCs (green) are also negative for the *byn* lineage. (**F**) *esg* lineage-traced stem cells (green; e.g. arrowhead) populate the posterior terminal midgut. (**G-J**) Transmission electron microscopy of the hindgut-midgut boundary region of the larva (G-I) and adult (J). Hindgut cells have an apical cuticle (cu) topping irregular microvilli (mv) and a junctional complex consisting of a sub-apical zonula adherens (za) and pleated septate junctions (psj) (H). Hindgut cells of the HPZ directly adjacent to the hindgut-midgut boundary (G,I) exhibit the same characteristics, with the exception of a much thinner cuticle (compare cu in I,H). Enterocytes of the posterior terminal midgut of the larva (lmg in G) and adult (J) form an apical brush border (bb), consisting of long, densely packed microvilli oriented in parallel. They lack the zonula adherens and have smooth septate junctions (ssj; compare appearance of ssj in J' with that of pleated septate junctions in H'). ahpz, adult hindgut proliferation zone; amg, adult midgut; amg_{ps}, posterior terminal midgut; amp, adult midgut progenitor; aure, adult ureter; bb, brush border; cu, cuticle; lhg, larval hindgut; lhpz, larval hindgut proliferation zone; lmg, larval midgut; mi, mitochondrion; mv, microvilli; pm, peritrophic membrane; psj, pleated septate junction; ssj, smooth septate junction; za, zonula adherens. Scale bars: 50 μm.

onto the Malpighian tubules and then become the renal stem cells (Singh et al., 2007). Throughout the adult phase, these renal stem cells maintain molecular and cellular characteristics of midgut stem cells; they remain as small diploid mesenchymal cells attached to the basal membrane of the Malpighian tubule epithelium and are positive for *esg* expression. Renal stem cells do not express markers specific for Malpighian tubules, such as Cut (Singh et al., 2007) (S.T. and V.H., unpublished). Only post-mitotic progeny of renal stem cells, once integrated in the tubule epithelium, turn on these markers. Whereas they share common origin and similar molecular characteristics with midgut ISCs, the repertoire of cells that they produce is entirely distinct from that of midgut ISCs, indicating that there must be an extrinsic signal(s) that specify the fate of their progeny according to where they reside.

The origin of *Drosophila* adult renal stem cells from midgut progenitors differs strongly from what has been reported for vertebrate kidney stem cells; this may in part reflect the fact that the developmental pathways by which the excretory systems of vertebrates and insects are formed show very little resemblance. Vertebrate kidney tubules arise from the metanephrogenic mesenchyme, an embryonic cell population that forms part of the intermediate mesoderm. In response to complex signaling mechanisms from the ureteric bud, as well as the ingrowing vascular system, these cells undergo a mesenchymal-epithelial transition to become polarized, epithelial cells (Schmidt-Ott et al., 2006). Vertebrate kidney tubules show a high degree of regenerative capacity. Following damage, tubule cells partially dedifferentiate and become proliferative (Humphreys and Bonventre, 2007; Maeshima, 2007). Recent fate-mapping experiments strongly support the notion that tubule epithelial cells are responsible for the generation of new kidney cells (Duffield and Humphreys, 2011). This then differs markedly from the situation in *Drosophila*, where mesenchymal cells originating from outside the excretory organs represent stem cells that replace renal cells under normal conditions and following injury (Singh and Hou, 2009).

A transition of ectoderm to endoderm: formation of the posterior terminal midgut

Cells of the posterior terminal midgut arise by delamination from the HPZ during the first few hours after puparium formation. Until about 24 hours into the pupal phase they form a plug of mesenchymal cells that fills the lumen of the HPZ. After another 24 hours, plug cells regain their polarity, epithelialize and form the posterior terminal midgut, whereas the lumen of this region is closed so that the midgut and the hindgut tubes are still disconnected, which opens right before eclosion. The sequential loss-and re-acquisition of epithelial properties of cells forming the posterior terminal midgut is reminiscent of midgut formation in the embryo. During gastrulation, the posterior endoderm and hindgut primordium form a common epithelial invagination (Skaer, 1993).

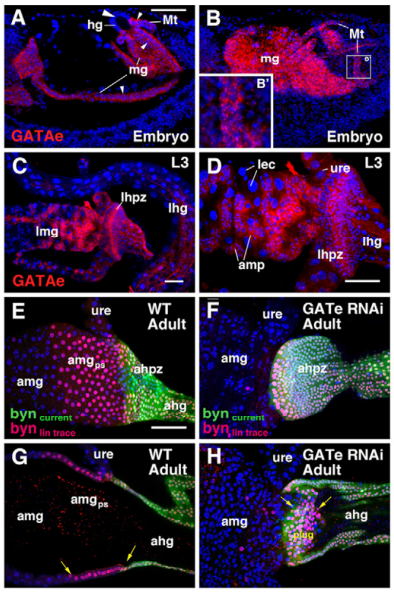

Fig. 6. Role of *GATAe* in the formation of the posterior terminal midgut. (**A-D**) Confocal sections of gut of late embryo (A,B) and third instar larva (C,D), showing expression of *GATAe* mRNA (red). Embryonic expression is found in the midgut (mg; small arrowheads) and Malpighian tubules (Mt) (B′), but not in the hindgut (hg; big arrowhead). In the larva, *GATAe* is expressed strongly in adult midgut progenitors (amp) and the hindgut proliferation zone (hpz); faint expression is seen in the Malpighian tubules and ureter (ure), and differentiated midgut enterocytes (lec). (**E-H**) Confocal *z*-projection images of the adult hindgut-midgut boundary of wild-type (E,G) and *GATAe* knock-down animals (F,H). Surface views (E,F) and sagittal views (G,H) are shown. Cells of the hindgut proliferation zone are lineage traced from late third instar using *byn-Gal4* driver. Current expression of *byn* is shown in green, the lineage is shown in red. In wild type, HPZ-derived cells come to lie within the posterior terminal midgut (amg_{ps}; arrows in G). Upon *GATAe* knock-down, HPZ-derived cells do not epithelialize and form a solid cluster of cells (plug; arrows) in the lumen of the hindgut (F,H). ahg, adult hindgut; ahpz, adult hindgut proliferation zone; amg, adult midgut; amg_{ps}, posterior terminal midgut; amp, adult midgut progenitor; hg, hindgut; lec, larval enterocyte; lhg, larval hindgut; lhpz, larval hindgut proliferation zone; lmg, larval midgut; mg, midgut; Mt, Malpighian tubule; ure, ureter. Scale bars: 50 µm.

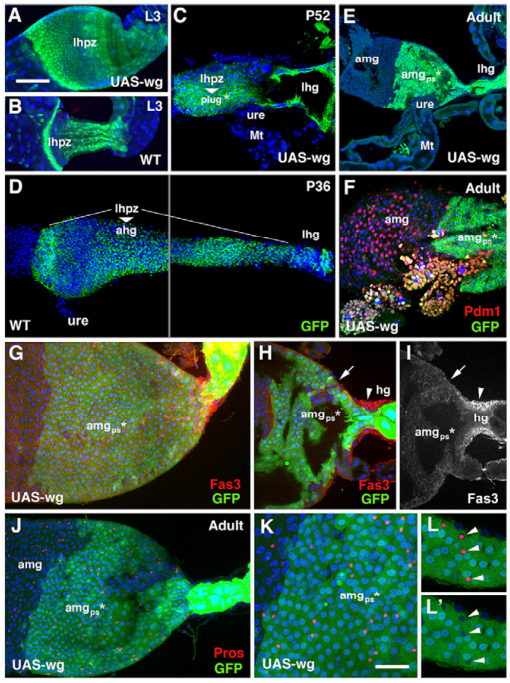

Fig. 7. Role of *wingless* in the formation of the posterior terminal midgut. (A-L) *Z*-projections of the hindgut-midgut boundary region following *byn-Gal4*-driven *wg* overexpression (A,C,E-L) and wild-type controls (B,D). HPZ-derived cells (lineage) are detected by the expression of mito-GFP (green), which has a long half life (C-F), or by use of anti-GFP antibody against conventional GFP to enhance the signal (G,H,J-L). (**A**,**B**) Wg overexpression from first to third instar causes expansion of the HPZ (anterior HPZ is detected by *10XStat92E-GFP*). (**C**) During mid-pupal stage (52 hours APF), the HPZ transforms into an enlarged plug (*) that has expanded anteriorly relative to the ureter (ure). (**D**) The HPZ of a wild-type pupa (36 hours APF) has expanded posteriorly to form the adult hindgut (ahg), which replaces the larval hindgut (lhg). (**E-I**) In adults of animals in which Wg was overexpressed from L1 onwards (E,F), cells of the plug become epithelial and form an abnormal, enlarged posterior terminal midgut (amg_{ps}*) lacking Pdm1 (F), but showing other midgut specific attributes, including low Fas3 (G-I). Thus, Fas3 is expressed at low levels at apical side of the midgut epithelium (arrows in H,I) and at high levels in the hindgut (arrowheads in H,I) (*z*-projection shown in G represents a surface view of the hindgut-midgut boundary, H and I represent sagittal sections). (**J-L′**) *Pros*-positive endocrine cells (arrowheads) form in the posterior terminal midgut as in wild type, but lack GFP expression, confirming that they are not of HPZ origin. ahg, adult hindgut; amg, adult midgut; amg_{ps}, posterior terminal midgut; hg, hindgut; lhg, larval hindgut; lhpz, larval hindgut proliferation zone; Mt, Malpighian tubule; ure, ureter. Scale bars: 50 µm in A-J; 25 µm in K-L′.

Around stage 10, the posterior endoderm undergoes an epithelial-mesenchymal transition, which then reverses during stage 12/13 with the formation of the definitive midgut epithelium (Tepass and Hartenstein, 1994b). It is tempting to speculate that the peculiar development of the epithelial HPZ giving rise to a small part of the midgut via a mesenchymal plug recapitulates a morphogenetic program that is active during early embryogenesis.

Interestingly, only enterocytes of the posterior terminal midgut are formed from the anterior HPZ. Midgut ISCs and endocrine cells found in this area emigrate from an anteriorly adjacent midgut region that is derived from endodermal AMPs. The boundary between hindgut and posterior midgut forms a conspicuous border at which the spread of pISCs stops. It is known that migrating cells interact with their environment via cell-cell adhesion molecules (e.g. cadherins, fasciclins) or cell-substrate adhesion molecules (e.g. integrins), and differential expression of these factors is likely to be involved in controlling pISC movement, causing them to stop at the hindgut-midgut boundary. In line with this hypothesis, several adhesion molecules, including DE-cadherin and Fas3, are expressed

very highly in the HPZ, and abruptly decline in the midgut (Fig. 5B and data not shown), which might prevent pISCs from invading into the hindgut territory.

Wg apparently has a role in controlling the balance between midgut and hindgut derivatives of the HPZ. It is well established that Wg promotes the maintenance of intestinal stem cells and inhibits differentiation in both vertebrates and *Drosophila* (Lin et al., 2008; Takashima et al., 2008; Faro et al., 2009; Haegebarth and Clevers, 2009; Silva et al., 2011). Overexpression of Wg in the *Drosophila* late larval HPZ causes these cells to continue to proliferate and prevents hindgut enterocytes from differentiating (Takashima et al., 2008). If Wg activity is enhanced in the HPZ long enough prior to metamorphosis, an additional phenotype is observed, consisting of an increased fraction of HPZ-derived cells developing as midgut. We speculate that the early overexpression of Wg prevents a 'determinative event' in the HPZ that predisposes all cells in the (larval) HPZ to initiate hindgut differentiation. Thus, the characteristic columnarization that one normally observes in the posterior HPZ of late larvae can be interpreted as the first step of hindgut differentiation. Cells undergoing this determinative step (in wild-type) are thereby unable to delaminate and contribute to the plug, which will become midgut. Overexpression of Wg, in line with its basic pro-proliferative and anti-differentiative function, prevents the hindgut determination and columnarization. As a result, most cells form a plug, and subsequently differentiate as midgut enterocytes. Why are cells allowed to differentiate (into midgut), rather than stay undifferentiated? The most likely answer is that expression of *byn-Gal4* driving Wg recedes from the plug, which then removes the block on differentiation.

Germ layers and the origin of the Malpighian tubules

In most animals, the specification of cell fates appears to be a long-lasting stepwise process. From an initial state of totipotency or pluripotency, cells become progressively more restricted in their fate. Gastrulation, the process by which cells are separated into three germ layers (ectoderm, endoderm, mesoderm) is widely considered as one of the most decisive, early occurring steps by which cell lineages with different fates become restricted. Subsequently, germ layers split into smaller units with even more restricted fates. Gastrulation in insects is a process by which the ventral domain and polar domain of the blastoderm become internalized to form the 'gastral groove' or 'ventral furrow' (Anderson, 1973; Alwes and Scholtz, 2006; Biffis et al., 2009; Wolff and Hilbrant, 2011; Brenneis et al., 2011). Cells of the gastral groove form the mesoderm (in the center) and the endoderm (anterior and posterior tip). After gastrulation, the outer surface epithelium adjacent to the anterior and posterior endoderm invaginates and forms the stomodeum (future foregut) and proctodeum (future hindgut). Their later time point of origin, as well as the fact that foregut and hindgut remain epithelial throughout development and later form cuticle, like the epidermis, were sufficient to consider these organs ectodermal, rather than endodermal, in much of the classical literature (e.g. Hertwig and Hertwig, 1881; Korschelt, 1936). The Malpighian tubules, including ureters, arise from the proctodeum, sometimes even before this tissue invaginates, and are therefore also usually counted as ectodermal structures. In Dipterans, matters are made difficult because invagination of the proctodeum occurs at the time of gastrulation, and the exact boundary between ectoderm and posterior endoderm is blurred. This has led some authors in the past to propose that the Malpighian tubules arise from the endoderm (e.g. Poulson, 1950). It is interesting to note that spiders, which became terrestrial independently of insects, have Malpighian tubules that are similar in ultrastructure and function to those of insects, but that are endodermal in origin, evaginating from the gastral groove well before the appearance of the proctodeum (Korschelt, 1936; Anderson, 1973).

The data presented in this paper as well as in previous genetic and molecular studies, suggest that a stable boundary between ectoderm and endoderm does not form in *Drosophila*, and that Malpighian tubules/ureters are supplied from all three germ layers. In the embryo, principal Malpighian tubule and ureter cells originate from the (structurally defined) ectoderm and mesodermal stellate cells, which later intercalate into tubule epithelium via mesenchymal-epithelial transition (Denholm et al., 2003). During metamorphosis, part of the ureter, as well as renal stem cells populating the (proximal) Malpighian tubules, are derived from endodermal midgut progenitors. Genetically, Malpighian tubules/ureters are also closely related to endoderm: transcriptional regulators associated with midgut (*srp*, *GATAe*) or Malpighian tubules (*Kr*) are transiently or permanently expressed in both tissues (Liu and Jack, 1992; Reuter, 1994; Okumura et al., 2005; Okumura et al., 2007) (see Fig. 6). Finally, ultrastructural features (lack of cuticle, presence of the brush border and smooth septate junctions) support the endodermal nature of the Malpighian tubules. Interestingly, these structural features are acquired secondarily during embryogenesis: Malpighian tubule progenitors start out like the ectodermal hindgut, as epithelial cells with pleated septate junctions and signs of apical cuticle secretion (Tepass and Hartenstein, 1994a), and, at a later time point, switch to an 'endodermal phenotype', replacing pleated septate junctions with smooth septate junctions and an apical brush border.

We speculate around the boundary between endoderm and ectoderm, a domain of germ layer of undefined identity exists that gives rise to the Malpighian tubules and posterior terminal midgut. It is puzzling what the developmental significance of this domain may be. In other words, why do Malpighian tubules, which at the anlagen stage as well as in their differentiated state express (at least some) attributes of endoderm, undergo a transient phase where they appear ectodermal? Comparative developmental-genetic studies, looking in other arthropods at the processes that shape the Malpighian tubules and adjacent intestine, may provide the answer to this puzzle. It will be particularly enlightening to gain more insight into the molecular mechanism that specifies Malpighian tubules in chelicerates, where these structures appear to be endodermal from start to finish, but where little is known about aspects of morphogenesis and gene expression patterns.

Acknowledgements
We thank Bloomington Stock Center, Vienna *Drosophila* Resource Center (VDRC) and the National Institute of Genetics (Japan) for providing flies. We are grateful to all our lab members for critical and helpful discussions.

Funding
This work is supported by the National Institutes of Health [1 R01 GM087373 to V.H.]. Deposited in PMC for release after 12 months.

Competing interests statement
The authors declare no competing financial interests.

Supplementary material
Supplementary material available online at
http://dev.biologists.org/lookup/suppl/doi:10.1242/dev.082933/-/DC1

References

Alwes, F. and Scholtz, G. (2006). Stages and other aspects of the embryology of the parthenogenetic Marmorkrebs (Decapoda, Reptantia, Astacida). *Dev. Genes Evol.* **216**, 169-184.
Anderson, D. T. (1973). *Embryology and Phylogeny in Annelids and Arthropods*. New York, NY: Pergamon Press.

Biffis, C., Alwes, F. and Scholtz, G. (2009). Cleavage and gastrulation of the dendrobranchiate shrimp Penaeus monodon (Crustacea, Malacostraca, Decapoda). *Arthropod Struct. Dev.* **38**, 527-540.
Brenneis, G., Arango, C. P. and Scholtz, G. (2011). Morphogenesis of Pseudopallene sp. (Pycnogonida, Callipallenidae) II: postembryonic development. *Dev. Genes Evol.* **221**, 329-350.
Denholm, B., Sudarsan, V., Pasalodos-Sanchez, S., Artero, R., Lawrence, P., Maddrell, S., Baylies, M. and Skaer, H. (2003). Dual origin of the renal tubules in Drosophila: mesodermal cells integrate and polarize to establish secretory function. *Curr. Biol.* **13**, 1052-1057.
Duffield, J. S. and Humphreys, B. D. (2011). Origin of new cells in the adult kidney: results from genetic labeling techniques. *Kidney Int.* **79**, 494-501.
Faro, A., Boj, S. F. and Clevers, H. (2009). Fishing for intestinal cancer models: unraveling gastrointestinal homeostasis and tumorigenesis in zebrafish. *Zebrafish* **6**, 361-376.
Haegebarth, A. and Clevers, H. (2009). Wnt signaling, lgr5, and stem cells in the intestine and skin. *Am. J. Pathol.* **174**, 715-721.
Hasebe, T., Kajita, M., Iwabuchi, M., Ohsumi, K. and Ishizuya-Oka, A. (2011). Thyroid hormone-regulated expression of nuclear lamins correlates with dedifferentiation of intestinal epithelial cells during Xenopus laevis metamorphosis. *Dev. Genes Evol.* **221**, 199-208.
Hertwig, O. and Hertwig, R. (1881). *Die Coelomtheorie: Versuch Einer Erkla"Rung Des Mittleren Keimblattes*, pp. 68-76. Jena: Verlag von Gustav Fischer.
Humphreys, B. D. and Bonventre, J. V. (2007). The contribution of adult stem cells to renal repair. *Nephrol. Ther.* **3**, 3-10.
Ishizuya-Oka, A. and Shi, Y. B. (2007). Regulation of adult intestinal epithelial stem cell development by thyroid hormone during Xenopus laevis metamorphosis. *Dev. Dyn.* **236**, 3358-3368.
Jiang, H. and Edgar, B. A. (2009). EGFR signaling regulates the proliferation of Drosophila adult midgut progenitors. *Development* **136**, 483-493.
Jiang, H., Patel, P. H., Kohlmaier, A., Grenley, M. O., McEwen, D. G. and Edgar, B. A. (2009). Cytokine/Jak/Stat signaling mediates regeneration and homeostasis in the Drosophila midgut. *Cell* **137**, 1343-1355.
Jiang, H., Grenley, M. O., Bravo, M. J., Blumhagen, R. Z. and Edgar, B. A. (2011). EGFR/Ras/MAPK signaling mediates adult midgut epithelial homeostasis and regeneration in Drosophila. *Cell Stem Cell* **8**, 84-95.
Korschelt, E. (1936). *Vergleichende Entwicklungsgeschichte der Tiere*. Jena, Germany: G. Fischer.
Lee, W. C., Beebe, K., Sudmeier, L. and Micchelli, C. A. (2009). Adenomatous polyposis coli regulates Drosophila intestinal stem cell proliferation. *Development* **136**, 2255-2264.
Lin, G., Xu, N. and Xi, R. (2008). Paracrine Wingless signalling controls self-renewal of Drosophila intestinal stem cells. *Nature* **455**, 1119-1123.
Liu, S. and Jack, J. (1992). Regulatory interactions and role in cell type specification of the Malpighian tubules by the cut, Krüppel, and caudal genes of Drosophila. *Dev. Biol.* **150**, 133-143.
Liu, W., Singh, S. R. and Hou, S. X. (2010). JAK-STAT is restrained by Notch to control cell proliferation of the Drosophila intestinal stem cells. *J. Cell. Biochem.* **109**, 992-999.
Maeshima, A. (2007). Label-retaining cells in the kidney: origin of regenerating cells after renal ischemia. *Clin. Exp. Nephrol.* **11**, 269-274.
Mathur, D., Bost, A., Driver, I. and Ohlstein, B. (2010). A transient niche regulates the specification of Drosophila intestinal stem cells. *Science* **327**, 210-213.
Micchelli, C. A. and Perrimon, N. (2006). Evidence that stem cells reside in the adult Drosophila midgut epithelium. *Nature* **439**, 475-479.
Ohlstein, B. and Spradling, A. (2006). The adult Drosophila posterior midgut is maintained by pluripotent stem cells. *Nature* **439**, 470-474.
Ohlstein, B. and Spradling, A. (2007). Multipotent Drosophila intestinal stem cells specify daughter cell fates by differential notch signaling. *Science* **315**, 988-992.
Okumura, T., Matsumoto, A., Tanimura, T. and Murakami, R. (2005). An endoderm-specific GATA factor gene, dGATAe, is required for the terminal differentiation of the Drosophila endoderm. *Dev. Biol.* **278**, 576-586.
Okumura, T., Tajiri, R., Kojima, T., Saigo, K. and Murakami, R. (2007). GATAe-dependent and -independent expressions of genes in the differentiated endodermal midgut of Drosophila. *Gene Expr. Patterns* **7**, 178-186.
Paladi, M. and Tepass, U. (2004). Function of Rho GTPases in embryonic blood cell migration in Drosophila. *J. Cell Sci.* **117**, 6313-6326.
Poulson, D. F. (1950). Histogenesis, organogenesis and differentiation in the embryo of Drosophila melanogaster Meigen. In *Biology of Drosophila* (ed. M. Demerec). New York, NY: John Wiley & Sons, Inc.
Reuter, R. (1994). The gene serpent has homeotic properties and specifies endoderm versus ectoderm within the Drosophila gut. *Development* **120**, 1123-1135.
Schmidt-Ott, K. M., Lan, D., Hirsh, B. J. and Barasch, J. (2006). Dissecting stages of mesenchymal-to-epithelial conversion during kidney development. *Nephron. Physiol.* **104**, 56-60.
Silva, A. C., Filipe, M., Steinbeisser, H. and Belo, J. A. (2011). Characterization of Cer-1 cis-regulatory region during early Xenopus development. *Dev. Genes Evol.* **221**, 29-41.
Singh, S. R. and Hou, S. X. (2009). Multipotent stem cells in the Malpighian tubules of adult Drosophila melanogaster. *J. Exp. Biol.* **212**, 413-423.
Singh, S. R., Liu, W. and Hou, S. X. (2007). The adult Drosophila malpighian tubules are maintained by multipotent stem cells. *Cell Stem Cell* **1**, 191-203.
Singh, S. R., Zeng, X., Zheng, Z. and Hou, S. X. (2011). The adult Drosophila gastric and stomach organs are maintained by a multipotent stem cell pool at the foregut/midgut junction in the cardia (proventriculus). *Cell Cycle* **10**, 1109-1120.
Skaer, H. (1993). The alimentary canal. In *The development of Drosophila melanogaster* (ed. M. Bate and A. Martinez-Arias), pp. 941-1012. Plainview, NY: Cold Spring Harbor Laboratory Press.
Takashima, S., Mkrtchyan, M., Younossi-Hartenstein, A., Merriam, J. R. and Hartenstein, V. (2008). The behaviour of Drosophila adult hindgut stem cells is controlled by Wnt and Hh signalling. *Nature* **454**, 651-655.
Takashima, S., Adams, K. L., Ortiz, P. A., Ying, C. T., Moridzadeh, R., Younossi-Hartenstein, A. and Hartenstein, V. (2011a). Development of the Drosophila entero-endocrine lineage and its specification by the Notch signaling pathway. *Dev. Biol.* **353**, 161-172.
Takashima, S., Younossi-Hartenstein, A., Ortiz, P. A. and Hartenstein, V. (2011b). A novel tissue in an established model system: the Drosophila pupal midgut. *Dev. Genes Evol.* **221**, 69-81.
Tepass, U. and Hartenstein, V. (1994a). The development of cellular junctions in the Drosophila embryo. *Dev. Biol.* **161**, 563-596.
Tepass, U. and Hartenstein, V. (1994b). Epithelium formation in the Drosophila midgut depends on the interaction of endoderm and mesoderm. *Development* **120**, 579-590.
Wolff, C. and Hilbrant, M. (2011). The embryonic development of the central American wandering spider Cupiennius salei. *Front. Zool.* **8**, 15.
Xu, N., Wang, S. Q., Tan, D., Gao, Y., Lin, G. and Xi, R. (2011). EGFR, Wingless and JAK/STAT signaling cooperatively maintain Drosophila intestinal stem cells. *Dev. Biol.* **354**, 31-43.
Yeo, S. L., Lloyd, A., Kozak, K., Dinh, A., Dick, T., Yang, X., Sakonju, S. and Chia, W. (1995). On the functional overlap between two Drosophila POU homeo domain genes and the cell fate specification of a CNS neural precursor. *Genes Dev.* **9**, 1223-1236.

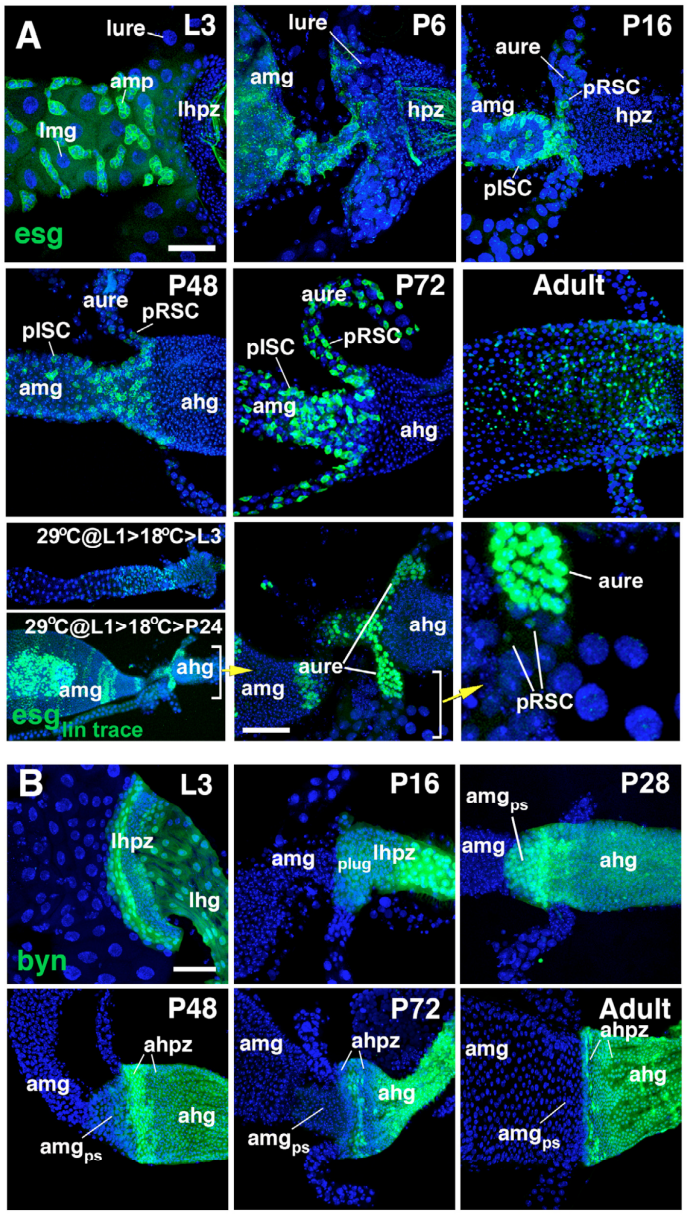

Fig. S1. Expression of Gal4 drivers. (**A**) Expression of *esg-Gal4>UAS-myr-mRFP* and (**B**) *byn-Gal4>UAS-GFP* in the hindgut-midgut boundary region at consecutive stages (both are shown in green). *esg-Gal4* lineage is also shown in the bottom row in A, where the lineage marker was briefly activated for 6 hours in first instar larvae and the animals were kept at 18°C until they reached L3 or the stage equivalent to P24 at 25°C (48 hours APF at 18°C) (current expression of *esg-Gal4* is not visible because of the inhibition of Gal4-UAS system by Gal80^{ts} at this temperature). Abbreviations: ahg, adult hindgut; amg, adult midgut; amg$_{ps}$, posterior terminal midgut; amp, adult midgut progenitor; aure, adult ureter; ahpz, adult hindgut proliferation zone; hpz, hindgut proliferation zone; L3, late third instar larva; lhg, larval hindgut; lhpz, larval hindgut proliferation zone; lmg, larval midgut; lure, larval ureter; P6, P16, P24, P28, P48, P72, pupa aged 6, 16, 24, 28, 48, 72 hours after puparium formation; pISC, presumptive intestinal stem cell; pRSC, presumptive renal stem cell. Scale bars: 50 μm.

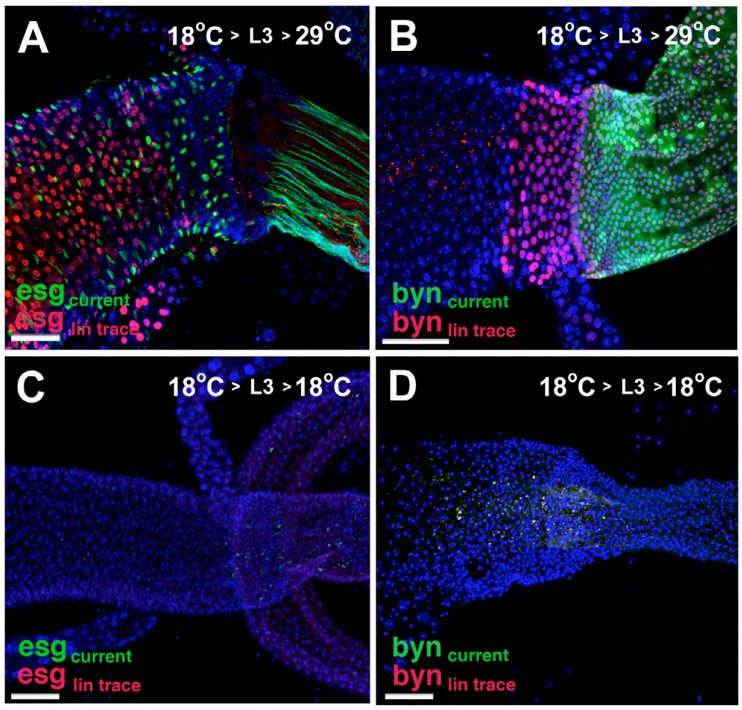

Fig. S2. Negative controls for lineage analysis. (**A-D**) Expression of a lineage marker (*lacZ*) driven by (A,C) *esg-Gal4* and (B,D) *byn-Gal4* in hindgut-midgut boundary region. Current expression of the *Gal4* drivers is shown in green and the lineage is shown in red. The lineage-tracing construct was activated by raising the temperature to 29°C at late third instar stage (A,B). Negative controls are shown in C,D, where the animals were reared at 18°°C, which prevents activation of the construct. In the negative controls, current expression of *Gal4* driver is also not visible because of the inhibition of Gal4-UAS system by Gal80^{ts} at this temperature. Scale bars: 50 µm.

Chapter 3: Changing lineage characteristics of developing *Drosophila* midgut stem cells depend on the control of prospero expression by the Wg and N signaling pathways

SUMMARY

Proliferating intestinal stem cells (ISCs) generate all cell types of the *Drosophila* midgut, including enterocytes, endocrine cells, and gland cells, throughout the lifetime of the animal. Among the signaling mechanisms controlling the balance between ISC self-renewal and the production of different cell types, Notch (N) and Wingless (Wg) play a pivotal role. To address some of the unanswered questions concerning the role of N and Wg in ISC proliferative behavior we focused on the developing midgut of the pupa. Precursors of the *Drosophila* adult intestinal stem cells (pISCs) can be first detected within the pupal midgut during the first hours after onset of metamorphosis as motile mesenchymal cells. PISCs of the pupa perform 2-3 rounds of parasynchronous divisions. The first mitosis yields only an increase in pISC number. During the following rounds of mitosis, dividing pISCs give rise to more pISCs, as well as the endocrine cells that populate the midgut of the eclosing fly. Enterocytes do not appear among the pISC progeny until around the time of eclosion. The "proendocrine" gene *prospero (pros)*, expressed from mid-pupal stages onward in pISCs, is responsible to advance the endocrine fate in these cells; following removal of *pros*, pISCs continue to proliferate, but endocrine cells do not form. Conversely, the onset of N activity that occurs around the stage when *pros* comes on restricts *pros* expression among pISCs. Loss of N abrogates proliferation and switches on an endocrine fate among all pISCs. Signals from the reorganizing visceral musculature, including Wg/Wnt4, are responsible to trigger the expression of *pros* and N activity in pISCs. Our results suggest that a switch depending on the activity of N and *pros* acts at the level of the pISC to decide between continued proliferation and endocrine differentiation.

INTRODUCTION

Stem cells of the intestine (ISCs) are responsible for the continuous replacement of all intestinal cell types. In vertebrates, ISCs are integrated in the intestinal epithelium lining the crypts, glandular invaginations of the gut. Progeny of the intestinal stem cells (transient amplifying cells) populate the upper region of the crypts and, after a limited number of cell divisions, become postmitotic to differentiate into absorptive cells (enterocytes), gland cells, or entero-endocrine cells (Crosnier et al., 2006; Scoville et al., 2008; Simon and Clevers, 2011). Clonal analyses, whereby individual ISCs were labeled, demonstrated that they are pluripotent: labeled clones included enterocytes, as well as secretory and/or endocrine cells (Bjerknes and Cheng, 2006). In the *Drosophila* midgut which lacks crypts or villi, ISCs are distributed as more or less evenly spaced, subepithelial cells which divide to produce enterocytes, endocrine cells, and secretory cells (Biteau et al., 2011; Jiang and Edgar, 2011; Strand and Micchelli, 2011; Takashima and Hartenstein, 2012; Luchetta and Ohlstein, 2012).

The genetic control of stem cell maintenance and intestinal cell fate specification appears to be highly conserved among vertebrate and insect systems. In both, Wnt/Wg acts to promote ISC proliferation and maintenance. Wnt proteins are secreted by myofibroblasts and glandular (Paneth) cells in the crypts of the vertebrate intestine, and by visceral muscle cells of the *Drosophila* intestine (Yen and Wright, 2006; Lin et al., 2008; Yeung et al., 2011; Farin et al., 2012). Excessive activation of the Wnt pathway, resulting from loss of the Adenopolyposis coli (Apc) protein, causes tumorous growth of intestinal stem cells in human patients, vertebrate model systems, and *Drosophila* (van Es et al., 2001; Kielman et al., 2002; Lee et al., 2009). Along with Wnt/Wg, the Notch (N) signaling pathway plays a complex role in ISC proliferation and differentiation. In the vertebrate gut, loss N activity results in the abrogation of proliferation

and the conversion of intestinal cells into secretory (glandular and endocrine) cells (Jensen et al., 2000; Crosnier et al., 2005; van Es et al., 2005; Fre et al., 2005; 2011). N overactivation promotes proliferation, blocks the formation of secretory cells, and also interferes with the differentiation of absorptive cells (Fre et al., 2005). The effect of N on stem cell proliferation and differentiation is mediated in large part by the bHLH transcription factor Math1, homolog of the *Drosophila* proneural gene *atonal* (Yang et al., 2001; Bossuyt et al., 2009). The model proposed for how N functions in the vertebrate intestine envisages a lateral inhibition mechanism taking place in the stem cell and/or amplifying progenitor compartment, whereby high N activity results in cells continuing to proliferate, and low activity allowed for the expression of Math1 causing cells to exit the cell cycle and differentiate as secretory cells (Fre et al., 2005, 2011; Stamataki et al., 2011).

In the *Drosophila* midgut, N activity has an equally inhibitory effect on the formation of secretory/endocrine cells, but appears to act differently from vertebrates in regard to enterocyte differentiation and stem cell maintenance. N-mediated interactions take place among small clusters of dividing ISCs which populate the basal surface of the midgut epithelium. Cells that end up with low levels of N activity turn on the bHLH proneural gene *asense* (*ase*; Bardin et al., 2010) and the homeobox gene *prospero* (*pros*) which promote exit from the cell cycle and differentiation as endocrine cells (Ohlstein and Spradling, 2006; 2007; Micchelli and Perrimon, 2006). Paradoxically, low N levels also favor proliferation, as seen in the strongly enlarged size of clones derived from ISCs with reduced or lacking N activity. High levels of N drive ISCs towards cell cycle exit and differentiation as enterocytes (Kapurina et al., 2012). It has been difficult to formulate a model encompassing N function in the ISCs of both *Drosophila* and vertebrates.

To gain more insight into the mechanisms controlling ISCs we analyzed the development of these cells in *Drosophila*. As a holometabolous insect, *Drosophila* has a biphasic life cycle where most organs of the larva, including the intestinal tract, are destroyed during metamorphosis and are replaced by adult-specific organs. Progenitor cells of the adult midgut (AMPs) form clusters ("nests") of proliferating cells dispersed throughout the differentiated larval gut, and undergo differentiation during the pupal stage (Jiang and Edgar, 2009; Mathur et al., 2010; Takashima et al., 2011). The future midgut stem cells originate from within the population of AMPs. We show in this paper that the precursors of ISCs (pISCs) are visible as small groups of dividing cells, set apart as motile, mesenchymal cells from the postmitotic, epithelial adult enterocyte precursors. Pupal pISCs perform 2-3 rounds of parasynchronous divisions which initially merely increase their own number. Around the mid-pupal phase, *pros* and N become active in the pISC population as a result of Wg signaling, likely originating from the visceral musculature. *Pros* prompts pISCs to abrogate proliferation and differentiate as endocrine cells; activity of N restricts *pros* expression among pISCs. The balance between *pros* and N activity determines the ratio of pISCs versus endocrine cells: following loss of *pros*, all cells develop as pISCs; loss of N results in all cells expressing an endocrine fate. Our results suggest that the relative activity of N vs *pros* represents a developmental switch that acts at the level of the pISC to decide between continued proliferation and endocrine differentiation.

MATERIALS AND METHODS

Fly stocks and maintenance

Fly lines used in this study were: *OregonR*^{w1118}, *UAS-myr-mRFP*, *UAS-mCD8GFP*, *UAS-flp, Act5C promoter-FRT-phl[+]-FRT-lacZ.nls* (*Act5C >stop>lacZ*), *UAS*-dominant negative TCF (*UAS-dnTCF*), *UAS-cdc2RNAi* (on 3rd chromosome), *UAS-DlRNAi* (on 3rd chromosome), *UAS-prosRNAi*, *24B(How)-Gal4* (all provided by the Bloomington Stock Center), *UAS-arm*^{S10}, *esg-Gal4* (the National Institute of Genetics, Mishima, Japan), *UAS-cdc2RNAi* (on 2nd chromosome), *UAS-DlRNAi* (on 2nd chromosome) (the Vienna Drosophila RNAi Center), *Gbe*$^{+}$*Su(H)-lacZ* (Furriols and Bray, 2001), *10XStat92E-GFP* (Bach et al. 2007), *UAS*-dominant negative Notch (*UAS-N*^{DN}), and *UAS-N*^{intra} (both provided by Dr. Utpal Banerjee). Flies were maintained with normal fly food at room temperature or in incubators set at 25°C or 18°C. In some experimental conditions, flies were transferred to the temperature at 29°C to suppress the function of *Gal80*^{ts}. Heat-shock was provided at 37°C variable lengths of time. MARCM clones (Lee and Luo, 2001) of pISC lineages were generated with the constructs *hsflp/+; FRTG13, UAS-mCD8GFP/FRTG13, tub-GAL80; tub-Gal4/+*, providing a heatpulse of 20-30min during the first hours following puparium formation.

Immunohistochemistry

Antibody and in situ staining was performed as described previously (Ashburner, 1989; Takashima et al., 2011). A digoxygenin-labeled RNA probe prepared against Wnt4 was used. Antibodies used were (dilutions in parentheses): mouse antibodies against armadillo (arm, 1:10), Delta (Dl, 1:10), discs large (dlg, 1:10), Fasciclin III (FasIII, 1;20), prospero (pros, 1:50) (all obtained from the Developmental Studies Hybridoma Bank, University of Iowa), □-galactosidase (□-gal, 1:100) (Promega, Madison, WI), rabbit antibodies against atypical protein

kinase C (aPKC, 1:200), FMRF-amide (1:500; Thermo Fisher Scientific, Waltham, MA), pdm-1 (1:1000; Yeo et al. 1995), Tachykinin (1:2000; a gift from Dr. Dick Nässel), goat secondary antibodies against mouse IgG labelled Alexa488 (1:100), mouse IgG Alexa 546 (1:300), rabbit IgG Alexa488 (1:100) (Life Technologies); rabbit Cy3 (1:200) (Jackson Immunoresearch, West Grove, PA).

Lineage trace experiments and mitotic clones

To trace the lineage of pISCs in normal condition, flies with genotype of *tub-Gal80ts/+; esg-Gal4 UAS-myr-mRFP/UAS-flp; Act5C>stop>lacZ/+* were used. In the case of the tracing lineage with a gene over-expression or down-regulation, one of the wild-type chromosomes (indicated as "+") was replaced with an UAS-harboring chromosome by crossing. Pupae raised at 18°C were transferred to 29^{o}C to inactivate Gal80ts repressor resulting in an elimination of a "Stop cassette" on the *Act5C>stop>lacZ* transgene by an UAS-driven flipase to permanently label the cells of the pISC lineage.

For mitotic (MARCM) clones we used progeny with the genotype *hsflp/+; FRTG13, UAS-mCD8GFP/FRTG13, tub-GAL80; tub-Gal4/+*. Clones were induced during the late third instar by heat-shocking at 38°C for 30 minutes to 1 hour.

BrdU incorporation assay

Labeling proliferative cells with BrdU was performed by injecting BrdU solution into pupa. After the pupal case was removed, the animal was injected with 20microL to 30microL of BrdU solution (approx. 1mg/mL; saturated in distilled water; Sigma, St Louis). After a given time interval, guts were dissected and fixed, treated with 2N HCl for 30 min on ice, and then processed for antibody staining.

Muscle ablation

To remove the visceral muscle during metamorphosis, female flies with genotypes *UAS-his UAS-rpr/(+ X-chromosome)*; *tub-Gal80^{ts}/(+, stat92E-GFP, or esg-GFP); 24B(How)-Gal4/+* (the latter expressed in muscle cells; Fyrberg et al., 1997) were used. Flies were grown until the beginning of metamorphosis at 18°C, then transferred to 29°C at varying pupal stages for a duration of 48 hours to deactive the Gal80^{ts} repressor in order to allow time for complete muscle deletion under the control of hid/rpr capsase mediated apoptosis. Controls for these experiments were grown under the same conditions, but were males without an affected X chromosome. When grown at 18°C growth developmental age is assumed to be about half that of normal development.

RESULTS

ISCs emerge at the beginning of gut metamorphosis

In the late larva, adult midgut progenitors form clusters ("islands" or "nests") of *esg*-positive, undifferentiated cells which are scattered over the basal surface of the larval midgut. Theses clusters split into two populations, the peripheral cells, which form a transient pupal midgut, and central cells, which give rise to the adult midgut, including its stem cell population (Mathur et al., 2010; Takashima et al., 2011). During the first hours after onset of metamorphosis, central cells undergo a mesenchymal to epithelial transition and start expressing a differentiation marker, Pdm-1 (Affolter et al., 1993; Fig. 1A-A''). Other markers that reflect the emerging polarization of the midgut epithelial cells are Fasciclin III (FasIII, Woods et al., 1997; Fig. 1B-B"), aPKC (Wodarz et al., 2000; Fig. 1C), and discs-large (Dlg; Woods and Bryant, 1991; Fig. 1D), all forming part of the junctional complex located near the apical pole of the midgut cells. *esg* initially remains expressed ubiquitously in these midgut epithelial cells, but soon becomes downregulated.

Presumptive intestinal stem cells (pISCs) can first be recognized by their failure to express Pdm-1 and continued high levels of *esg* (Fig. 1A', A''). These cells do not become an integral part of the adult midgut epithelium; they do not contact the luminal surface, and do not express apical markers like FasIII, Dlg and aPKC (Fig. 1A', B, C, D, H). Armadillo/□-catenin, expressed in a polarized manner around the basal pole of differentiated midgut cells, is found throughout the cytoplasm of pISCs (Fig. 1E). Electron microscopy confirms that pISCs do not contact the midgut lumen (Fig. 1F, G). During the pupal and into the adult phase, they remain as small, basal, mesenchymal cells that do not partake in the apical junctional complex formed in between enterocytes (Fig. 1H).

Pupal pISCs are motile cells undergoing several parasynchronous divisions

We speculated that pISCs should be motile cells because, following cell divisions, they move away from each other to evenly distribute over the midgut epithelium. To directly assess pISC motility we performed live imaging analyses of dissected pupal guts over periods of 10-20 hours. These studies confirmed that live pISCs, labeled by the expression of *esg-Gal4 UAS-mCD8GFP*, are multipolar, highly motile cells which rapidly extend and withdraw filopodia (Fig. 2A, B). Some pISCs move over distances of multiple cell diameters (Fig. 2B, C). Their filopodia can be frequently observed to touch neighboring pISCs (Fig. 2B, 160min). Live imaging also indicated that pISCs divide in a wave-like, parasynchronous fashion. Thus, during a 150min interval around 24 hours APF the large majority of pISCs captured in the frame shown in Fig. 2D doubled. Daughter cells initially stay in contact, but then move away from each other.

The injection of BrdU into staged pupae confirmed that the mitosis of pISCs, as well as endoreplication of differentiating enterocytes, occurs in parasynchronous waves. During the late larval stage until the first few hours after puparium formation, all midgut progenitors are mitotically active (data not shown). BrdU injections between 3 and 18h APF, followed by 4h intervals after which animals were fixed and dissected, did not result in any labeling of the cells of the midgut. By contrast, injections around 24 hours APF labeled most pISCs (Supplementary Fig. S1A-C). A second wave of pISC mitosis takes place approximately 48 hours APF (Fig. S1G-I); a third wave, which may not affect every pISC, occurs in the late pupa, around 72 hours APF (not shown). Applying BrdU in the intervals in between these time points (Fig. S1D, E, F, J) did not result in labeling of pISCs. Differentiating Pdm-1-positive enterocytes do not divide, but undergo a few rounds of endoreplication. Two waves affecting most, if not all, enterocytes

take place around 6 hour and 43 hours APF (Fig. S1E, F), where BrdU injection left pISCs unlabeled, but stained most enterocytes. Another wave affecting only the middle segment of the midgut takes place around 67 hours APF (Fig. S1K, L).

Pupal pISC proliferation augments the number of stem cells and generates endocrine cells, but no enterocytes

To identify the cell types that the pISCs produce during different developmental time points, their lineage was examined by a flip out-mediated cell labelling technique (see Materials and Methods). Flies of the genotype *esg-Gal4 UAS-mRFP tub-Gal80ts; UAS-flp Act5c>stop>lacZ* were initially kept at 18^{o}C to inactivate the Gal4-UAS system, thus leaving cells unlabeled. They were then transferred to 29^{o}C upon reaching a particular developmental stage and remained at that temperature until dissection and analysis. The flip out event stimulated under the non-permissive termperature enabled cells to permanently activate the lacZ lineage reporter in *esg*-expressing pISCs and their progeny. Between 24 hours and 48 hours APF, lineage traced cells are restricted to the Esg-positive pISC population (Fig. 3A). Pros-positive endocrine precursors start to appear after the second pISC division, between 48 hour and 72 hours APF (Fig. 3B, D, E). We confirmed this finding by a clonal analysis (see Materials and Methods). The GFP labeled clones induced at the onset of metamorphosis and fixed around 72 hours APF had an average of approximately 5 small, subepithelial cells (pISCs or endocrine cells), half of which expressed Pros (Fig. 3E). None of the clones contained enterocytes. Enterocytes, recognizable by their large size and lack of *esg* and Pros expression, were labeled for the first time by lineage analysis shortly after eclosion (Fig. 3C, D, F). At this stage, the GFP clones averaged approximately 8

cells (Fig. 3F), supporting the idea that most pISCs undergo one more round of division in the late pupa.

After production from pISCs, many, if not all Pros-positive endocrine precursors still undergo at least one cell division before becoming postmitotic. Pros starts to be expressed around 50-60h APF in a small sub-population of *esg*-positive pISCs (Fig.S2B; Takashima et al., 2011). At this stage, all of the Pros-positive cells also express *esg*. By 72 hours APF, most Pros-positive cells have lost *esg* expression (Fig. S2C). Pulses of BrdU labeling between 54 hour and 72 hours APF yielded multiple BrdU/Pros-double positive cells, which typically form pairs of closely spaced cells (Fig. S2D, E). In some cases, BrdU signal could be seen in cells expressing both *esg* and Pros. These findings suggest that after 54 hours APF, a subset of pISCs turn on *pros*; subsequently, they lose *esg* during/after undergoing their final mitosis.

Prospero **is required in pISCs to adopt an endocrine fate**

What mechanism accounts for the changing compositon of pISC lineages during pupal development? We first focused on the gene *prospero,* which represents the earliest marker for midgut endocrine cell fate; it is expressed in pISCs while they are still *esg*-positive (see above). Reducing *pros* function by *esg*-Gal4-driven *pros*-RNAi (*esg-Gal4 UAS-mRFP/+; tub-Gal80ts/UAS-prosRNAi*) from 24 hour to 72 hours APF results in the loss of endocrine cells (Fig. 4A, B). At the same time, the number of *esg*-positive cells is significantly increased. Thus, in late pupal/early adult midguts of wild type flies, the ratio of *esg*-positive stem cells to *esg*-negative enterocytes is 22.1%; in *pros*-RNAi midguts it is 45.9% (Fig. 4H). Lineage tracing pISCs in the *pros*-RNAi background (*esg-Gal4 UAS-mRFP tub-Gal80ts/+; UAS-flp Act5c>stop>lacZ/UAS-*

prosRNAi) confirms that all early pISCs, labeled by the expression of *esg*-lacZ lineage reporter, develop as pISCs in late pupal midguts (Fig. 4B, inset). These findings indicate that Pros inhibits both *esg* expression and the continuation of mitosis: pISCs that would normally turn on *pros*, lose *esg*, and stop dividing, maintain *esg* and continue to proliferate in *pros*-RNAi flies.

To investigate the role of mitosis in triggering *pros* expression, pISC division was blocked by driving a *cdc2*-RNAi construct using *esg*-Gal4 (*esg-Gal4 UAS-mRFP/+; tub-Gal80ts/UAS-cdc2RNAi*). *cdc2-RNAi* was expressed starting at 12 hours APF, and pupae fixed at various time points (48, 60, 72, 78, and 96 hours APF) were assayed for expression of *esg* and *pros* (Fig. 4G, G'). At all time points the fraction of *esg*-positive pISCs was less than 10% (Fig. 4H). Significantly, all pISCs were Pros-positive (Fig. 4G, G', H), indicating that the expression of *pros* and subsequent endocrine development is the default fate of pISCs and is independent of cell division.

Regulation of Prospero by Notch signaling

The first appearance of endocrine cells is tied to the expression of *pros*. How is *pros* expression controlled in the pupa? It was shown previously that Delta-Notch signaling is active in the adult and pupal midgut to control the number of endocrine cells (Ohlstein and Spradling, 2006; Micchelli and Perrimon, 2006; Takashima et al., 2011). Delta expression begins in a subpopulation of pISCs around 50-60 hours APF (Fig. 5A) and increases during later pupal stages. Notch activity, monitored by a N signal reporter, *Gbe*$^{+}$*Su(H)-lacZ*, can be first detected at around 72 hours APF in a subset of mostly Pros-negative pISCs (Fig. 5B-D). To investigate the interaction between N signaling and *pros* in the developing midgut, we reduced N activity by

esg-Gal4 driven *Dl*-RNAi (*esg-Gal4 UAS-mRFP/+; tub-Gal80^{ts}/UAS-DlRNAi* or *esg-Gal4 UAS-mRFP/UAS-DlRNAi; tub-Gal80^{ts}/+*) and a dominant negative form of N (N^{DN}) (*esg-Gal4 UAS-mRFP/+; tub-Gal80ts/UAS-N^{DN}*) from 24 hours APF to 72 hours APF or to 96 hours APF (eclosion). Reduction of N activity in pupal pISCs resulted in a strong increase in the number of Pros-positive cells, and a loss of *esg* expression (Fig. 5E-H). In 72 hour *esg*-Gal4>*Dl*-RNAi pupae, we counted 52% *pros*+ cells, compared to 16% in wild type controls (Fig. 5E, F, K). Few or none of these cells also expressed *esg*, supporting the notion that *pros* inhibits *esg*. Counts at 96 hours APF yielded 34% Pros-positive cells (Fig.5I, J, K), which indicates that after turning on Pros, cells cease to divide; the reduced fraction of Pros-positive cells compared to 72 hour samples is likely due to the sequestration of cells into the lumen, followed by cell death.

Aside from suppressing *pros* in pISCs, N activity also slows down proliferation in these cells. At 48 hours APF, no numerical difference in the fraction of pISCs between wild-type and *N* or *Dl* knock-down could be detected (Fig. 5K). However, at 72hAPF, the sum total of pISCs and their endocrine progeny amounts to 34% (of all gut cells) in wild-type, and 52% in *Dl*-RNAi flies (Fig. 5K), indicating that pISCs perform an average of at least two divisions between P48 and P72, whereas in wt, these cells only undergo only one division (see above).

Wingless activity is required for *prospero* expression in pISCs

Wg/Wnt activity promotes stem cells in many systems, including the *Drosophila* intestine (Lin et al., 2008) and neurectoderm (Chu-LaGraff and Doe, 1993). To investigate the possibility that Wg turns on the proendocrine gene *pros* in the pISCs we expressed a dominant negative form of TCF (van de Wetering et al., 1997) from 24 hours APF and assayed for *esg* and *pros* expression

in 72 hour pupae and freshly eclosed adults (Fig. 6). Reduced Wg activity resulted in a phenotype opposite to the one observed for blocking N or Dl: the number of *esg*-positive cells was decreased (11.3%, compared to 20.7% in wild-type), and *pros* expression was completely absent (Fig. 6A, B). Expressing a constitutive active form of armadillo protein, Arm^{S10}, which activates Wg target genes in the absence of Wg signal (Pai et al., 1997), did not cause a change in the number of *esg*-positive or Pros-positive cells (Fig. 6C), indicating that Wg activity is necessary, but not sufficient, to promote pISC proliferation and trigger *pros* expression. To test the genetic relationship between Wg and N in pupal pISCs, *dnTCF* and *DlRNAi* were expressed concomitantly (*esg-Gal4 UAS-mRFP/UAS-DlRNAi; tub-Gal80^{ts}/UAS-dnTCF*). This experiment, similar to blocking Wg alone, resulted in the absence of Pros-positive cells (Fig.5E). We conclude that only after Wg has triggered *pros* in the pISC pool does the N pathway act on this pool to restrict the number of cells that end up as *pros*-positive endocrine cells.

It has been suggested that, in the adult midgut, the visceral muscles represent the source of the Wg signal (Lin et al., 2008). In the larva and early pupapupa, Wg (detected by antibody or the Wg-lacZ reporter) is restricted to a narrow band at the midgut-hindgut boundary (Fig. 6G, H); from mid-pupal stages onward, Wg signal also appears in visceral muscle cells flanking the middle segment of the midgut (Fig. 6I). Another member of the Wnt family, DWnt-4, is expressed in a widespread manner in the visceral musculature (Fig. 6F).

A role for visceral muscle in supplying signals regulating N and Pros

Given that a likely source for signals acting on the pISCs is the visceral musculature, we hypothesized that the dynamically changing lineages produced by pupal pISCs might be due to

the metamorphic reorganization of the visceral musculature. Previous reports (Klapper, 2001) and our own analysis (Aghajanian et al., 2014) show that the adult visceral musculature is derived from larval visceral muscle cells. During the first 24h of metamorphosis, the larval visceral musculature de-differentiates; myofibrils and extracellular matrix is lost (Fig. 7A P24), even though the muscle cells survive. Around 30-40 hours APF these cells re-differentiate into adult visceral muscle (Fig. 7A P36, P72). The stage when muscle re-differentiates coincides with the time when detectable levels of Dl appear in pISCs, and when pISCs start producing endocrine cells (see above).

We used a muscle-specific driver line, how (24B)-Gal4 (Fyrberg et al., 1997; Jiang and Edgar, 2009) and tub-Gal80ts to simultaneously drive apoptosis promoting genes, *hid* and *reaper* (*rpr*) and thereby kill visceral musculature in a time-specific manner. By using phalloidin and a nuclear marker to monitor for the presence of myofibrils and muscle nuclei, respectively, we observed that the activation of *hid* and *rpr* at 24hAPF effectively ablated muscle cells (Fig. 7B, C). In pupae fixed at approximately 72h APF (corrected for accelerated development at increased temperatures), the lack of visceral muscles caused a significant reduction in the number of *Pros*-positive endocrine cells (Fig.7D, E). Taken together, these data suggest a model whereby signals (including Wg/Wnt4) stimulating pISC proliferation, *pros* expression, and Notch activity during pupal development originate from the visceral muscle. As the visceral muscle re-differentiates into its adult state, these signals gradually build up. Consequently, at low/intermediate levels of Notch activity reached at around mid pupal stages, cells of the pISC lineage first begin to differentiate as endocrine cells. High levels of Notch activity, required to push stem cells towards the enterocyte fate, are not reached until around the time of adult eclosion.

DISCUSSION

Notch activity and the balance between enterocytes, endocrine/secretory cells, and proliferating stem cells

The genetic control of intestinal stem cell proliferation and differentiation shows a high degree of conservation among the model systems studied, including mouse, chicken, *Xenopus*, zebrafish, and *Drosophila* (Takashima et al., 2013). Still, a number of fundamental issues remain unresolved. In the mammalian gut, two types of pluripotent stem cells (Tian et al., 2011) are distinguished from a population of committed, rapidly proliferating "amplifying progenitors". Based on loss and gain of function experiments, Notch activity appears to control proliferation of both stem cells and amplifying progenitors: loss of N signaling causes the absence of cell division in both populations, and the conversion of all cells into secretory gland/endocrine cells (Stamataki et al., 2011). Increased N activity promotes proliferation (Fre et al., 2005), presumably also in both stem cells and amplifying progenitors, although this distinction has not been made explicit in the literature. Heightened N activity appears to be detrimental to enterocyte terminal differentiation, as evidenced by the ultrastructural analysis of Fre et al. (2005). In the *Drosophila* adult midgut, increased N activity seems to have the opposite effect as in vertebrates: it inhibits stem cell proliferation, and drives stem cells to terminally differentiate as enterocytes (Wang and Hou, 2010; Jiang and Edgar, 2011; Micchelli, 2012). Does N activity control two different networks of genes in flies and vertebrates?

Another feature that appears to be different in the vertebrate vs *Drosophila* ISC system concerns the sequence in which the decisions between (1) continued proliferation vs cell cycle exit, and (2) enterocyte vs secretory/endocrine cell take place. For the *Drosophila* adult midgut,

it was proposed that these two decisions are made in two steps, and are both dependent on N activity (reviewed in Wilson and Kotton, 2008; Luchetta and Ohlstein, 2012). The model is based upon the assumption that ISCs divide according to the same, simple pattern, into a renewed ISC and a postmitotic enteroblast. ISCs express the N ligand Dl. Following each division, one of the daughter cells loses Dl, and at the same time, is induced by its Dl-positive sibling turn on N activity. The Dl-positive cell then enters the next cell cycle, continuing its role as an ISC. The Dl-negative/Su(H)-positive enteroblast faces the choice between enterocyte and endocrine cell. Again, N-activity plays a decisive role: a high level of N in the enteroblast promotes the enterocyte fate; a low level the endocrine fate. In contrast to this model, a one step mechanism of N-dependent fate determination appears to operate in vertebrates. Thus, based on the available evidence, ISCs, or amplifying progenitors, or both, "decide" in a N-dependent manner between continued proliferation and the secretory/endocrine fate. How can one resolve these apparent differences between the *Drosophila* and mammalian ISC systems?

The role of N in pupal and adult pISC lineages

One significant difference between pupal and adult ISC lineages in *Drosophila* is the complete lack of enterocytes from the former. During their first round of division, pISCs simply double their own number; none of the daughter cells show any sign of differentiation. Around the second division, between 48 and 60 hours APF, we see the appearance of *pros* and *ase* in a subset of pISCs. Initially (around 54 hours APF), all pISCs, including the *pros*-positive ones, still express the marker *esg*; a short time later (72 hours), *pros*-positive cells turn off *esg*. If N activity is inhibited during this phase, all pISCs turn on *pros*, and loose *esg*. These findings imply a N-dependent mechanism whereby, similar to the scenario in the mammalian crypt, stem cells

decide between continued proliferation on the one hand, and a postmitotic, endocrine/secretory fate on the other hand. Can one reconcile this proposal, where we detect a good correspondence between the *Drosophila* pupal pISCs and mammalian ISCs, with the two step model (ISC>enteroblast>endocrine cell or enterocyte) that has been suggested for the adult fly midgut?

One important argument for the adult model was the finding that ISC clones lacking N activity possess a strongly increased number of undifferentiated ISCs (Ohlstein and Spradling, 2006; Micchelli and Perrimon, 2006). This would support the idea that the initial N-dependent step is to decide between continued proliferation (ISC) and cell cycle exit (enteroblast). According to the same studies, clones persistently also contained a strongly increased fraction of *pros*-positive endocrine cells, or were entirely composed of these cells, but these findings were interpreted as an effect of perdurance: if one of the daughter cells of the ISC in which the N gene was eliminated still inherited a certain level of N protein, it might still enter the enteroblast stage, in which *pros* might be turned on, even though this daughter cell (like its completely N-negative signaling) continued to proliferate. This then would lead to mixed clones with strongly enhanced cell number, of which one fraction was also *pros*-positive. However, there are alternative explanations for the N-negative clones that were composed entirely, or partially, of *pros*-negative cells. Recent findings suggest that local "insults" to the midgut, typically coupled with oxidative stress, activate signaling pathways; among them Hippo and Wg (Poernbacher et al., 2012; Cordero et al., 2012), which strongly promote ISC proliferation. Removal of N from an ISC might just represent such an insult. In that scenario, several activated pathways will impinge on the ISC, and cause tumorous overproliferation. Lack of N per se may cause a (moderate) overproliferation, as also observed in the pupa, but the main effect will be the de-repression of *pros*. This would explain why the number of *pros*-positive cells in adult midgut N-mutant clones

is strongly elevated. The fact that in addition to the many *pros*-positive cells there are also many *pros*-negative cells could be attributed to the fact that the onset of *pros* expression in cells of the growing "tumor" cannot keep up with the proliferation driven by other pathways.

Another possible explanation for the diversity of clones resulting from removing N-activity in adult ISCs may lie in the fact that ISC division in the adult midgut is far less homogenous than initially assumed. Thus, a recent clonal analysis (de Navascues et al., 2011) showed that only a fraction of ISCs divides in the "canonical" asymmetric manner, producing one Dl-positive and one Dl-negative daughter; in a substantial number of cases (which may also depend on the age of the midgut or availability of food; O'Brian et al., 2011) both daughter cells lacked Dl, or expressed, Dl. It is possible that the diversity of clone types resulting from removal of N is related to the diversity of division patterns among ISCs. For example, clones derived from an ISC that was about to undergo a division into two ISC daughters might develop into a "tumor" containing only *pros*-negative cells; clones derived from asymmetrically dividing ISCs might encompass predominantly *pros*-positive cells.

The reorganizing visceral musculature: a dynamic niche

Our findings suggest that the reorganization of the musculature during metamorphosis may explain the changing lineage of pISCs at different stages. Previous published findings had identified the visceral musculature of the adult midgut as a major source of "niche signals": Wingless and EGFR ligands (Lin et al., 2008; Jiang etn al., 2011; Xu et al., 2011; Biteau and Jasper, 2011) are expressed in the visceral musculature. In addition, differentiated enterocytes, as well as endocrine cells may emit signals that modulate the proliferation of ISCs. Here we have another similarity between fly and vertebrate system: the myofibroblasts underlying the crypt

epithelium have also been identified as one likely element of the ISC niche (Scoville et al., 2008; Yeung et al., 2011). Our finding that visceral muscle ablation in pupae strongly reduces pISCs and endocrine cells, in conjunction with the fact that Wg and Wnt4 are expressed in the visceral muscle, and when mutated also cause a reduction in both cell types, support the idea of a diffuse "visceral muscle niche" acting upon the pISCs. This then would represent a straightforward explanation for the changing proliferative behavior of pISCs during pupal development. Visceral muscle cells de-differentiate during the first day after puparium formation, "melting down" myofibrils, and losing their basement membrane covering (Aghajanian et al., 2014). We speculate that production/presentation of the "niche signal" acting upon pISCs diminishes during this time of muscle involution. From about 36h onward the muscle is rebuilt into its adult shape, and that may also be accompanied by niche signal re-appearance. Thus, from about 48h onward, signals (possibly among them Wg/Wnt4) stimulating Pros expression cause the appearance of endocrine cells. Other, unknown (but also possibly muscle related) signals responsible for the levels of N activity that drives ISCs towards the enterocyte pathway only appear around the time of eclosion.

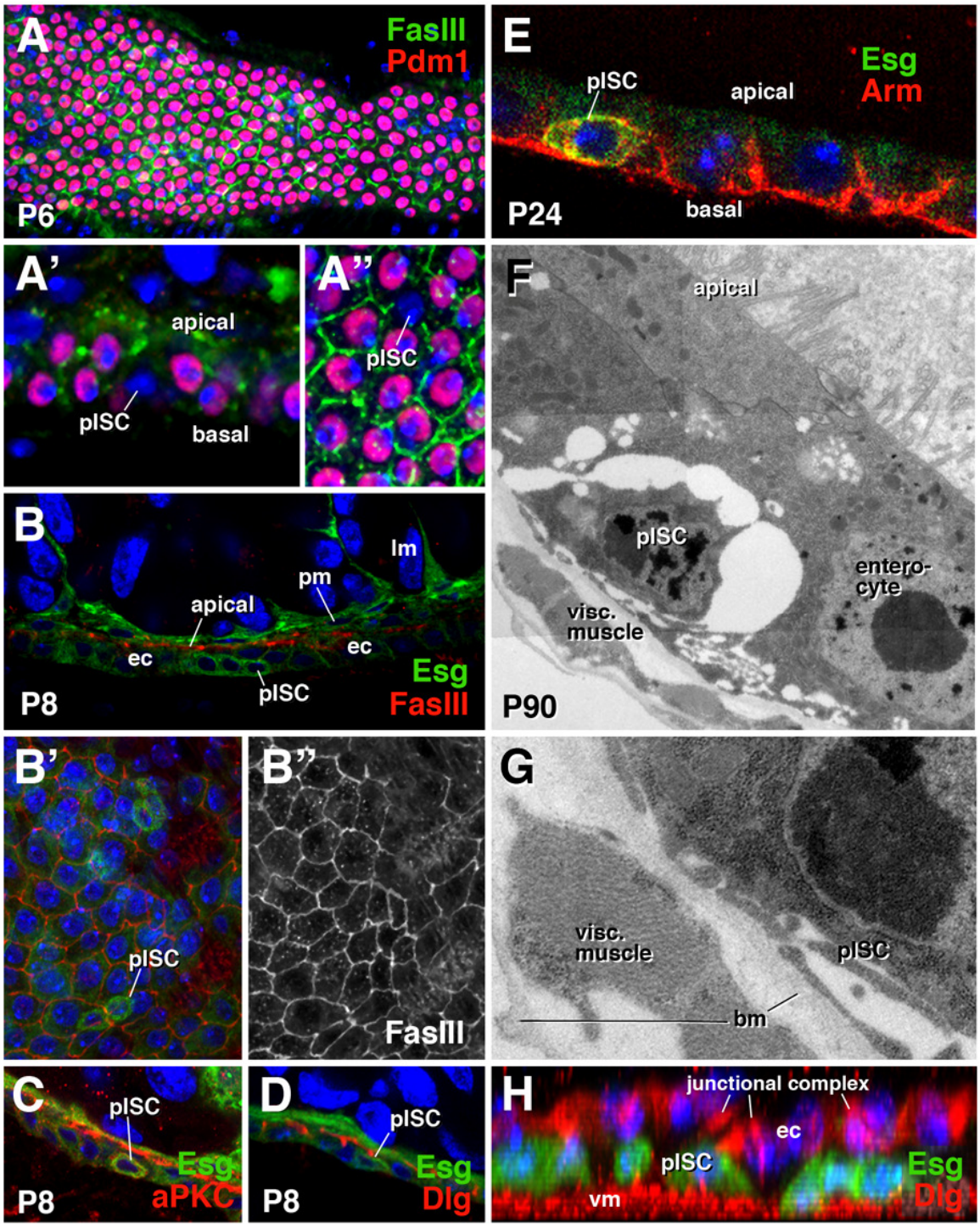
A
FasIII
Pdm1
P6
E
pISC
apical
Esg
Arm
P24
basal
A'
apical
pISC
basal
A''
pISC
F
apical
pISC
entero-
cyte
visc.
muscle
P90
B
lm
pm
apical
ec
ec
pISC
Esg
FasIII
P8
B'
pISC
B''
FasIII
G
visc.
muscle
pISC
bm
C
pISC
Esg
aPKC
P8
D
pISC
Esg
Dlg
P8
H
junctional complex
ec
pISC
Esg
Dlg
vm

Fig. 1. Origin of pISCs during early metamorphosis. **(A-E)** Z-projections of confocal sections displaying the pupal midgut at different stages of metamorphosis. At 6 hours APF (P6) adult midgut progenitors have formed a continuous epithelial layers of enterocytes (ec) expressing the nuclear marker Pdm-1 (red; **A-A''**) and the polarity marker FasIII (green). pISCs can be observed by their lack of Pdm-1 **(A-A'')** and FasIII **(A-A'')** expression. At 8 hours APF (P8) pISCs also do not express the apical markers FasIII (red) **(B-B')**, aPKC (red) **(C)**, Dlg (red) **(D)**, but do express high levels of *esg* (green) **(B-E)** and are located on the basal side of the midgut **(A')**. At 24 hours APF Armadillo/□-catenin (red) is localized on the basal pole of the midgut epithelium, but occurs throughout the cytoplasm in pISCs. **(F,G)** Electron micrographs of midguts at 90 hours APF (P90) displaying the localization of pISCs in between the basal membrane of enterocytes and the visceral muscle (vm) and basement membrane (bm). **(H)** Tilted z-projection of confocal section of adult midgut labeled with Dlg (red; apical marker of enterocytes, as well as visceral muscle) and Esg (ISCs). In the adult, as in the pupa, ISCs are mesenchymal cells located basal of the enterocyte epithelium, and are negative for Dlg. Nuclei are stained with TOTO-3 or TOPRO-3 (indicated in blue) in all confocal images. Abbreviations: bm, basement membrane; ec, enterocyte; lm, larval midgut; pm, pupal midgut; pISC, presumptive intestinal stem cell. Bars: 20μm **(A)**; 5μm **(A', A'')**, 10μm **(B-D, H)**; 2μm **(E)**; 1μm **(F)**; 0.25μm **(G)**

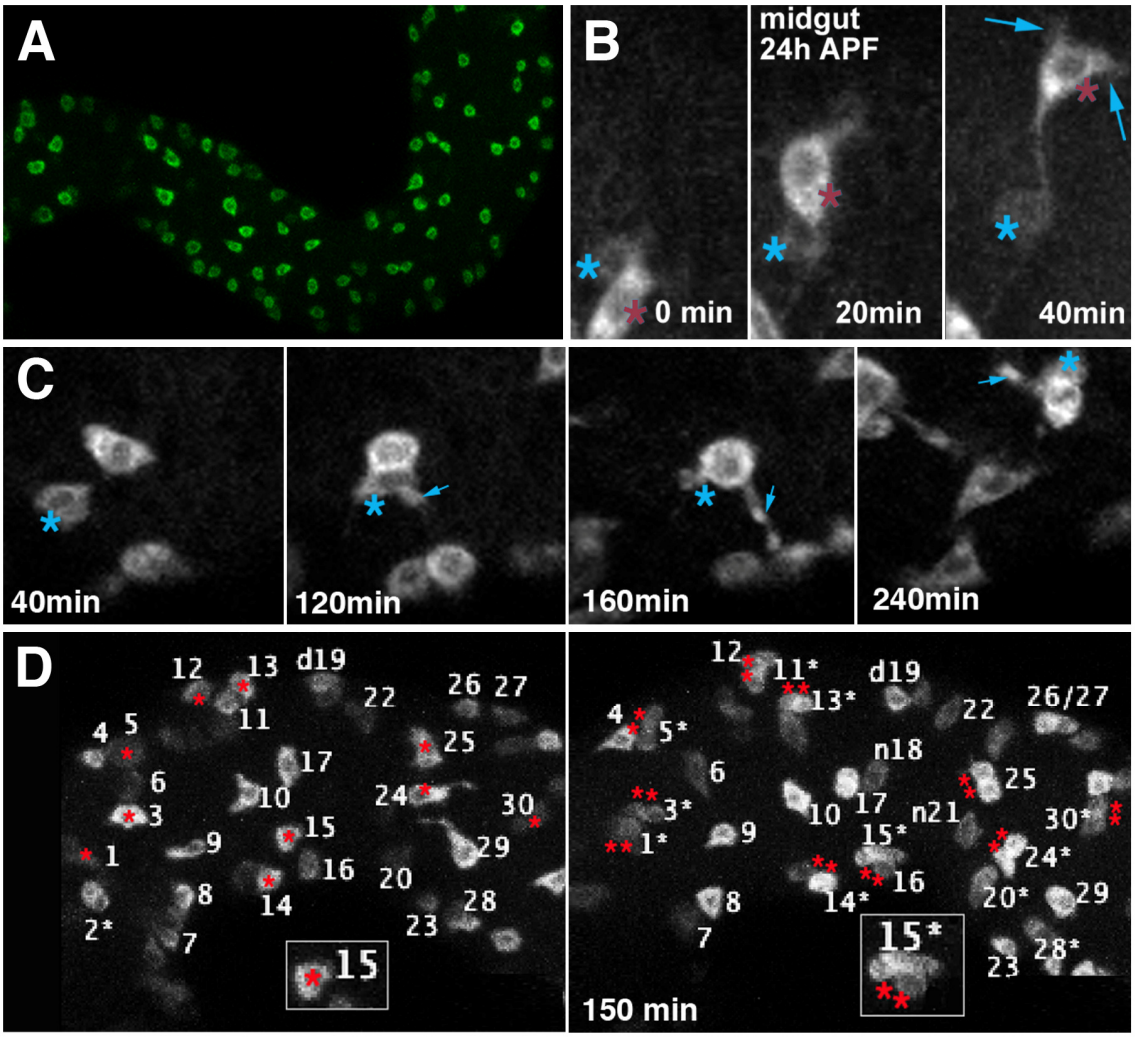

Fig. 2. pISCs migrate and divide during metamorphosis. Live confocal images of pupal midguts, pISCs visualized via *esg-mRFP*. **(A)** Pupal midgut around 20h APF; pISCs (green). **(B)** Three frames of a 40 minute live video of a pupal midgut around 20h APF., A single pISC (red asterisk) extends filopodia (arrows) and, within 40 minutes, migrates past an adjacent pISC (blue asterisk). **(C)** A migrating pISC (blue asterisk) extends and retracts its filipodia (arrow) to interact with neighboring cells. **(D)** pISCs divide in a parasynchronus fashion around P24. After a 150 minute period, cells 1, 3, 5, 11, 13, 14, 15, 24, 25, and 30 (initially denoted by a single red asterisk) divide to form cell doublets 1*, 3*, 5*, 11*, 13*, 14*, 15*, 24*, 25*, and 30* (each daughter is marked by a red asterisk; cell #15 framed). Bars: 20µm (A); 5µm (B, C); 10µm (D)

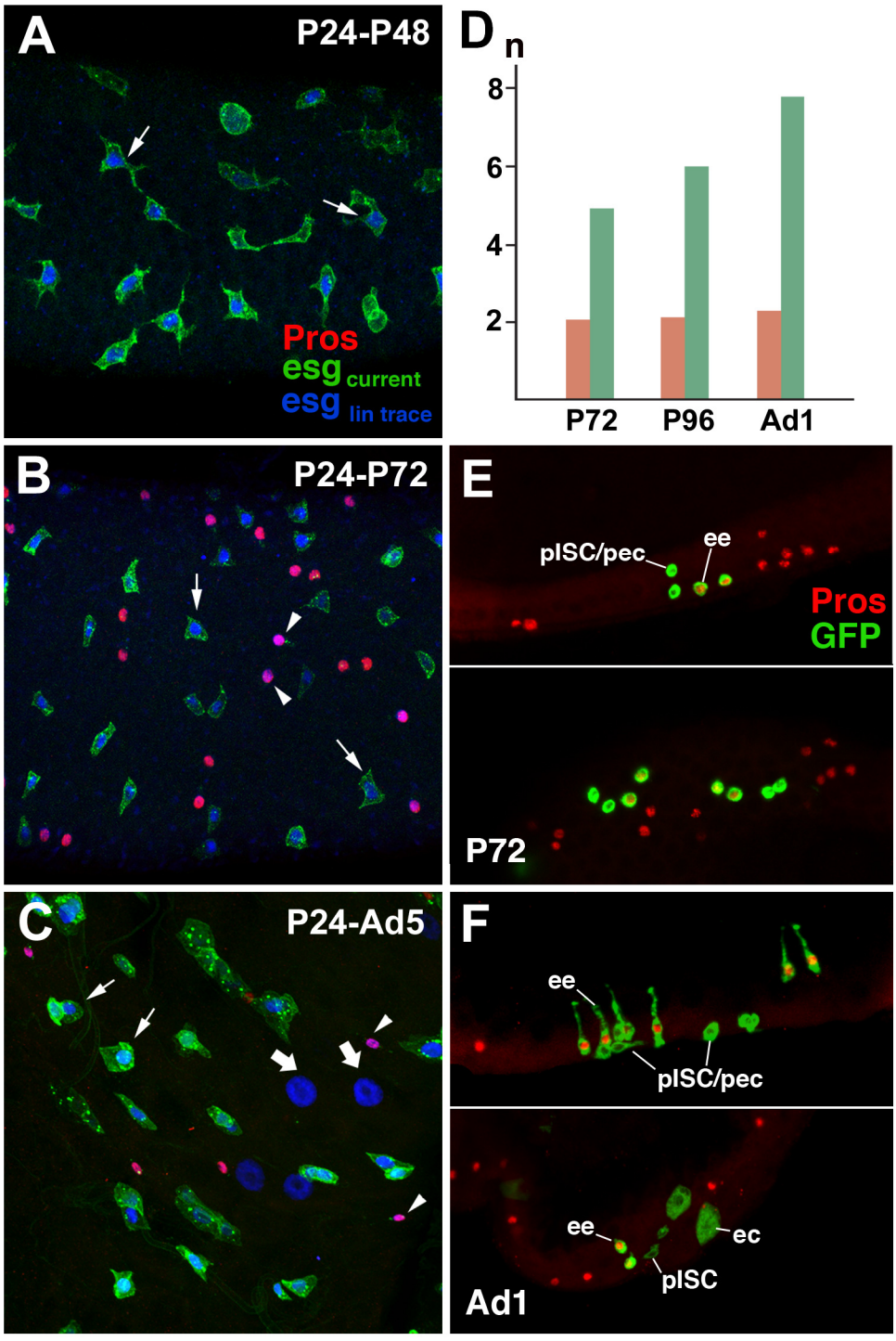
A
P24-P48
Pros
esg current
esg lin trace
B
P24-P72
C
P24-Ad5
D
n
8
6
4
2
P72
P96
Ad1
E
pISC/pec
ee
Pros
GFP
P72
F
ee
pISC/pec
ee
ec
pISC
Ad1

Fig. 3. Lineages of pISC change during metamorphosis. (A-C) Lineage trace analyses using a *tub-Gal80^{ts}* controlled *esg-Gal4 driving UAS-flp Act5C>stop>lacZ*. LacZ expression (lineage) is indicated in blue. **(A)** Lineage tracing activated at early metamorphosis shows no Pros-positive cells between P24-P48 (small arrows indicate pISCs). **(B)** Following the second division event around 72h APF, Pros-positive endocrine cells (red, arrow heads) can be seen beside undifferentiated pISCs (green). **(C)** Adult enterocytes (large arrows) are formed at early adult stages from pISC lineage as indicated by blue nuclei. **(D-F)** GFP-labeled MARCM clones descended from single pISCs, Clone induction around puparium formation. Histogram in (D) indicates average clone size (green bar) observed at P72, P96, and one day after eclosion (Ad1). Red bars indicate number of Pros-positive cells contained within one clone. (E) and (F) show representative clones at 72h APF (E; top panel: one clone; bottom panel: two neighboring clones) and one day after eclosion (F). At P72, most clones contain four cells, two of which are Pros-positive. Shortly after eclosion, clones have grown to an average of eight cells, but vary in size from six cells (bottom panel in (F) to more than 12 cells (top panel). In most clones, Pros-positive cells have differentiated into endocrine cells (ee), sending out characteristic apical processes towards the gut lumen (arrow in F). Among the Pros-negative cells are undifferentiated pISCs which continue to cycle, presumptive enterocytes (pec), as well as differentiated enterocytes (ec). Bars: 5µm (A-C); 10µm (E-F)

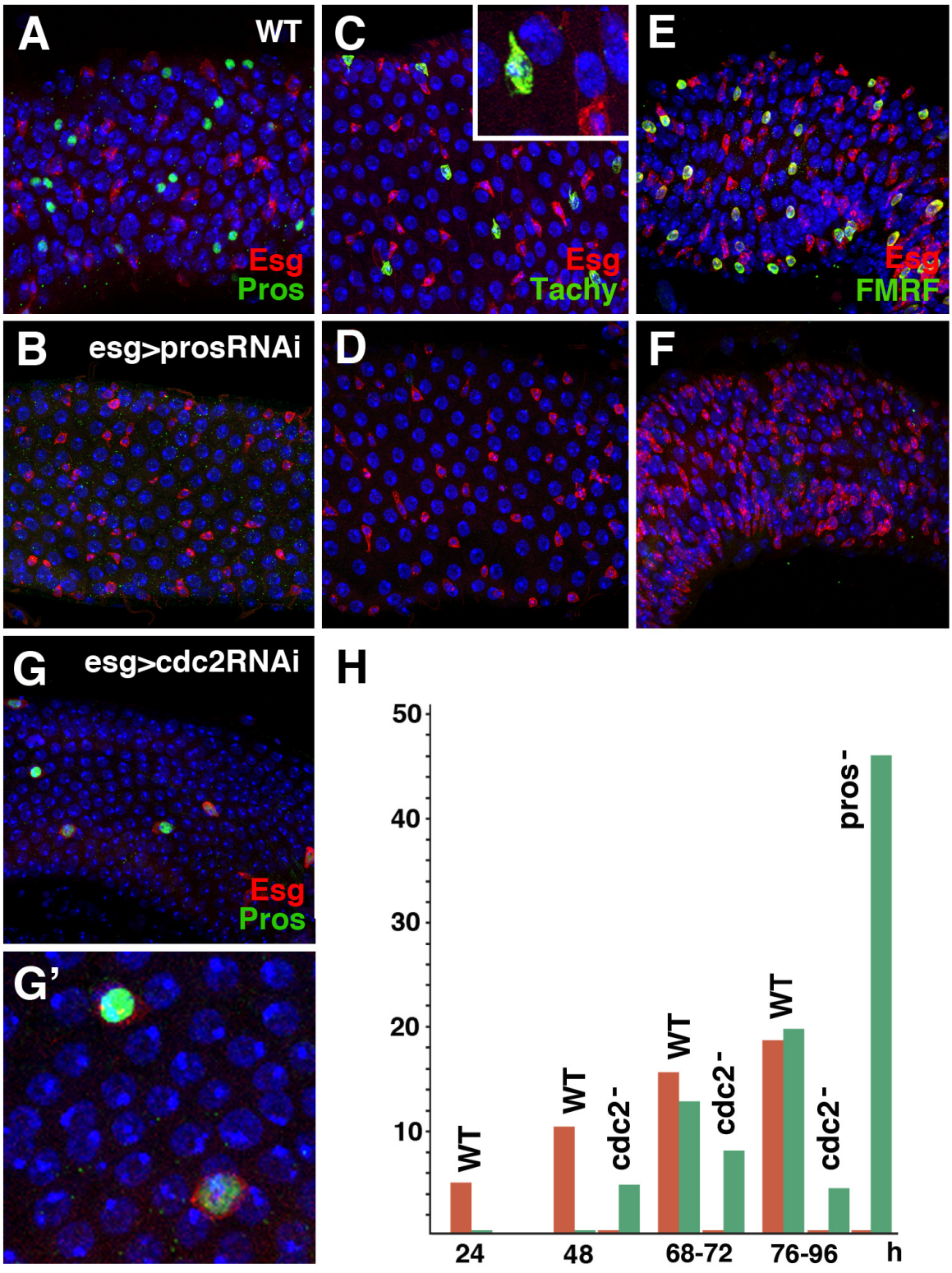
A
WT
Esg
Pros
C
Esg
Tachy
E
Esg
FMRF
B
esg>prosRNAi
D
F
G
esg>cdc2RNAi
Esg
Pros
G'
H
50
40
30
20
10
WT
WT
cdc2-
WT
cdc2-
WT
cdc2-
pros-
24
48
68-72
76-96
h

Fig. 4. Prospero, but not cell division is required for endocrine fate. (A-G) Z-projections of confocal sections of P96 pupal guts, showing the effect of knockdown of *prospero* (*esg*-Gal4>*pros*RNAi; A-F) and *cdc2* (*esg*-Gal4>*cdc2*RNAi (G, G') Histogram **(H)** visualizes fraction of pISCs (*esg*-positive) vs enterocytes (red bars) and endocrine cells (Pros-positive) vs enterocytes (green bars) in wild-type controls and experimental guts at different stages. **(A,C,E)** Wild-type control; inset in (C) shows enlarged Tachy-positive endocrine cell; **(B, D, F)** *prospero* knockdown. *Esg*-positive pISCs are shown in red; green label indicates expression of Prospero **(A, B)**, Tachykinin **(C, D)**, and FMRF **(E, F)**. Note increased fraction of *esg*-positive pISCs and absence of endocrine cells in *prospero* knockdown. Inset in (B) shows lineage traced *esg*-positive cells (esg-lacZ lineage marker, green, turned on before 24h APF) that all develop as esg-RFP-positive stem cells (red). **(G)** Pros (green) is still activated in *esg*-positive cells (red) that were mitotically arrested in pupa via *cdc2-RNAi*. **(G')** A high magnification image of **(G)**. Note large size of mitotically arrested pISC. Nuclei are stained with TOTO-3 or TOPRO-3 (indicated in blue) in all confocal images. Bars: 20μm (A-G); 5μm (G').

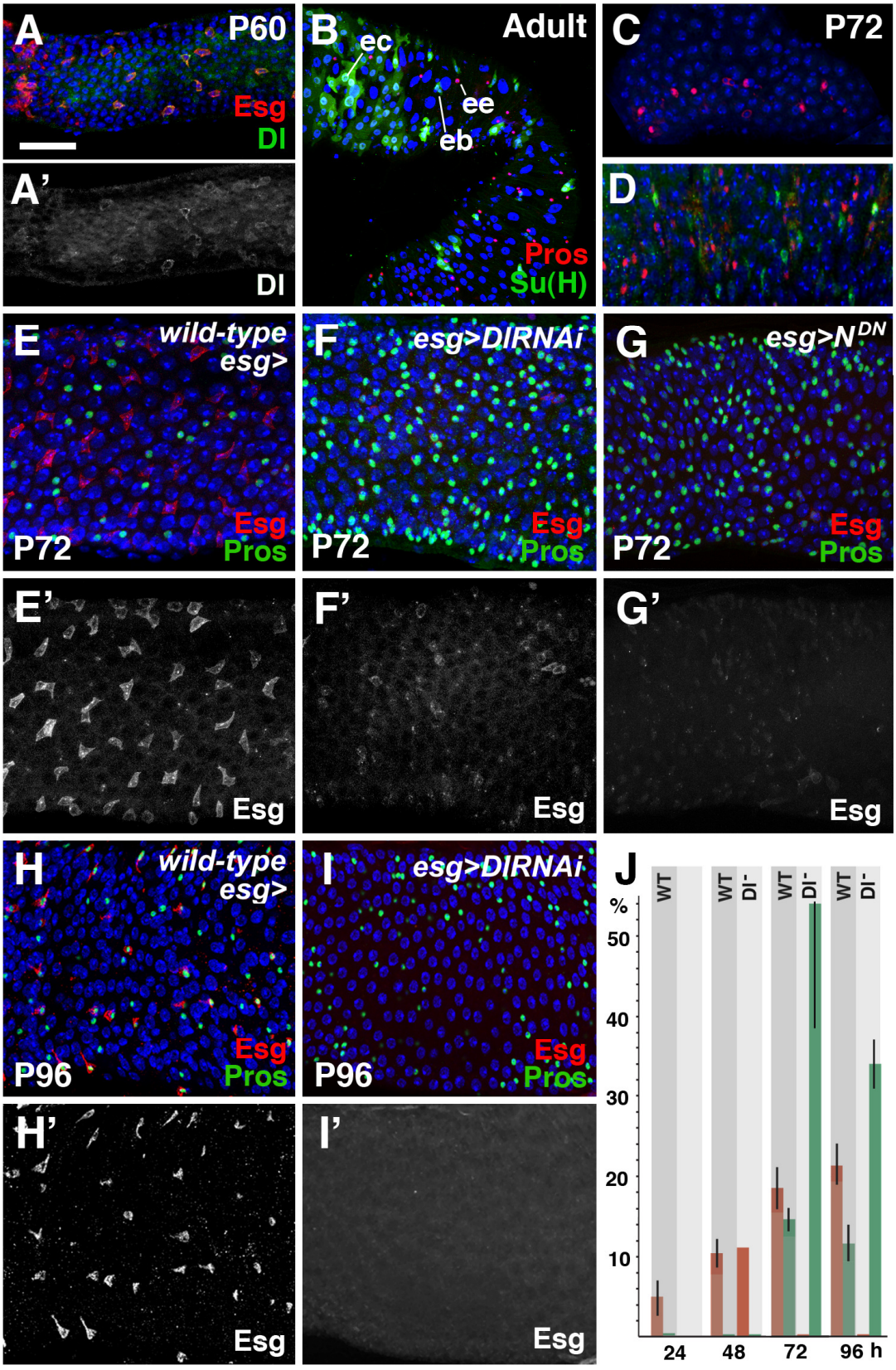
A
P60
Esg
Dl
A'
Dl
B
Adult
ec
ee
eb
Pros
Su(H)
C
P72
D
E
wild-type
esg>
Esg
Pros
P72
F
esg>DlRNAi
Esg
Pros
P72
G
esg>N^DN
Esg
Pros
P72
E'
Esg
F'
Esg
G'
Esg
H
wild-type
esg>
Esg
Pros
P96
I
esg>DlRNAi
Esg
Pros
P96
H'
Esg
I'
Esg
J
%
50
40
30
20
10
WT
Dl-
WT
Dl-
WT
Dl-
WT
Dl-
24
48
72
96 h

Fig. 5. Notch signaling is a regulator of endocrine differentiation and pISC self-renewal in the pupal midgut. (A, A') Dl (in situ probe) first appears around 60h APF in pISCs (A, A'). **(B-D)** Notch signaling pathway activity is monitored by the reporter *Gbe^{+}Su(H)-lacZ.* In the adult (B), this construct is expressed in the progeny of ISCs which undergo the transition towards enterocytes ("enteroblasts"; eb), as well as some mature enterocytes (ec), but no Pros-positive endocrine cells (ee). *Gbe^{+}Su(H)-lacZ* starts being expressed at low levels at around P72. In panel (C) laser intensity was adjusted to the same level used in B, resulting in no detectable signal for *Gbe^{+}Su(H)-lacZ*; laser intensity in D was increased, showing subset of pISCs and enterocytes positive for *Gbe^{+}Su(H)-lacZ*). Signal was generally, though not strictly, excluded from Pros-positive cells. **(E-J)** Knock down of the Notch pathway between 24h and 72h APF (F, F': *esg*-Gal4>*UAS-DlRNAi*; G-G': *esg*-Gal4>*UAS-N^{DN}*) increases the number of Pros-positive cells (green) while decreasing or eliminating the number of *esg*-positive pISCs. H-I') Following knock down of Notch activity between 24h and 96h APF number of Pros-positive cells does not further increase (compare F and I, as opposed to the wild-type control E and H, where Pros-positive and *esg*-positive cells increase between P72 and P96). Nuclei are stained with TOTO-3 or TOPRO-3 (indicated in blue) in all confocal images. **(J)** Histogram showing the ratio of *esg*-positive pISCs/ enterocytes (red bars) and Pros-positive endocrine cells/enterocytes (green bars) in the presence of Notch signaling (WT) or absence of Notch signaling. (Dl-). Bar: 20μm

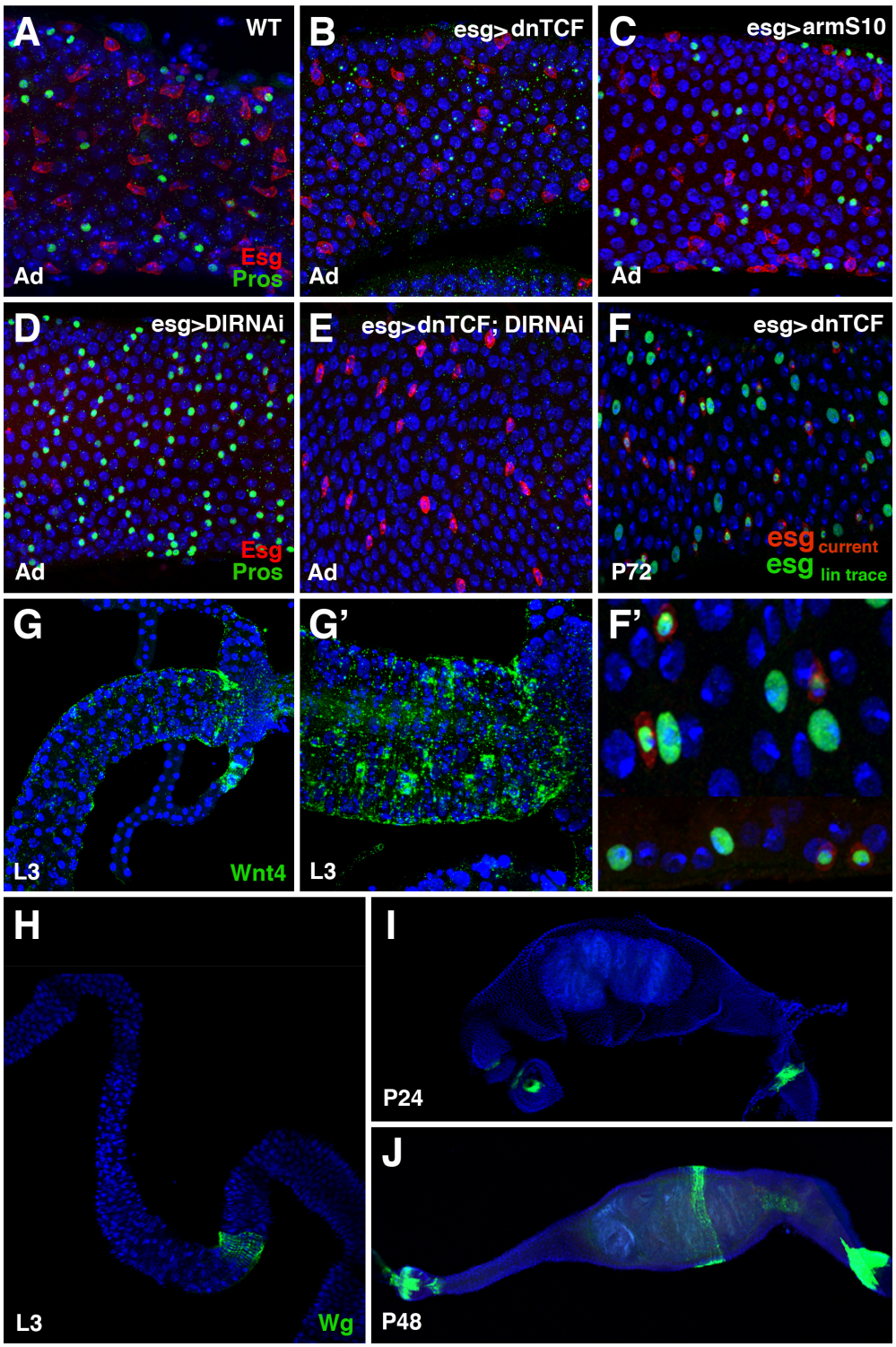
A
WT
Esg
Pros
Ad
B
esg>dnTCF
Ad
C
esg>armS10
Ad
D
esg>DIRNAi
Esg
Pros
Ad
E
esg>dnTCF; DIRNAi
Ad
F
esg>dnTCF
esg current
esg lin trace
P72
G
Wnt4
L3
G'
L3
F'
H
Wg
L3
I
P24
J
P48

Fig. 6. Wg controls endocrine fate by regulating Notch activity. (A-E) Z-projections of adult midguts (1 day post eclosion), showing effects of modified Wg or Dl expression. All constructs are under the control of *esg*-Gal4. **(A)** A wild type control. **(B)** Expression of dnTCF, an inhibitor of the Wg pathway, eliminates Pros expression (green) in pISCs **(C).** Constitutively active Wg signal induced in pISCs has no effect on the number of Pros-positive or *esg*-positive cells. **(D)** *Dl*RNAi greatly reduces *esg*-positive cells while increasing the number of Pros-positive cells as seen in Fig. 5. **(E)** Expression of *dnTCF* in conjunction with *Dl*RNAi results a similar phenotype to that one following *dnTCF* alone (see panel B). **(F,F')** Lineage tracing *esg*-positive pISCs expressing dnTCF between P12 and P72 shows that, in the absence of Wg signaling, pISCs develop as enterocytes (ec; arrows in F). **(G,G')** Expression of Wnt4 (in situ probe) in visceral muscle of L3 larva **(H-J)** Restricted expression of wg-lacZ reporter (green). In the larval gut (H) and early pupal gut (I), expression is confined to a narrow band of muscles anterior to the midgut-hindgut junction. Around mid-pupal stages **(J)** Wg is also expressed in the visceral muscle surrounding the central midgut. Nuclei are stained with TOTO-3 or TOPRO-3 (indicated in blue) in all confocal images. Bars: 20μm (A-F, G'); 50μm (G, H-J); 10μm (F').

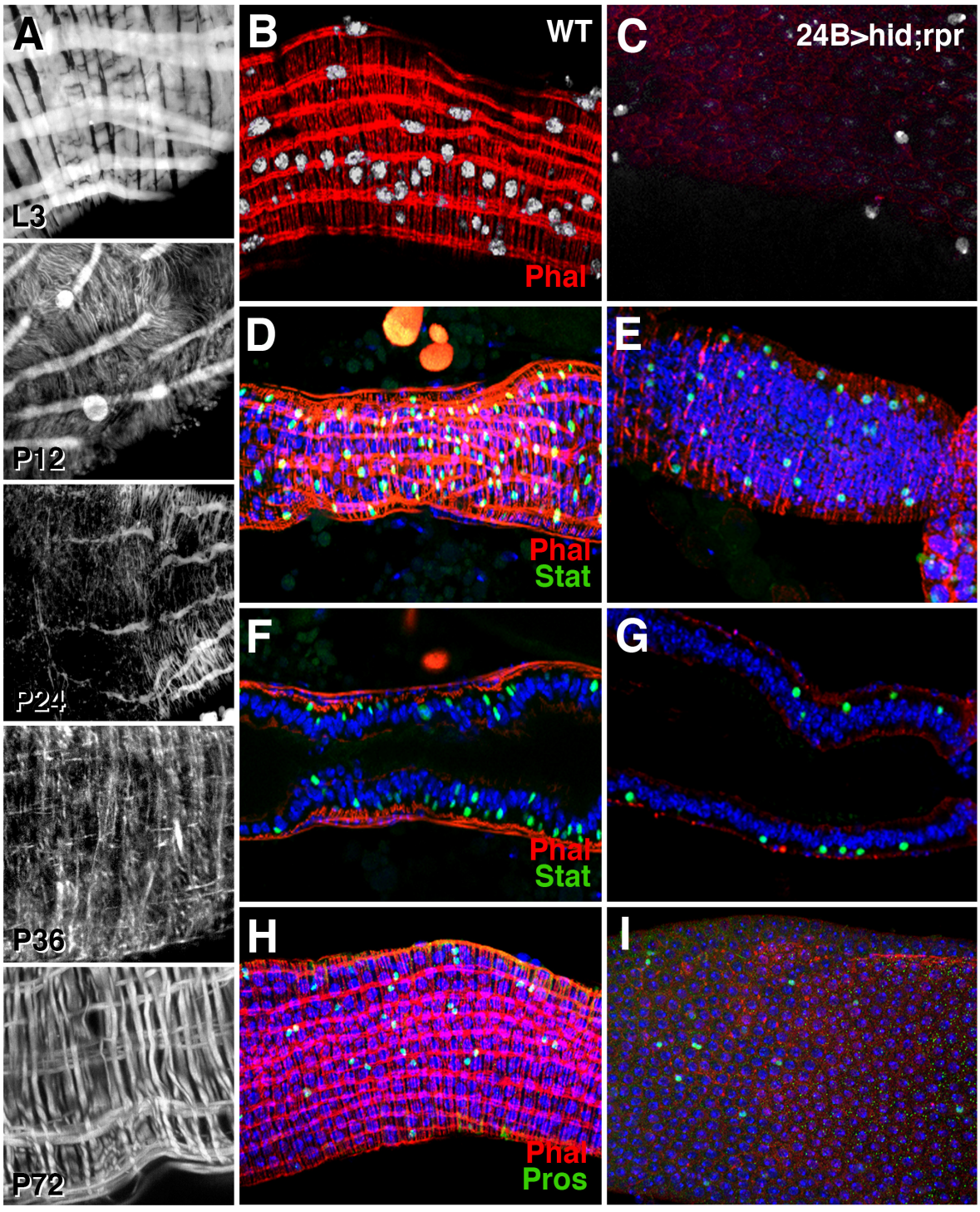
A
L3
P12
P24
P36
P72
B
WT
Phal
C
24B>hid;rpr
D
Phal
Stat
E
F
Phal
Stat
G
H
Phal
Pros
I

Fig. 7. The visceral muscle is responsible for regulating pISC differentiation during metamorphosis. (A) Z-projections of confocal stacks showing visceral muscle fiber morphology (Phalloidin, white) during different stages of metamorphosis. Stage L3 larva have strong fiber structure in both the longitudinal and circular fibers of the midgut. Myofibrils begin to retract at P12 and are virtually absent by P24. Muscle fibers begin to reform around P36. At P72, the adult orthogonal muscle pattern is established. **(B-E)** Effect of muscle ablation. (B and C) show P72 control midguts with circular and longitudinal muscle fibers (red). Topro-labeled muscle nuclei (separable by their superficial location from the deeper intestinal epithelial nucle) are shown in white in panel (B). Expression of a UAS-*hid;rpr* construct under the control of 24B(*How*)-Gal4 (D, E) from P24 to P72 results in apoptosis of visceral muscle cells**.** Absence of muscle is accompanied by a strong reduction in the number of Pros-positive endocrine cells. Bars: 10μm (A, B, D); 20□m (C, E)

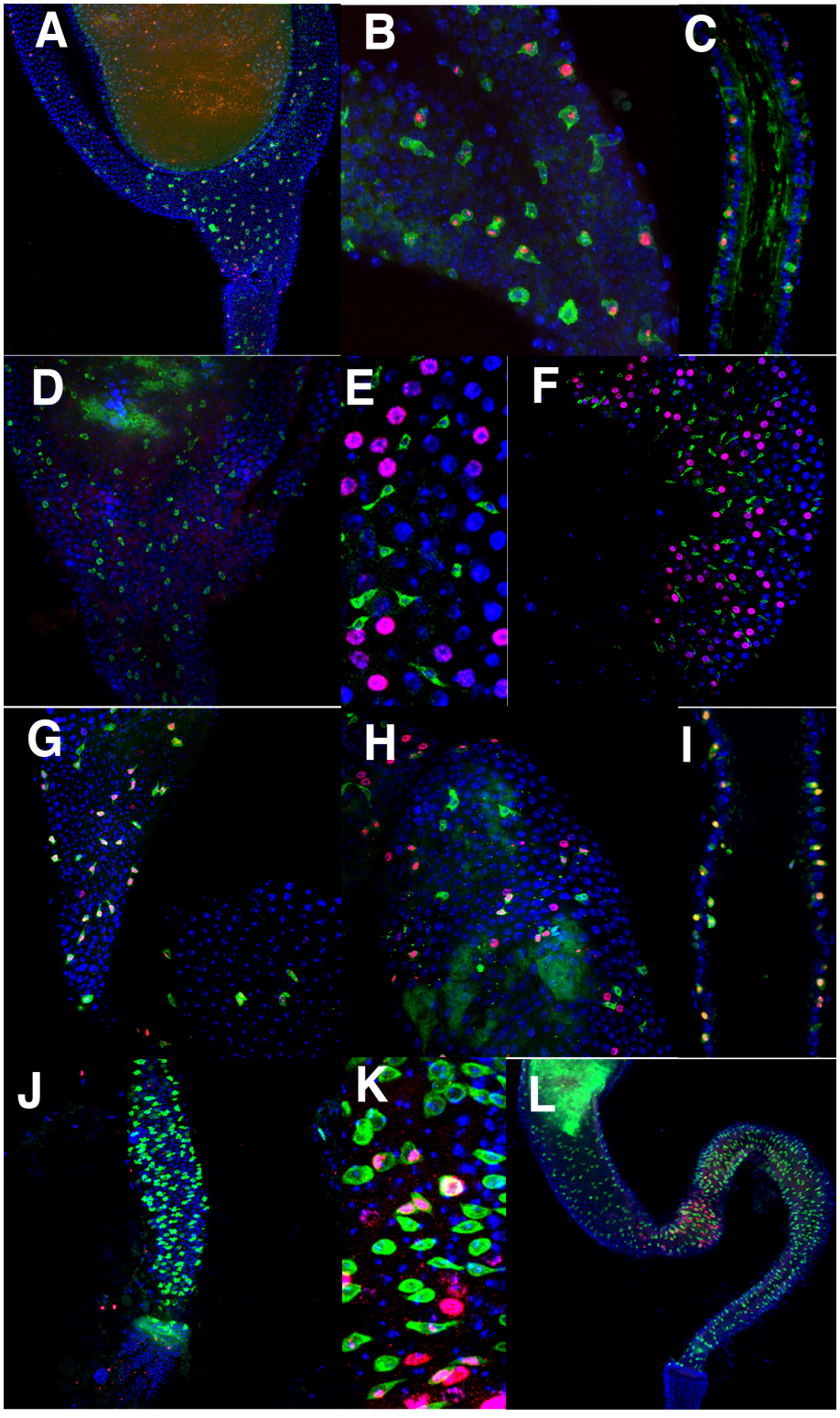
A
B
C
D
E
F
G
H
I
J
K
L

Supplementary Fig.S1. Proliferation in the pupal midgut. All panels show z-projections of midgut that have incorporated BrdU, following injection into pupa, during time intervals indicated at lower left. BrdU immuno-reactivity is in red; esg-positive pISCs are shown in green, nuclei (TOPRO-3) blue. (A-C): Global BrdU labeling of pISCs (first round of pISC mitosis). (D): No BrdU labeling of midgut during interval P30-32. (E, E') Global BrdU labeling of enterocytes (endoreplication; arrow). (F-H): Global laveling of pISCs (second round of pISC mitosis), scattered labeling of endoreplicating enterocytes (arrow). (I) No BrdU incorporation during P62-65 interval. (J, J'): Global labeling of enterocytes of middle segment of midgut (arrow); scattered labeling of pISCs (onset of third round of mitosis of pISCs). Abbreviations: ec enterocyte; vm visceral muscle; Bars: 50μm (A, J), 10μm (B, E', J'), 20μm (C-I)

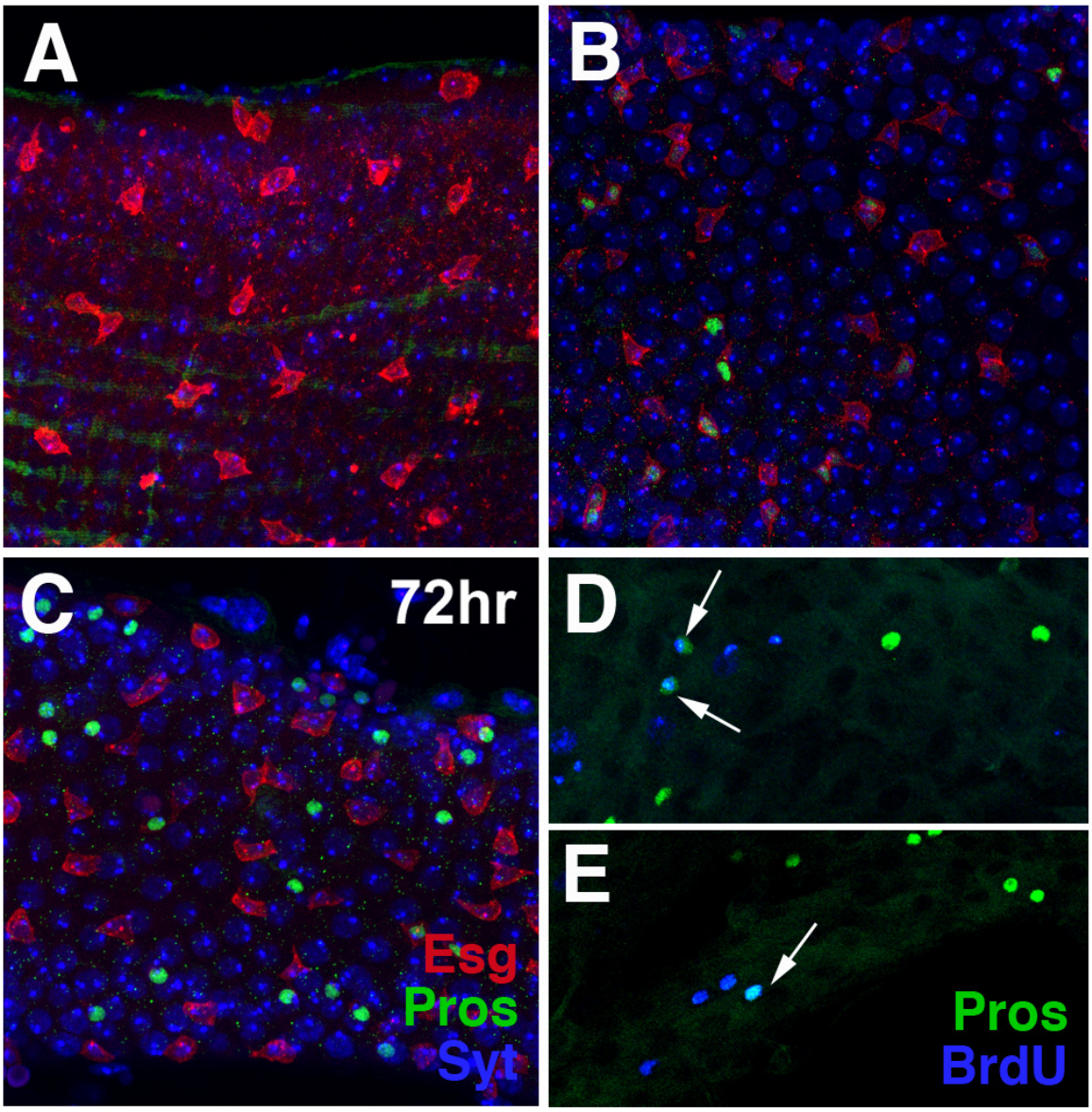

Supplementary Fig.S2. Expression of the proendocrine genes *prospero* and *asense* in the pupal midgut. (A-C) Pros (green) is not expressed at P24; it comes on in a few pISCs (red) around P54. By P72 most Pros-positive cells have switched off esg. (D, E) Pairs of neighboring Pros-positive cells (arrows in D)), or isolated Pros-positive cells (arrow in E) incorporate BrdU, suggesting that Pros-positive endocrine precursor still undergo a round of mitosis. (F, G) nExpression of Asense (Ase, green) in Pros-positive endocrine precursors at P72 and P96. Bar: 20μm (A-G).

References

Affolter, M., Walldorf, U., Kloter, U., Schier, A. F. and Gehring, W. J. (1993). Regional repression of a Drosophila POU box gene in the endoderm involves inductive interactions between germ layers. Development 117, 1199-1210.

Ashburner M (1989) *Drosophila. A Laboratory Manual*, pp214-217. New York: Cold Spring Harbor Laboratory Press.

Bardin, A. J., Perdigoto, C. N., Southall, T. D., Brand, A. H. and Schweisguth, F. (2010). Transcriptional control of stem cell maintenance in the Drosophila intestine. Development 137, 705-714.

Biteau, B. and Jasper, H. (2011). EGF signaling regulates the proliferation of intestinal stem cells in Drosophila. Development 138, 1045-1055.

Biteau, B., Hochmuth, C. E. and Jasper, H. (2011). Maintaining tissue homeostasis: dynamic control of somatic stem cell activity. Cell Stem Cell 9, 402-411.

Bjerknes, M. and Cheng, H. (2006). Neurogenin 3 and the enteroendocrine cell lineage in the adult mouse small intestinal epithelium. Dev Biol 300, 722-735.

Bossuyt W, Kazanjian A, De Geest N, Van Kelst S, De Hertogh G, Geboes K, Boivin GP, Luciani J, Fuks F, Chuah M, VandenDriessche T, Marynen P, Cools J, Shroyer NF, Hassan BA.(2009) Atonal homolog 1 is a tumor suppressor gene. PLoS Biol. 2009 Feb 24;7(2):e39.

Chu-LaGraff, Q., and Doe, C.Q. (1993). Neuroblast specification and formation regulated by wingless in the Drosophila CNS. Science 261, 1594-7.

Cordero, J. B., Stefanatos, R. K., Scopelliti, A., Vidal, M. and Sansom, O. J. (2012). Inducible progenitor-derived Wingless regulates adult midgut regeneration in Drosophila. Embo J 31, 3901-3917.

Crosnier, C., Vargesson, N., Gschmeissner, S., Ariza-McNaughton, L., Morrison, A. and Lewis, J. (2005). Delta-Notch signalling controls commitment to a secretory fate in the zebrafish intestine. Development 132, 1093-1104.

Crosnier, C., Stamataki, D. and Lewis, J. (2006). Organizing cell renewal in the intestine: stem cells, signals and combinatorial control. Nat Rev Genet 7, 349-359.

de Navascues, J., Perdigoto, C. N., Bian, Y., Schneider, M. H., Bardin, A. J., Martinez-Arias, A. and Simons, B. D. (2012). Drosophila midgut homeostasis involves neutral competition between symmetrically dividing intestinal stem cells. Embo J 31, 2473-2485.

Farin, H. F., Van Es, J. H. and Clevers, H. (2012). Redundant sources of Wnt regulate intestinal stem cells and promote formation of Paneth cells. Gastroenterology 143, 1518-1529 e1517.

Fre, S., Huyghe, M., Mourikis, P., Robine, S., Louvard, D. and Artavanis-Tsakonas, S. (2005). Notch signals control the fate of immature progenitor cells in the intestine. Nature 435, 964-968.

Fre, S., Bardin, A., Robine, S. and Louvard, D. (2011). Notch signaling in intestinal homeostasis across species: the cases of Drosophila, Zebrafish and the mouse. Exp Cell Res 317, 2740-2747.

Furriols, M. and Bray, S. (2001). A model Notch response element detects Suppressor of Hairless-dependent molecular switch. Curr Biol 11, 60-64.

Fyrberg, C., Becker, J., Barthmaier, P., Mahaffey, J., and Fyrberg, E. (1997) A Drosophila muscle-specific gene related to the mouse quaking locus. Gene 197, 315-23.

Jensen, J., Pedersen, E. E., Galante, P., Hald, J., Heller, R. S., Ishibashi, M., Kageyama, R., Guillemot, F., Serup, P. and Madsen, O. D. (2000). Control of endodermal endocrine development by Hes-1. Nat Genet 24, 36-44.

Jiang H, Edgar BA. (2009) EGFR signaling regulates the proliferation of Drosophila adult midgut progenitors. Development 136, 483-93.

Jiang, H., Grenley, M. O., Bravo, M. J., Blumhagen, R. Z. and Edgar, B. A. (2011). EGFR/Ras/MAPK signaling mediates adult midgut epithelial homeostasis and regeneration in Drosophila. Cell Stem Cell 8, 84-95.

Jiang, H. and Edgar, B. A. (2011). Intestinal stem cells in the adult Drosophila midgut. Exp Cell Res 317, 2780-2788.

Kapuria, S., Karpac, J., Biteau, B., Hwangbo, D. and Jasper, H. (2012). Notch-mediated suppression of TSC2 expression regulates cell differentiation in the Drosophila intestinal stem cell lineage. PLoS Genet 8, e1003045. doi: 1003010.1001371/journal.pgen.1003045. Epub 1002012 Nov 1003048.

Kielman, M. F., Rindapaa, M., Gaspar, C., van Poppel, N., Breukel, C., van Leeuwen, S., Taketo, M. M., Roberts, S., Smits, R. and Fodde, R. (2002). Apc modulates embryonic stem-cell differentiation by controlling the dosage of beta-catenin signaling. Nat Genet 32, 594-605.

Klapper, R., Heuser, S., Strasser, T., and Janning, W. (2001). A new approach reveals syncytia within the visceral musculature of Drosophila melanogaster. Development 128, 2517-24.

Lee, T., Luo, L. (2001). Mosaic analysis with a repressible cell marker (MARCM) for Drosophila neural development. Trends Neurosci. 24, 251-254.

Lee, W. C., Beebe, K., Sudmeier, L. and Micchelli, C. A. (2009). Adenomatous polyposis coli regulates Drosophila intestinal stem cell proliferation. Development 136, 2255-2264.

Lin, G., Xu, N. and Xi, R. (2008). Paracrine Wingless signalling controls self-renewal of Drosophila intestinal stem cells. Nature 455, 1119-1123.

Lucchetta, E. M. and Ohlstein, B. (2012). The Drosophila midgut: a model for stem cell driven tissue regeneration. Wiley Interdiscip Rev Dev Biol 1, 781-788.

Mathur, D., Bost, A., Driver, I. and Ohlstein, B. (2010). A transient niche regulates the specification of Drosophila intestinal stem cells. Science 327, 210-213.

Micchelli, C. A. (2012). The origin of intestinal stem cells in Drosophila. Dev Dyn 241, 85-91.

Micchelli, C. A. and Perrimon, N. (2006). Evidence that stem cells reside in the adult Drosophila midgut epithelium. Nature 439, 475-479. Epub 2005 Dec 2007.

O'Brien, L.E., Soliman, S.S., Li, X., and Bilder, D. (2011). Altered modes of stem cell division drive adaptive intestinal growth. Cell 147, 603-14.

Ohlstein, B. and Spradling, A. (2006). The adult Drosophila posterior midgut is maintained by pluripotent stem cells. Nature 439, 470-474. Epub 2005 Dec 2007.

Ohlstein, B. and Spradling, A. (2007). Multipotent Drosophila intestinal stem cells specify daughter cell fates by differential notch signaling. Science 315, 988-992.

Pai, L. M., Orsulic, S., Bejsovec, A. and Peifer, M. (1997). Negative regulation of Armadillo, a Wingless effector in Drosophila. Development 124, 2255-2266.

Poernbacher, I., Baumgartner, R., Marada, S. K., Edwards, K. and Stocker, H. (2012). Drosophila Pez acts in Hippo signaling to restrict intestinal stem cell proliferation. Curr Biol 22, 389-396.

Scoville, D. H., Sato, T., He, X. C. and Li, L. (2008). Current view: intestinal stem cells and signaling. Gastroenterology 134, 849-864.

Simons, B. D. and Clevers, H. (2011). Stem cell self-renewal in intestinal crypt. Exp Cell Res 317, 2719-2724.

Stamataki, D., Holder, M., Hodgetts, C., Jeffery, R., Nye, E., Spencer-Dene, B., Winton, D. J. and Lewis, J. (2011). Delta1 expression, cell cycle exit, and commitment to a specific secretory fate coincide within a few hours in the mouse intestinal stem cell system. PLoS One 6, e24484.

Strand, M. and Micchelli, C. A. (2011). Quiescent gastric stem cells maintain the adult Drosophila stomach. Proc Natl Acad Sci U S A 108, 17696-17701.

Takashima, S., Adams, K. L., Ortiz, P. A., Ying, C. T., Moridzadeh, R., Younossi-Hartenstein, A. and Hartenstein, V. (2011). Development of the Drosophila entero-endocrine lineage and its specification by the Notch signaling pathway. Dev Biol 353, 161-172.

Takashima, S. and Hartenstein, V. (2012). Genetic control of intestinal stem cell specification and development: a comparative view. Stem Cell Rev 8, 597-608.

Takashima, S., Gold, D. and Hartenstein, V. (2013). Stem cells and lineages of the intestine: a developmental and evolutionary perspective. Dev Genes Evol 223, 85-102.

Tian, H., Biehs, B., Warming, S., Leong, K.G., Rangell, L., Klein, O.D., and de Sauvage, F.J. (2011) A reserve stem cell population in small intestine renders Lgr5-positive cells dispensable. Nature 478, 255-9.

van de Wetering, M., Cavallo, R., Dooijes, D., van Beest, M., van Es, J., Loureiro, J., Ypma, A., Hursh, D., Jones, T., Bejsovec, A. et al. (1997). Armadillo coactivates transcription driven by the product of the Drosophila segment polarity gene dTCF. Cell 88, 789-799.

van Es, J. H., Giles, R. H. and Clevers, H. C. (2001). The many faces of the tumor suppressor gene APC. Exp Cell Res 264, 126-134.

van Es, J. H., van Gijn, M. E., Riccio, O., van den Born, M., Vooijs, M., Begthel, H., Cozijnsen, M., Robine, S., Winton, D. J., Radtke, F. et al. (2005). Notch/gamma-secretase inhibition turns proliferative cells in intestinal crypts and adenomas into goblet cells. Nature 435, 959-963.

Wang, P. and Hou, S. X. (2010). Regulation of intestinal stem cells in mammals and Drosophila. J Cell Physiol 222, 33-37.

Wilson, A. A. and Kotton, D. N. (2008). Another notch in stem cell biology: Drosophila intestinal stem cells and the specification of cell fates. Bioessays 30, 107-109.

Wodarz, A., Ramrath, A., Grimm, A. and Knust, E. (2000). Drosophila atypical protein kinase C associates with Bazooka and controls polarity of epithelia and neuroblasts. J Cell Biol 150, 1361-1374.

Woods, D. F. and Bryant, P. J. (1991). The discs-large tumor suppressor gene of Drosophila encodes a guanylate kinase homolog localized at septate junctions. Cell 66, 451-464.

Woods, D.F., Wu, J.W., and Bryant, P.J.(1997). Localization of proteins to the apico-lateral junctions of Drosophila epithelia. Dev Genet. 20, 111-8.

Xu, N., Wang, S. Q., Tan, D., Gao, Y., Lin, G. and Xi, R. (2011). EGFR, Wingless and JAK/STAT signaling cooperatively maintain Drosophila intestinal stem cells. Dev Biol 354, 31-43.

Yang, Q., Bermingham, N. A., Finegold, M. J. and Zoghbi, H. Y. (2001). Requirement of Math1 for secretory cell lineage commitment in the mouse intestine. Science 294, 2155-2158.

Yen, T. H. and Wright, N. A. (2006). The gastrointestinal tract stem cell niche. Stem Cell Rev 2, 203-212.

Yeung, T. M., Chia, L. A., Kosinski, C. M. and Kuo, C. J. (2011). Regulation of self-renewal and differentiation by the intestinal stem cell niche. Cell Mol Life Sci 68, 2513-2523.

Chapter 4: The dedifferentiation and redifferentiation of the metamorphosing visceral muscle influences the extension of the adult hindgut in *Drosophila melanogaster*

Introduction

The visceral muscle fibers of the *Drosophila melanogaster* gut form a striated structure for contraction used for food transport as well as an environment that provides growth and differentiation signals to the intestinal stem cells (ISCs) of both the midgut and the hindgut (Mclin et al., 2009; Jiang et al., 2012). While much of the early development of the visceral muscle is known, very little description of its maturity during metamorphosis exists apart from preliminary studies focused mainly on longitudinal muscle development (Klapper et al., 2000). In the *Drosophila* embryo, visceral muscle develops from two populations of myoblasts and forms syncytial fibers of 2 nuclei (circular muscle) and 3-5 nuclei (longitudinal muscle) per fiber (San-Martin et al., 2001). In the adult the visceral musculature has a striated orthogonal configuration of longitudinal and circular muscle fibers in the midgut, and a single layer of circular muscles in the hindgut. The fibers are located basal to the epithelium and surrounded by a basement membrane (Fig. 1A-C arrowheads denote circular muscle nuclei, arrows denote longitudinal muscle nuclei; Fig. 1D,D'). Each muscle fiber contains ~4 myofibrils, which can be observed with the F-actin binding molecule, phalloidin (Fig. A-C). Each myofibril is formed by a dense and regularly patterned array of myofilaments (Fig. 1E). The longitudinal muscles are comprised of 12 fibers that extend along the entire length of the midgut (Fig. 1B). The presence of visceral muscle can be monitored by the driver 24B(How)-Gal4 which marks muscle fibers (Brand et al., 1993; Fig. 1B,B') regardless of the polymerization state of its myofilaments.

Even though the Drosophila gut has become a favorable model system to study the biology of intestinal stem cells (Jiang et al., 2012; Takashima et al., 2012; Zeng et al., 2013), few studies have paid attention to the origin of the adult visceral muscle cells, and specifically the question

whether these cells are formed by a set of stem cells outside the larval musculature, or are retained from the larval stage. Klapper et al. (2000) has shown that the longitudinal muscle of the larval midgut is maintained through metamorphosis and at P20 (20 hours after puparium formation), and presented images of metamorphosing longitudinal muscle cells. By contrast, the developmental pathway shaping the circular fibers of the midgut and hindgut remained elusive. One goal of the present study was to use a variety of markers, in conjunction with electron microscopy and lineage tracing, to establish the metamorphic changes occurring in the visceral musculature and, specifically, the origin of the adult fibers.

The second goal was to determine the role of visceral muscle in shaping the development of the adult intestinal epithelium. Previous studies had shown that the gut undergoes a series of morphological changes during metamorphosis. Though dissimilar in the manner in which cells are replaced, both the midgut and the hindgut create a new set of cells for the functioning adult gut, while the larval gut undergoes programmed cell death (Denton et al., 2009; Lee et al., 2002). In the midgut, the dying larval gut becomes surrounded by a layer of cells known as the pupal midgut, which originate from a class of Stat+ positive adult midgut progenitors (peripheral cells; Takashima et al., 2011). During the larval period, the peripheral cells are responsible for maintaining the developing islands of presumptive intestinal stem cells (pISCs) of the midgut during larval development (Mathur et al., 2010). In the hindgut, the larval cells are replaced by a new set of adult cells which develop from a narrow domain, the hindgut proliferation zone, located at the midgut-hindgut boundary (Takashima et al., 2008; 2013). The process by which hindgut metamorphosis occurs, however, has not previously been investigated. The present study

establishes the stages of hindgut metamorphosis, and describes the morphogenetic changes leading up to the adult gut shape.

Finally, our study addressed the questions of interactions between the metamorphosing visceral musculature and the formation of adult intestinal stem cells (ISCs). In the adult, midgut ISC differentiation or self-renewal is under the control of Notch/Delta signaling (Ohlstein et al., 2007; Michelli et al., 2006), but is also influenced by many other factors such as Jak/Stat (Beebe et al., 2010), EGF (Jiang et al., 2009; Xu et al., 2011) and Wg(Lin et al., 2009; Xu et al., 2011) signaling, the latter two which are mediated by the visceral muscle. Similar to the midgut ISCs, hindgut ISCs are under the control of Wg signaling and also express Stat, though their differentiation is mediated via Hh signaling (Takashima et al., 2008). Given the role of the adult visceral musculature as a "global niche environment" in adult midgut, we speculated that signals from the metamorphosing musculature might also play a role in the formation of ISCs in the pupa. The development of these cells has been analyzed in a recent study (Takashima et al., 2014).

The goal of this study is to (1) investigate the morphological changes undergone by the visceral muscle and its surrounding membrane. (2) Determine the origin of the adult visceral muscle in both the midgut and the hindgut. (3) Establish a time course for adult hindgut extension and examine how the larval hindgut is discarded. (4) Document the role of the muscle in the progression of the adult midgut and hindgut as well as it's influence on the stem cell progenitor populations of those respective tissues.

MATERIALS AND METHODS

Fly stocks and maintenance

Fly lines used in this study were: *24B(How)-Gal4*, *tub-Gal80^{ts}*, *UAS-myr-mRFP*, *UAS-mCD8GFP*, *UAS-flp, Act5C promoter-FRT-phl[+]-FRT-lacZ.nls* (*Act5C >stop>lacZ*) (all provided by the Bloomington Stock Center), *esg-Gal4* (the National Institute of Genetics, Mishima, Japan), *UAS-hid UAS-rpr*, *10Xstat92E-GFP* (Bach et al., 2007) *ZCL1973X* (*Trol-GFP*) (Kelso et al., 2004), *wg-lacZ* (Struhl and Basler, 1993), *esg-GFP* (*YB0232*) (Cooley Lab). Flies were maintained with normal fly food at room temperature or in incubators set at 25^{o}C or 18^{o}C. In some experimental conditions, flies were transferred to the temperature at 29^{o}C to suppress the function of *Gal80^{ts}*.

Immunohistochemistry

Antibody staining was performed as described previously (Takashima et al., 2011). Shortly, dissected gut was fixed by 4% formaldehyde diluted with PBS-Tween (PBS containing 0.1% Tween20). After washing with PBS-Tween, gut samples were incubated with primary antibody for overnight at 4^{o}C. The unbound antibody was washed out with PBT then the samples were incubated with secondary antibody labeled with fluorescent dye for overnight at 4^{o}C. After washing, samples were stained with TOTO-3 or TOPRO-3 (Life Technologies, Carlsbad, CA) nuclear dye (1:1000 dilution in Vectashield) while mounting in Vectashield mounting medium (Vector Laboratories, Burlingame, CA). Throughout the procedure samples were kept in a tube placed on ice to prevent sample degradation. Antibodies used were (dilutions in parentheses): mouse antibodies against armadillo (arm, 1:10), Delta (Dl, 1:10), prospero (pros, 1:50) (all obtained from the Developmental Studies Hybridoma Bank, University of Iowa), Rhodamine

Phalloidin (Phal 1:500) (Molecular Probes), β-galactosidase (β-gal, 1:100) (Promega, Madison, WI), goat secondary antibodies against mouse IgG labeled Alexa488 (1:100), mouse IgG Alexa 546 (1:300), rabbit IgG Alexa488 (1:100) (Life Technologies); and rabbit Cy3 (1:200) (Jackson Immunoresearch, West Grove, PA).

BrdU incorporation assay

Labeling proliferative cells with BrdU was performed by injecting BrdU solution into pupa. After the pupal case was removed, the animal was injected with 20microL to 30microL of BrdU solution (approx. 1mg/mL; saturated in distilled water; Sigma, St Louis). After a given time interval, guts were dissected and fixed, treated with 2N HCl for 30 min on ice, and then processed for antibody staining.

Lineage trace experiments

To trace the lineage of pISCs in normal condition, flies with genotype of *tub-Gal80^{ts}/+; UAS-flp; Act5C>stop>lacZ/24B(How)-Gal4* were used. In the case of the tracing lineage with a gene over-expression or down-regulation, one of the wild-type chromosomes (indicated as "+") was replaced with an UAS-harboring chromosome by crossing. L3 Larvae raised at 18°C were transferred to 29^{o}C to inactivate the Gal80^{ts} repressor resulting in an elimination of "Stop cassette" on *Act5C>stop>lacZ* transgene by an UAS-driven flipase to permanently label the cells of the visceral muscle lineage until P48 or adult stages.

Muscle ablation experiments

To effectively remove the visceral muscle during metamorphosis, female flies with genotypes *UAS-his UAS-rpr/(+ X-chromosome)*; *tub-Gal80^{ts}/(+, stat92E-GFP, or esg-GFP); 24B(How)-Gal4/+* were used. Flies were grown at least until the beginning of metamorphosis at 18°C, then were transferred to 29°C at varying pupal stages for a duration of 48 hours to deactivate the Gal80^{ts} repressor in order to allow time for complete muscle deletion under the control of hid/rpr caspase mediated apoptosis. Controls for these experiments were grown under the same conditions, but were males without an affected X chromosome. When grown at 18°C growth developmental age is assumed to be about half that of normal development.

Clonal analysis

Clones were created using a hsFLP UAS-GFP; tub>GAL80>GAL4 provided by Gary Struhl via the Banerjee Lab. Flip-outs would occur spontaneously, providing single celled clones for analysis.

Transmission electron microscopy

Guts were fixed with 2.5% glutaraldehyde and 1% osmium tetroxyde and embedded in Epon resin following standard procedures optimized for pupal tissue (Grigorian et al. 2011). Ultra-thin sections were stained with uranyl acetate and lead citrate. JEOL 100CX transmission electron microscope was used for observation.

Results

The visceral muscle de-differentiates and later re-differentiates during metamorphosis

During larval and adult stages of the *Drosophila* lifespan, the visceral muscle of the midgut maintains an orthogonal patterned configuration of longitudinal muscle layered on top of circular muscle (Fig. 2A-B'). The muscle of the hindgut is composed of only circular muscle (Fig. 2B-C'). Using a muscle specific How-Gal4<Uas-GFP transgenic fly line and the actin binding molecular phalloidin, we were able to monitor the morphological changes of the visceral muscle during metamorphosis.

During early metamorphosis (P0 - P12), few morphological changes can be observed in the visceral muscle itself (data not shown). By P24, however, the visceral muscle reaches a point of substantial degradation. The longitudinal muscle syncytia begin to dissociate into single cells, leaving compact linear clusters of 1-4 nuclei, which can be confirmed by expression of How-Gal4<Uas-GFP (Fig. 2D-E'). The circular muscles reduce cell size as well, this takes place in both the midgut (Fig. 2D-E') and the hindgut (Fig. 2F-F'). Clonal analysis of circular muscle cells shows a weakened muscle syncytial membrane at P29. Binucleated circular muscle cells lose their attachments and frequently become mononucleated (Fig. 5D-F, arrows). In the midgut, this loss of muscle filaments begins in the central midgut and progresses from there to the anterior and posterior ends of the gut. This pattern of myocyte contraction maybe be due to loss muscle fiber connection to their attachment points, facilitated by a loss of the basement membrane (see below). Cells remain, however as a clusters of mononucleated cells or small 2-3 nuclei syncytia. Moreover, muscle filaments appear to have degraded to the point that few polymerized filaments can be detected. This depolymerization or degraded state of muscle filaments is sustained

continuously through P36, however muscle syncytia begin to reestablish themselves at this stage (Fig. 2G-J'). Polymerization of the muscle filaments can be observed at P48, though not fully restored to their full capacity. This can most readily be detected in the hindgut which seems to lag in its morphological changes when compared to the midgut (Fig. 2L-M'). By P72, the visceral muscle has adopted a striated filamental muscle structure that is maintained for the duration of the fly's life span (Fig. 2N-O').

The basement membrane surrounding the visceral muscle disappears during metamorphosis and reforms to envelope the adult tissue

The basement membrane completely surrounds cells of the visceral muscle, creating a layer of extracellular matrix between cells of the gut epithelium and the muscle fibers. Terribly reduced optic lobes (Trol), the *Drosophila* homologue of the heparan sulfate proteoglycan Perlecan, which is known to interact with multiple signaling molecules in the extracellular matrix, is expressed within and can be detected as a marker for the basement membrane (Grigorian et al., 2013). Using a Trol-GFP protein trap fly line we were able to monitor the morphological changes exhibited by the basement membrane during metamorphosis. Additionally, this process was examined by the use of transmission electron microscopy in order to determine the integrity of the ultrastructure of cells in the epithelial/mesenchymal junction of the metamorphosing gut. During late larval development, reaching into the early pupal phase (P6), Trol can be detected as a confluent membrane layer surrounding both the circular and longitudinal visceral muscle. This includes the muscle of the hindgut and the midgut (Fig. 3A-D'). Electron microscopically, the electron dense ECM appears as a layer of 30-50nm thickness surrounding visceral muscle, similarly to what can be detected with Trol (Fig. 4A-B', arrows)

At P12 the Trol-GFP signal is expressed around the visceral muscle in a punctate manner. This process occurs before the muscle fibrils themselves begin to show any signs of degeneration (Fig. 3E-J'). At P24, the Trol-GFP-positive material has been broken up into globular particles located basally to the visceral muscle in the midgut and the hindgut (Fig. 3K-M, arrows). Interestingly, in the Malpighian tubules which are largely retained from larval to adult stage (Singh et al., 2009), Trol-GFP signal persists as a continuous layer around the visceral muscle (Fig. 3K-M'). Examination of the basement membrane ultrastructure around this stage indicates a severely reduced ECM to the point at which almost none exists to separate the visceral muscle from the gut epithelium (Fig. 4D', arrows). P20 muscle myofibrils also exhibit a much more fragmented phenotype than when compared to those of the early pupa (Fig. 4C-D').

Trol-GFP signal begins to reappear in its normal expression pattern at ~P36, initially more highly expressed in the midgut (Fig. 3O,O') than the hindgut (Fig. 3P,P'). Ultrastructural analysis, however, of the P48 stage shows that the ECM has not fully regenerated by this stage (Fig. 4E,E'). Instead, it forms but a thin (10-20nm), relatively light layer of floccular material around the muscle and basal membrane of the intestinal epithelium (Fig. 4E' arrowheads). We conclude that a strong Trol-GFP signal is detectable at a stage before the ECM has assembled into a dense basement membrane. By contrast, at P72, the strong Trol-GFP-positive layers around muscle fibers seen in the confocal microscope (Fig.3Q-S') parallels the electron microscopic image, which shows an ECM dense basement membrane of 50nm diameter (Fig. 4F,F').

Lineage tracing and clonal analysis demonstrate that visceral muscle cells are maintained during metamorphosis

Through the use of lineage trace analysis under the control of How-Gal4 AF2 we were able to monitor the fate of metamorphosing visceral muscle cells. After a 24hr heat shock flip out starting from the late L3 larva, flies were grown at the permissive temperature until P48 (Fig. 5A,A') or Adult (Fig. 5B,B'). The heat shock initiated expression of the LacZ lineage trace construct in larval visceral muscle fibers, to which the driver line used, 24B-Gal4, is confined. At P48 and in the adult we observed the lineage-trace construct in the visceral muscle cells, including both longitudinal and circular fibers. This finding indicates that the muscle cells present at this stage did not come from a de novo non-muscle source (Fig. 5A,A'), but were the descendants of larval fibers.

Additional proof of muscle fiber longevity comes via the use of clones, induced in larva and fixed at different stages of pupal development (Fig. 5C-G). Clones were present during every tested stage of pupal development as either single binucleated syncytia, or pairs of separate cells. Thus, during mid-metamorphosis (P24-P48), clones typically are composed of two separate mononucleated cells (Fig. 5D-D' thin fibers (arrowheads), Fig. 5E-F, mononucleated clones (arrows)). Where pairs of nuclei still inhabit a single fiber, this fiber is typical very thin and irregular in shape (Fig. 5D-E). These same fibers will reform binucleated syncytia by P72 (Fig. 5G). Important to note is that the adult syncytia still surround one half of the gut perimeter, as in the larva (Fig. 5G,G').

BrdU pulses initiated at various times during metamorphosis indicate that visceral muscle cells proliferate little, if any, during gut metamorphosis (Fig. S1). Thus, whereas epithelial cells of the intestine incorporate BrdU at defined time points of development (see below), we could not detect BrdU signal in muscle nuclei, recognizable by their position peripheral to the intestinal epithelium (Fig.S1G-H Arrows). Our finding matches counts of longitudinal visceral muscle nuclei, which established a number of ~500-530 muscle nuclei from the late larva to adulthood (Klapper et al., 2000), further indicating that visceral musculature not only persists, but also remains mitotically quiescent.

Structural changes of the hindgut and midgut during metamorphosis take place within a persisting muscular sheath

Through our findings above we have been able to exhibit that the muscle layer persists through metamorphosis, even though the attachment of fibers and the syncytial structure of fibers transiently breaks down. Within this "sleeve" formed by the muscle cells, the intestinal epithelium changes from its larval to adult configuration. In contrast to what we see in the visceral muscle, larval intestinal cells undergo programmed cell death, and are replaced by a new set of adult specific cells which descend from the adult gut progenitors. In Fig. 1F, both populations of midgut(arrowheads) and hindgut (arrows) progenitors can be observed in a late stage pupal gut.

Midgut metamorphosis: In the early pupa, adult midgut progenitors undergo a mesenchymal to epithelial transition, forming a layer of adult polarized epithelial cells that surround the larval gut, while maintaining scattered mesenchymal pISCs (Takashima et al. 2014). The adult midgut

epithelium encloses the degenerating larval midgut ("yellow body"; Fig. 6A). A recent study had shown that a third layer, the transient pupal midgut, is sandwiched in between adult and dying larval gut cells (Takashima et al., 2012; Fig. 6A,B). During the first 12h of metamorphosis, the yellow body, pupal midgut and adult midgut are in very close proximity. Subsequently the yellow body contracts and looses contact to the adult midgut epithelium. The adult epithelium expands in diameter to form a wide spindle-shaped structure, enclosing the yellow body in its center (Fig. 6B). After 36h of pupal development, the adult midgut epithelium undergoes a change in shape towards long and tubular. This process, which is likely accompanied by a convergence-extension movement of the epithelial cells, coincides temporally with the reconstitution of adult visceral muscle fibers, as described above (Fig. 6C).

Proliferation does not appear to play a major role in the metamorphic expansion of the midgut epithelium. BrdU injection experiments revealed that once polarized, midgut epithelial cells do no longer divide (Takashima et al., 2014). However, cells incorporate BrdU in two rounds of endoreplication, resulting in increased cell size. By contrast, the cells set aside as progenitors of intestinal stem cells (pISCs) undergo 2-3 rounds of mitosis, increasing there number, as well as producing endocrine cells that become incorporated in the intestinal epithelium (Takashima et al., 2014)

Hindgut metamorphosis: The adult hindgut arises from adult hindgut progenitors which are concentrated in the HPZ of the late larva. Initially, expansion of the adult hindgut during metamorphosis proceeds slowly. Thus, between the white prepupa stage and P24, the hindgut mainly consists of large larval hindgut epithelium with the cells of the adult hindgut being

limited to a short HPZ at the midgut-hindgut boundary (Fig. 6D-I). Interestingly, beginning at late larval stages, the larval hindgut expresses Stat in a polarized manner, marking only half of the hindgut cells. It is unknown, however, whether this is the dorsal or ventral portion of the larval hindgut. This Stat signal does not overlap with the Stat detectable in the HPZ.

Between P24 and P48 the HPZ, the larval hindgut cells compress and are slowly replaced by expanding adult cells in an anterior to posterior manner. At this stage, Stat becomes ubiquitously expressed in all of the larval hindgut cells. As the larval hindgut cells disappear between P36 and P48, a new domain of Stat expression appears at the leading edge of the adult hindgut (Fig. 6G-H). This expression pattern, along with the much smaller nuclei of the adult gut, marks a clear boundary for monitoring the extending adult hindgut and the dying larval hindgut. A possible functional reason for this ubiquitous dispersal of Stat may be a function of regulating apoptosis as Stat-1 has been mentioned as a regulator of apoptosis (Stephanou et al., 2003). While this occurs, the rectum begins to form at the posterior most end of the hindgut (Fig. 6H). Apoptotic larval hindgut cells, are expelled from the developing hindgut region and may be endocytosed by macrophages surrounding the hindgut between P24-P36 (Fig. 6I arrow). Thus by P48, only adult hindgut cells remain.

In previous comparative cell counts between the larva and adult hindgut, Fox et al. had described an increase of cell numbers from 990 cells in the larva to 2200 cells in the adult hindgut (Fox et al., 2009). In order to determine how and when cells proliferate, we performed BrdU incorporation assays at varying lengths during metamorphosis. BrdU pulses in the hindgut in the pupa suggest only one doubling of cells in early hindgut metamorphosis, which occurs between

P1-P6 (Fig. S1A-C). Shortly before the expansion of the adult hindgut another phase of global BrdU incorporation can be observed (Fig. S1D-F). We surmise that this phase of DNA synthesis corresponds to endoreplication, based on the fact that hindgut cells increase in size, and that the number of adult cells is only about twice that of larval cells (Fox et al., 2009; see above). BrdU incorporation in the hindgut ceases after the full extension of the adult hindgut (Fig. S1J,K arrows) and does not reactivate in the adult unless induced by tissue damage (Fox et al., 2009).

Development of intestinal stem cells during metamorphosis

Stem cells of the midgut are scattered more or less evenly over the different regions of the midgut and give rise to a variety of enterocytes and enteroendocrine cells (Marianes et al., 2013). Precursors of midgut stem cells (pISCs) are derived from the adult midgut progenitors at the time when the majority of these cells undergo their mesenchymal to epithelial transition into adult gut epithelium during the first hours of pupal development (see above; Takashima et al., 2014). Thus, around P6, one can observe a population of cells which remain located basally of the epithelium and maintain high levels of the stem cell marker esg (Fig. 7I-I'). These cells undergo a round of mitosis around P24 (Fig. 7J), and one or two additional rounds at P48 and later (Fig. 7K). Starting around the second round of mitosis, a fraction of the progeny of pISCs start to differentiate as endocrine cells (Fig. 7K); new enterocytes are not produced until after eclosion (Takashima et al., 2014).

Progenitors of the adult hindgut, located in the HPZ of the larval hindgut, can be recognized by the expression of high levels of Stat92E-GFP (Takashima et al., 2008). Furthermore, a row of cells right in front of the HPZ expresses Wg, a signal required to maintain hindgut progenitor

cells in an undifferentiated, dividing state. The same configuration of Wg and Stat is seen in the HPZ of the adult hindgut, where cells continue to divide, albeit at a much lower rate than in the midgut (Takashima et al., 2008; Fox et al., 2009). To investigate the emergence of the adult hindgut stem cells we labeled pupal hindgut preparations with Stat92E-GFP (Fig. 7A,C,E,G) and a wg-lacZ reporter (Fig. 7B,D,F,H). During early metamorphosis, the expression level of both markers decreases. At this stage, the larval HPZ undergoes its transition into the adult hindgut epithelium; in addition, the most anterior cells of the larval HPZ, which remain faintly positive for Stat (Fig. 7C), as well as Wg (Fig. 7D,D'), expand anteriorly, to become incorporated into the adult midgut (Takashima et al., 2013).

Expression of Stat and Wg in what will become the adult HPZ is re-initiated around P48. Stat expression is restricted to the anterior 5-7 rows of cells of the HPZ, which become the so called spindle cell zone (SCZ) of the adult HPZ (Fig. 7E,G arrow). Wg signaling reappears at the midgut-hindgut boundary at P48 (Fig. 7F arrow/arrowhead). Initially, this new Wg signal is localized in two rows of midgut circular muscle directly adjacent to, but not overlapping with the Wg signal present in the aSCZ (Fig. 7F',F", arrowhead denotes muscle, arrow denotes epithelial signal). By P72, a bright Wg signal is present in both the SCZ and the two circular muscle cells at the midgut/hindgut boundary (Fig. 7H-H", arrowhead muscle, arrow epithelium). These Wg signals are maintained in the adult, however, in the HPZ, Wg becomes a more compact signal and is only localized in the aSCZ. The Wg signal in the circular muscle is no longer directly adjacent to the Wg signal in the HPZ (data not shown).

The effect of the muscle on the normal development of the hindgut and midgut

We speculated that the visceral muscle may play multiple roles with regards to its effect on gut metamorphosis. First, it may be important for gut morphogenesis, in particular the convergent extension resulting in the elongated tubular structure of both midgut and hindgut; secondly, in the re-constitution of intestinal stem cells. To test these roles, we used a tub-Gal80ts How-Gal4 mediated activation of UAS-hid/UAS-rpr, proteins known to activate caspase mediated apoptosis, to selectively ablate the visceral muscle at specific time points during pupal development. Muscle ablation was then verified via a disruption in phalloidin binding to polymerized actin (note lack of striated red signal in Fig. 8G compared to Fig. 8D).

During the course of normal metamorphosis, the pISCs undergo multiple waves of division and the midgut lengthens itself (Fig. 8A). Ablating the muscle before the second wave of proliferative activity also prevents the midgut from developing and growing. Inducing muscle ablation at P36 generates a phenotypes similar to a P36-P48 midgut rather than that of a P84 midgut, which is very similar to the early adult gut (Fig. 8C). In addition to the midgut epithelium, ablation of the visceral muscle can also modify pISC numbers as well. When assayed with pISC specific Esg-GFP, the pISC number in the affected midguts is visibly reduced when compared to the control (Fig. 9E-F').

In the midgut, visceral muscle ablation also stunts morphogenesis and the emergence of pISCs. Thus, following ablation between 12 and 60h, or 36 and 84h, the adult midgut epithelium forms a continuous layer and expands, but retains its short, wide configuration that is seen in early control midguts (Fig. 8A). The subsequent extension towards an elongated tube that is typical for

the late pupal wild-type midgut fails to occur (Fig. 8B,C), which is likely due to either a lack of signaling or scaffolding functionality of the muscle. A reduction of pISC number, in comparison to the control, can also be correlated to muscle ablation(Fig. 9E-F'). This phenomenon is likely due to an inhibition of pISC proliferation during various stages of metamorphosis as a result of a lack of muscle derived signals. Additionally, it has been shown that late stage pupal midguts that have undergone muscle ablation exhibit an decreased number of prospero-positive endocrine cells, indicating that the muscle plays a roll not only in pISC maintenance, but also it's development (Takashima et al., 2014).

In the hindgut, ablation of visceral muscle at the onset of puparium formation abrogates extension of the HPZ and removal of the larval hindgut. The larval hindgut persists, even though increased amount of macrophages and signs of apoptosis exist among its cells. (Fig.8E-F arrow). At the same time, the HPZ often bulges outward, forming a short, wide structure co-existing with a persisting larval hindgut (Fig.8G). Muscle ablation at later stages (between 36hrs and 84hrs) were correlated with more extended HPZs and the disappearance of larval hindgut cells; still, the emerging hindgut was considerably shorter than that of control animals (Fig. 8H). With regards to its effect on the re-emergence of the adult HPZ, we observed that following muscle ablation the pattern of expression of Stat changed. Whereas in control animals, expression is restricted to a narrow domain bordering the midgut hindgut boundary, expression in ablated animals is more diffuse, and occupies a much wider zone (Fig. 9A-D arrowheads).

Discussion

It is known that all tissues in the metamorphosing fly are dynamic to a variable degree. As a well studied model for stem cell/niche interactions, the *Drosophila* gut has been a provocative target of study. Therefore, alterations that take place in the *Drosophila* intestines were an important bridge for understanding how a dynamic niche may function. In this study we were able to determine that (1) the muscle filaments and basement membrane in both the midgut and hindgut are degenerated and regenerated, possibly due to a dedifferentiation of the muscle. (2) The muscle present in the adult is the same muscle that is present in the larva and circular muscle is composed of two binucleated cells. (3) The hindgut fully replaces all larval tissue with newly generated adult cells by P48. (4) The muscle plays a role in influencing gut development during metamorphosis by influencing proliferative and undifferentiated populations of cells.

The maintenance of the visceral muscle during metamorphosis

Preliminary studies into the metamorphosis of visceral muscle mentioned the disorganization of muscle tissue during metamorphosis, however, there was limited investigation into the details of these processes or source of the adult muscle tissue (Klapper et al., 2000; Klapper et al., 2001). In this study, we examined the complete time course of muscle metamorphosis in the gut in addition to determining the lineage of the adult visceral muscle. Our results confirmed that the visceral muscle fibers undergo a disorganization phase and form clusters of 1-5 nucleus cells with weak attachments. These results are comparable to studies of muscle cell de-differentiation in mouse skeletal muscle, which were able to de-differentiate myotubes from syncytia into single nucleus myoblasts able to contribute to the regeneration of muscle tissue (Mu et al., 2013). We have deduced that our results are a product of dedifferentiation. The myofibers then begin

reattachment to form syncytia and subsequently repolymerize their myofilaments. Similarly, in sea cucumbers (*Holothuria glaberrima*) myofiber regeneration, an analogous reformation of myofiber syncytia, occurs before the myofilament polymerization (Murray et al., 2004).

Concomitantly with the dissociation of the muscle fibers, the myofibrils break down. This could be a result of a number of mechanisms. One possibility is the simple depolymerization of the actin myofilaments, which is a normal process in cell motility. In *H. glaberrima* filaments condense to form spindle like structures when myocytes dedifferentiate (García-Arrarás et al., 2011, Candelaria et al., 2006). Another study which examines a homologous process in *Aedes aegypti* during its metamorphosis suggests that proteosomes may play a role in filamental degradation (Bernick et al., 2007). However, this was based purely on ultrastructural observations of small structures by the myofilaments within the same size range as proteosomes without any further investigation to their function. Our studies also demonstrated a loss of the basement membrane (Fig. 3; Fig. 4), which plays a role in providing attachment points for the myofilaments. Loss of the basement membrane is a plausible mechanism for facilitating myofilamental depolymerization. As it seems when the ECM is reestablished, the myofilaments also reorganize and form their classic striated phenotype (Fig. 4D,F). A similar phenomenon has also been described for *H. glaberrima*, when muscle layers become disorganized, the ECM breaks down (Quiñones et al., 2002).

Adult hindgut metamorphosis at a glance

The hindgut of *Drosophila* is functionally important for water and ion absorption. It is currently known that the anterior most region of the hindgut, the HPZ, is responsible for forming the adult

hindgut epithelium (Takashima et al., 2008). In the adult, proliferation continues at a low rate in the HPZ under normal conditions, but can be activated by hindgut tissue damage (Fox et al., 2009). In this study, we documented the process wherein the larval HPZ morphs into adult hindgut that replaces the larval gut, and the adult HPZ reappears at the anterior end of the hindgut . In the early stages of extension, the adult hindgut undergoes one to two rounds of mitosis while not extending very far. Around P17-P22 the hindgut activates massive DNA proliferation and subsequently extends completely from p20-P40. A known quality of the adult hindgut is that the cell number is over double the amount present in the larva, therefore a substantial cell proliferation must take place (Fox et al., 2009). As the hindgut extends to replace the dying larval gut, it us unknown whether this is coupled by and increase is cell number or whether this lengthening of the adult gut is due to increased cell size via endoreplication. Therefore, the question still remains: does adult hindgut proliferation occur in multiple waves or in one large stage localized at the HPZ? This can be answered with more periodic BrdU assays and cell counts.

The larval hindgut shows few changes through P12, however, it becomes seemingly shorter and thinner by P24. Macrophage like bodies can be observed surrounding the larval hindgut during this stage, likely for the purpose of endocytosing apoptotic larval cells (Fig. 6I arrow). The larval hindgut expresses Stat-GFP initially in a polarized manner, eventually expressing it in all larval hindgut cells. The functional relevance of this is unknown, however, as mentioned earlier, the Jak/Stat pathway plays multiple roles. In the case of the larval gut, it may act as an activator or enhancer of apoptosis (Stephanou et al., 2003). In addition, recent studies have suggested that Stat-1 may act as a negative regulator in mitophagy, further demonstrating its role as a promoter

of apoptotic activity (Bourke et al., 2013). Stat is also highly expressed in the pupal midgut which surrounds the green body during metamorphosis as it proceeds through autophagocytosis, though the role of its expression in this region has not been investigated (Takashima et al., 2011). Preliminary experiments of Stat-RNAi activation specific to the hindgut has shown little effect on the extension of the hindgut (data not shown). This data is inconclusive, but the role of Stat as it is expressed in the larval hindgut, may be an important avenue to investigate.

The metamorphosing muscle and its role as a transient niche

The role that the visceral muscle plays in the providing signals that are known to provide maintenance and differentiation cues to the adult midgut (EGF, Wg) have been well documented (Jiang et al., 2009; Xu et al., 2011; Lin et al., 2009). Overexpression of Wg leads to undifferentiated tumor formation. Notch (N) which is required for enterocyte fate determination, interacts downstream of Wg in an epistatic fashion. N overexpression can override the influence of Wg on ISCs and induce differentiation to enterocytes (Lin et al., 2009). Furthermore, it is known that the pISCs in the midgut undergo multiple waves of division during metamorphosis, including a stage of endocrine differentiation (Takashima et al., 2014; Fig. 7I-K). Notch signaling is undetectable during metamorphosis between P4 and P50, however, ectopic expression of N can induce enterocyte differentiation in even the metamorphosing pISCs (Takashima et al., 2014). Incidentally, a major round of pISC division takes place during p24-48, a time when visceral muscle is de-differentiated. In addition to this, a round of differentiation to endocrine fate occurs at a point between P48 and P72, which coincides with the return of the muscle and basal membrane to a somewhat normal capacity (Fig. 2; Fig. 3). In this paper we have also shown that deletion of the visceral muscle during metamorphosis leads to a reduced

number of pISCs present in the metamorphosing adult gut (Fig. 9E-F'). Further corroborating the muscle's role as a signal provider is the presence of a ring of Wg signal which is known to provide self-renewal cues (Lin et al., 2009; Xu et al., 2011), in the central midgut through larval development that weakens during mid metamorphosis (P24) and returns at ~P48 with the visceral muscle (Takashima et al., 2014). The muscle also plays a role in the convergent extension of the midgut (Fig. 8A-C). Developmental stagnation observed in muscle ablated midguts may be explained by either a scaffolding function or a lack of signaling. These data taken together suggest a significant influence on adult midgut epithelial and mesenchymal development by the surrounding muscle.

Though the visceral muscle is known to play an important role in midgut maintenance, little thought has been given to its role in maintenance of the hindgut despite the similarities in the active signal transduction pathways that are seemingly shared between the midgut ISCs and the hindgut ISCs (Takashima et al., 2008). While its specific function has not been investigated, a possible maintenance cue for the HPZ may come from the active Wg signal in the visceral muscle at the midgut/hindgut boundary. This signal does not become active until the complete adult hindgut has formed at P48 and stays active at least to early adulthood (Fig. 7F",H"). Wg signal is also present as a sharp band in the aSCZ in the HPZ epithelium, however, this band does not form until the Wg signal in the visceral muscle is expressed. It would be reasonable to suggest that this Wg signal in the muscle may interact with the Wg expressing cells of the HPZ and induce a quiescence in the cells of the aSCZ. The findings in Fox et al. 2009 may in fact support this hypothesis, as in the adult, the HPZ is somewhat quiescent unless induced to repair damaged tissue. The function of the Wg signal in the hindgut/midgut boundary could be the next

avenue for study in this region. Ablating the muscle during metamorphosis additionally has two separate functions; (1) it allows for an increase in Stat expression in the HPZ and (2) prevents larval hindgut detachment. Stat is known to be expressed in the SCZ of the hindgut, this region is essentially the transient amplifying zone of the hindgut. Consequently, it is possible that the increase in stat expression in the HPZ is responsible for the bulge formation in the anterior hindgut after muscle ablation. As the function of the visceral muscle has not been studied in the hindgut, these data can give insight as to its function in maintaining the HPZ in the larva and the adult.

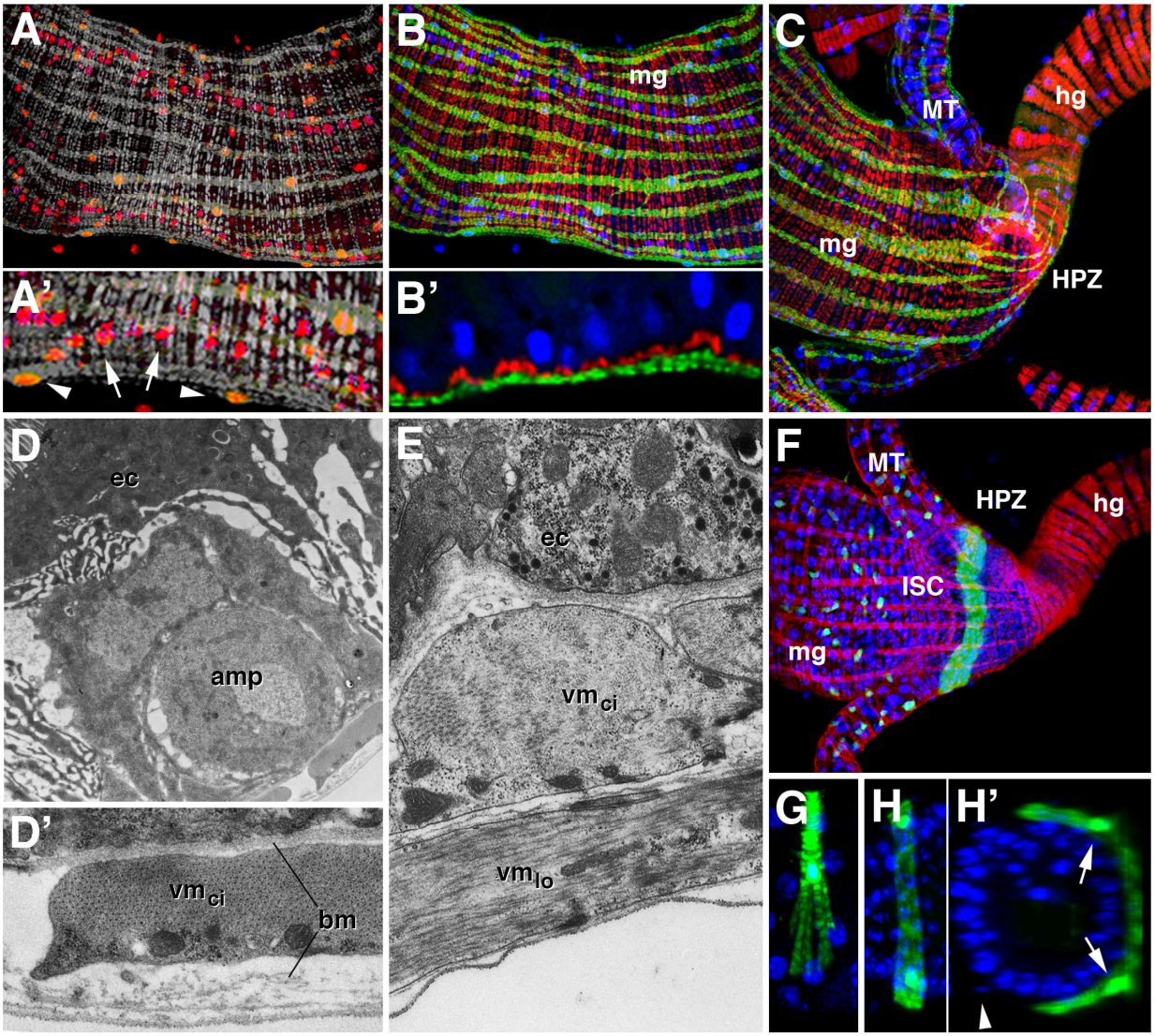
A
B
mg
C
MT
hg
mg
HPZ
A'
B'
D
ec
amp
E
ec
vm ci
vm lo
F
MT
HPZ
hg
ISC
mg
D'
vm ci
bm
G
H
H'

Fig. 1. An Introduction to the visceral muscle. (A-C, F) Confocal z-projections of an adult midgut**. (A)** Muscle nuclei are depicted in red **(A')** longitudinal nuclei are denoted with arrowheads, circular nuclei are denoted with arrows. **(B,B')** Myofilaments are marked with red (phalloidin) and myofibers are marked in green (How-Gal4) in this image, the GFP signal is strongest in the longitudinal fibers. **(C)** Midgut/hindgut junction region. Longitudinal and circular fibers from the midgut transition to just circular fibers in the hindgut. **(D, D', E)** Electron micrograph of a late L3 larval gut. **(D)** Image of an adult midgut progenitor **(D')** Circular visceral muscle located basal to the amp. **(E)** Enterocyte in relation to basally located visceral muscle. **(F)** Midgut/hindgut boundary. ISCs of the midgut, hindgut, and Malpighian tubules marked with Stat/Esg (green), myofibrils (red). **(G, H, H')** Single celled circular muscle clones of a late stage pupal gut. **(H')** Transverse section indicating that two syncytial cells make one circular muscle fiber. Arrows point to clone nuclei, arrowhead points to unlabeled cell nucleus. Nuclei for confocal images marked with Topro (blue). Abbreviations: amp, adult midgut progenitor; bm, basement membrane; ec enterocyte; HPZ, Hindgut Proliferative Zone; hg, hindgut; ISC, intestinal stem cell mg, midgut; MT, Malpighian Tubules; vm_{ci}, circular visceral muscle; vm_{lo}, longitudinal visceral muscle

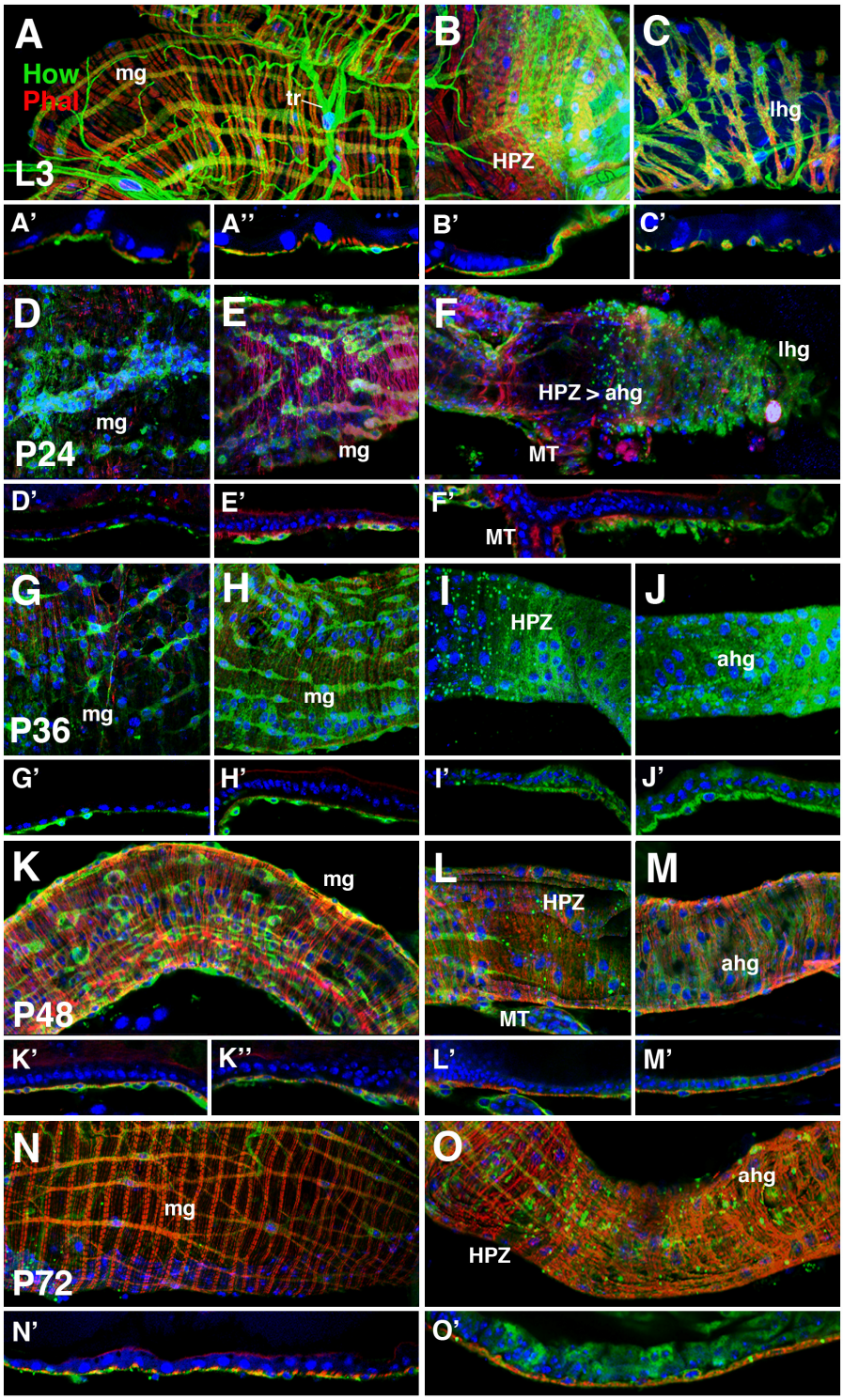
A
How
Phal
mg
tr
L3
B
HPZ
C
lhg
A'
A''
B'
C'
D
mg
P24
E
mg
F
lhg
HPZ > ahg
MT
D'
E'
F'
MT
G
mg
P36
H
mg
I
HPZ
J
ahg
G'
H'
I'
J'
K
mg
P48
L
HPZ
MT
M
ahg
K'
K''
L'
M'
N
mg
P72
O
ahg
HPZ
N'
O'

Fig. 2. Visceral muscle metamorphosis. Z-projections of confocal sections used to visualize the development of visceral muscle from the late larva through metamorphosis. **(A-C)** At the late L3 Larva myofilaments in the migut **(A-A'')**, HPZ **(B-B')** and hindgut **(C-C')** stained with phalloidin (red) can be visualized as orthogonal layers of circular and longitudinal fibers. Muscle cells can be identified via How-Gal4 UAS-GFP (green). **(D-F)** At P24 myofilaments in the migut **(D-D')**, HPZ **(E-E')** and hindgut **(F-F')** show substantial signs of depolymerization. Additionally, longitudinal muscle nuclei (blue) have separated into units of 1-3 nuclei within a cell and cell size for circular muscle has reduced. **(D', E', F')** Filament visualization appears disorganized in sagittal sections as well. **(G-J)** P36 confocal sections of the midgut **(G-H)**, HPZ **(I)**, and hindgut **(J)** indicate that muscle fibers have completely dissociated from one another leaving only the muscle cells. **(G', H', I', J')** **S**agittal sections show no sign of intact muscle filaments. (**K-M)** P48 muscle filaments show signs of repolymerizing in the midgut **(K)**, HPZ **(L)** and hindgut **(M)**. **(K', K'', L', M')** Filaments can be observed within muscle cells. **(N-O)** Muscles have developed a normal structure that is maintained through the rest of metamorphosis and the adult life cycle. **(N',O')** Strong filamental staining in the muscle cells, indicating intact muscle structures. **(')** and **('')** frames denote sagittal sections. Nuclei marked with Topro (blue). Abbreviations: mg, midgut; tr, trachea; HPZ, Hindgut Proliferative Zone; ahg, adult hindgut; MT, Malpighian Tubules

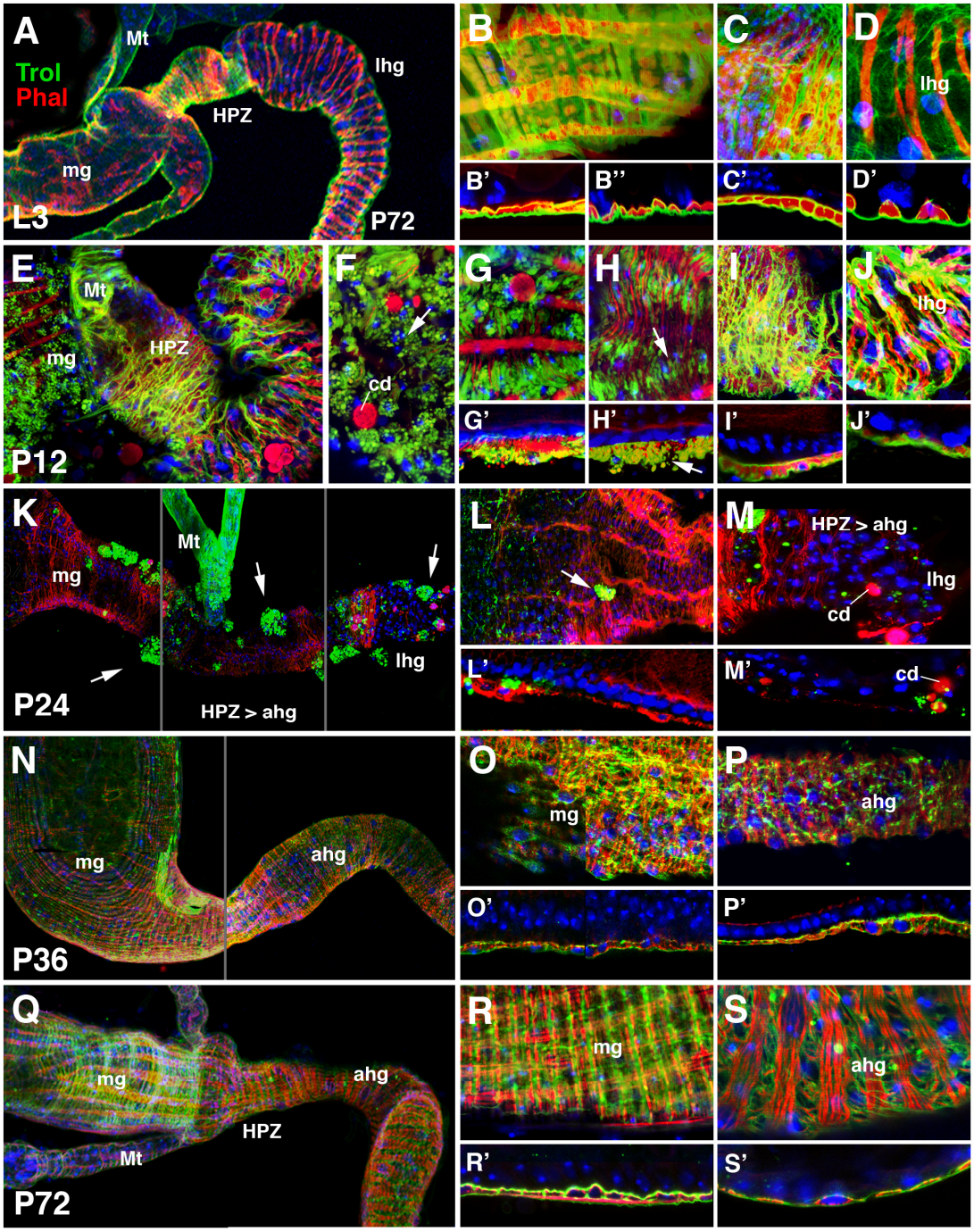
A
Mt
Trol
Phal
lhg
HPZ
mg
L3
P72
B
B'
B''
C
C'
D
lhg
D'
E
Mt
mg
HPZ
P12
F
cd
G
G'
H
H'
I
I'
J
lhg
J'
K
mg
Mt
lhg
P24
HPZ > ahg
L
L'
M
HPZ > ahg
lhg
cd
M'
cd
N
mg
ahg
P36
O
mg
O'
P
ahg
P'
Q
mg
ahg
HPZ
Mt
P72
R
mg
R'
S
ahg
S'

Fig. 3. Disintegration of Trol expression in the basement membrane during metamorphosis. **(A-S)** Z-projections of confocal sections used to visualize the development of visceral muscle and surrounding basement membrane from the late larva through metamorphosis. **(A)** Low magnification projection of the midgut-hindgut junction region of a late L3 larval gut. **(B-D)** High magnification images of the L3 gut show a layer of Trol (green) located in the basement membrane, completely surrounding each muscle cell (Muscle filaments marked by phalloidin in red) **(B', B'', C', D')**. **(E, F)** Low magnification image of the midgut-hingut boundary region at P12 shows signs of Trol layer disorganization (arrow). **(G-J)** High magnification projections show regions where the Trol layer is dissolving (arrows). **(G', H', I', J')** Sagittal segments displaying the Trol layer no longer surrounds the visceral muscle. **(K)** Low magnification projection of P24 gut with virtually no Trol layer (arrows), though a layer remains on the Malpighian Tubules and Ureter. **(L, M)** Trol expression is limited to islands of degrading protein (arrow). Muscle filaments are also partially degraded. **(L', M')** Sagittal segments confirm a lack of Trol expression around muscle cells. **(N)** Low magnification projection of the midgut-hindgut junction at P36. **(O, P)** High magnification projections of P36 gut indicate the return of Trol-expression in the basement membrane surrounding the visceral muscle which can be seen in the sagittal sections **(O', P')**. **(Q)** Low magnification projection of the midgut-hindgut junction at P72. **(R, S)** High magnification projection of P72 gut displays a complete layer surrounding intact muscle cells **(R', S')**. **(')** and **('')** frames denote sagittal sections. Nuclei marked with Topro (blue). Abbreviations: mg, midgut; tr, trachea; HPZ, Hindgut Proliferative Zone; ahg, adult hindgut; lhg, larval hindgut; MT, Malpighian Tubules

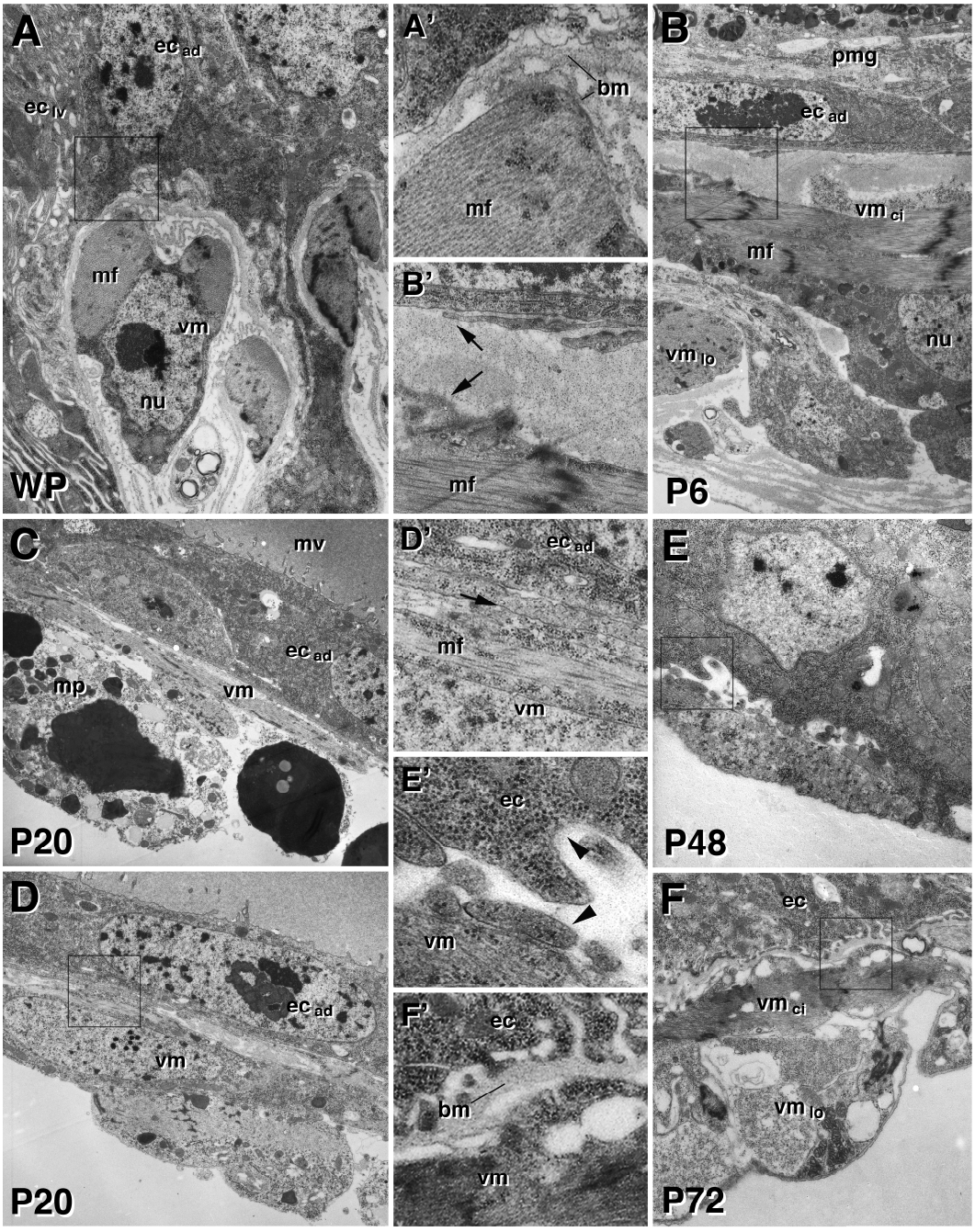
A
ec ad
ec lv
mf
vm
nu
WP
A'
bm
mf
B
pmg
ec ad
vm ci
mf
vm lo
nu
P6
B'
mf
C
mv
ec ad
mp
vm
P20
D'
ec ad
mf
vm
E
P48
E'
ec
vm
D
ec ad
vm
P20
F'
ec
bm
vm
F
ec
vm ci
vm lo
P72

Fig. 4. Ultrastructure of the metamorphosing visceral muscle and surrounding basement membrane. (A-F) Electron micrographs of the junction between the visceral muscle and midgut epithelium during multiple stages of pupal development. **(A)** Muscle and enterocytes of a white prepupa. **(A')** Enlarged boxed region from **(A)**, a basal membrane with an intact extracellular matrix (ECM) separates a muscle cell from the gut epithelium. **(B)** P6 basal membrane provides a boundary between the circular muscle and midgut epithelium **(B')** (arrows). **(C-D)** At P20, the ECM and the basement membrane virtually disappear **(D')** (arrow) as do most the intact muscle filaments. **(E)** At P48 the basement membrane returns, ECM also begins to reform **(E')** (arrowheads). **(F)** A P72 gut reestablishes complete basement membrane **(F')**. Abbreviations: bm, basement membrane; ec, enterocyte; ec_{ad}, adult enterocyte; ec_{lv}, larval enterocyte; mf, microfilament; mv, microvilli; nu, nucleus; pmg, pupal midgut, vm, visceral muscle; vm_{ci}, circular visceral muscle; vm_{lo}, longitudinal visceral muscle

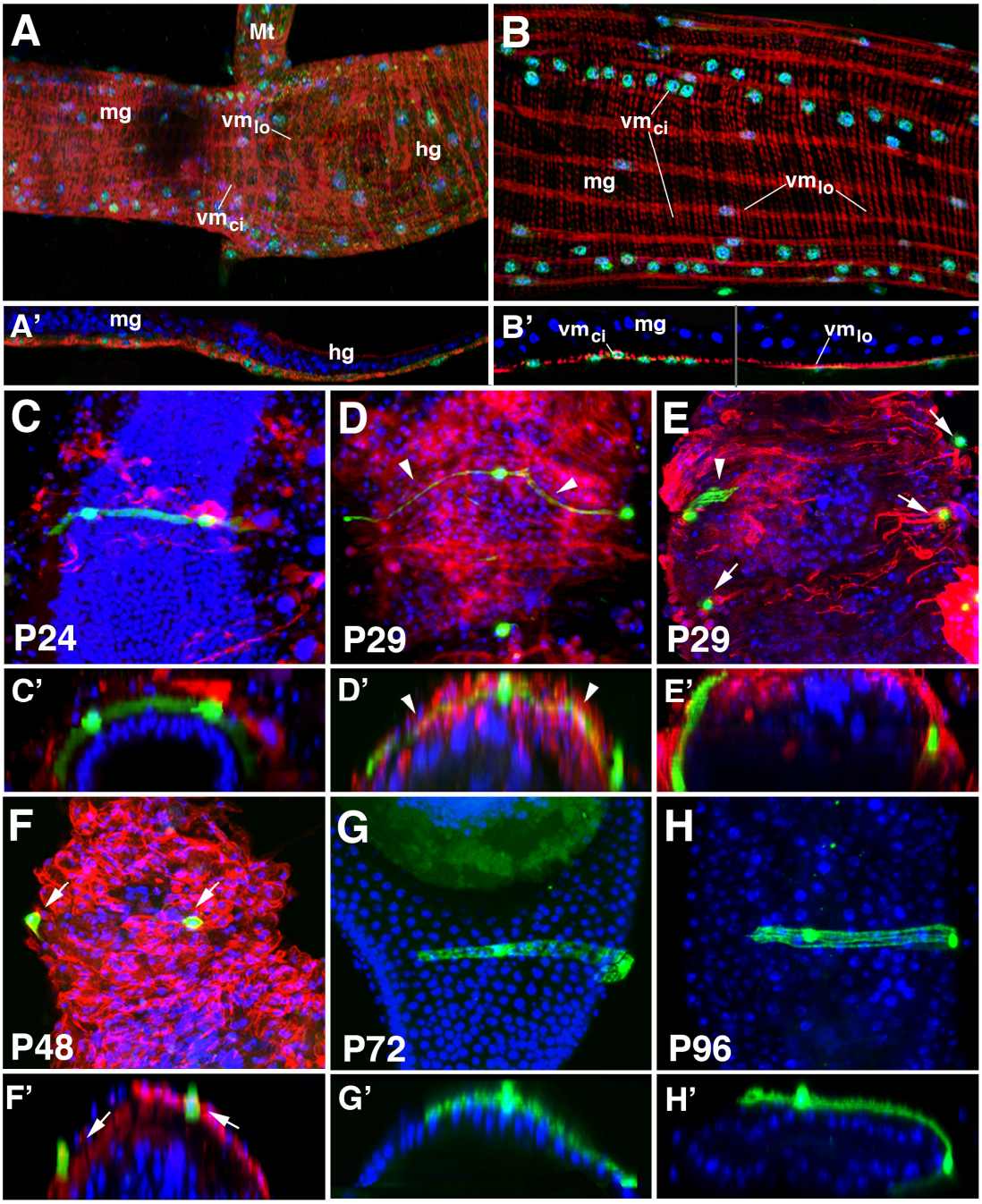
A
Mt
mg
vm lo
hg
vm ci
B
vm ci
mg
vm lo
A'
mg
hg
B'
vm ci
mg
vm lo
C
P24
D
P29
E
P29
C'
D'
E'
F
P48
G
P72
H
P96
F'
G'
H'

Fig. 5. The visceral muscle persists through metamorphosis. (A-B) Confocal z-projections of lineage traced muscles. **(A)** 48 hr gut, lineage trace initiated at Late L3, all muscle cells marked with How-Gal4 **(A')** sagittal section, muscle nuclei (Green) **(C-H)** Confocal z-projections of single celled circular muscle clones during various stages of metamorphosis. **(C'-H')** Transverse sections. **(C)** Tangential sections of the midgut when muscle filaments (red) are in a deteriorated state show the presence of muscle cells (green). **(C')** Transverse sections of the same region in **(C)** show binucleated clones which envelope half of the circumference of the midgut. **(D-F)** Tangential views of visceral muscle upon the return of muscle filaments. **(D'-F')** Transverse sections of **(D-F)** show the muscle clones overlapping with the muscle filaments (arrowheads point to thinned muscle attachments, arrows; clone nuclei). **(G-H)** Late stage pupal guts (not stained with phalloidin) show redifferentiated single celled circular muscle clones. Abbreviations: hg, hindgut; mg, midgut; MT, Malpighian Tubules; vm_{ci}, circular visceral muscle; vm_{lo}, longitudinal visceral muscle

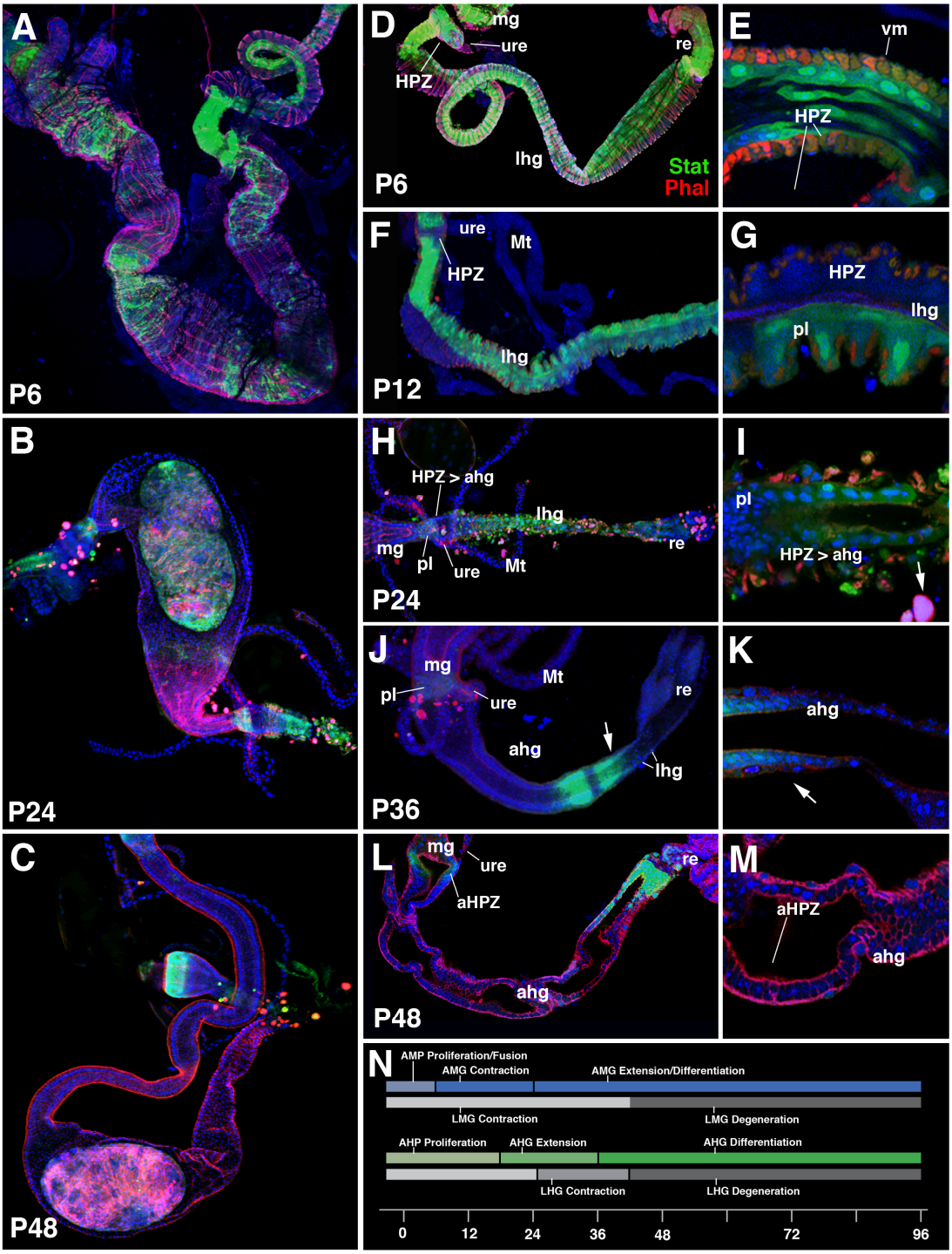
A
P6
D
mg
ure
re
HPZ
lhg
Stat
Phal
P6
E
vm
HPZ
F
ure
Mt
HPZ
lhg
P12
G
HPZ
lhg
pl
B
P24
H
HPZ > ahg
lhg
mg
pl
ure
Mt
re
P24
I
pl
HPZ > ahg
J
mg
Mt
pl
ure
re
ahg
lhg
P36
K
ahg
C
P48
L
mg
ure
re
aHPZ
ahg
P48
M
aHPZ
ahg
N
AMP Proliferation/Fusion
AMG Contraction
AMG Extension/Differentiation
LMG Contraction
LMG Degeneration
AHP Proliferation
AHG Extension
AHG Differentiation
LHG Contraction
LHG Degeneration
0
12
24
36
48
72
96

Fig. 6. The concerted cell movements of the midgut and hindgut during metamorphosis. (A-M) Confocal z-projections portraying the morphological changes of the midgut and hindgut from early to late metamorphosis. Nuclei marked with Topro (blue) **(A-C)** Post larval development, the midgut begins as a long epithelium **(A)**. The gut subsequently contracts and widens until ~P24 **(B)** and through convergent extension lengthens itself again by P48 **(C)**. **(D-E)** At P6, the adult hindgut is limited to the cells of the HPZ. **(F-G)** At P12 the adult hindgut is still restricted to the HPZ, but has extended. **(H-I)** At P24, the adult hingut extends to where stat (green) is faintly being expressed in the hindgut. The rectum begins to form. **(J-K)** At P36, the majority of the hindgut is composed of the adult epithelium after convergent extension. Few larval cells remain between the adult hindgut and the rectum (arrows). **(L-M)** At P48, the entire hindgut is composed of adult tissue. **(N)** A diagram explaining adult gut extension/contraction in relation to the larval tissues during the time course of metamorphosis. Larval tissues (gray), adult midgut (blue), adult hindgut (green). Abbreviations: ahg, adult hindgut; aHPZ, Adult Hindgut Proliferative Zone; HPZ, Hindgut Proliferative Zone; lhg, larval hindgut; ma, macrophage; mg, midgut; Mt, Malpighian Tubules; pl, plug; re, rectum; tr, trachea; ure, ureter

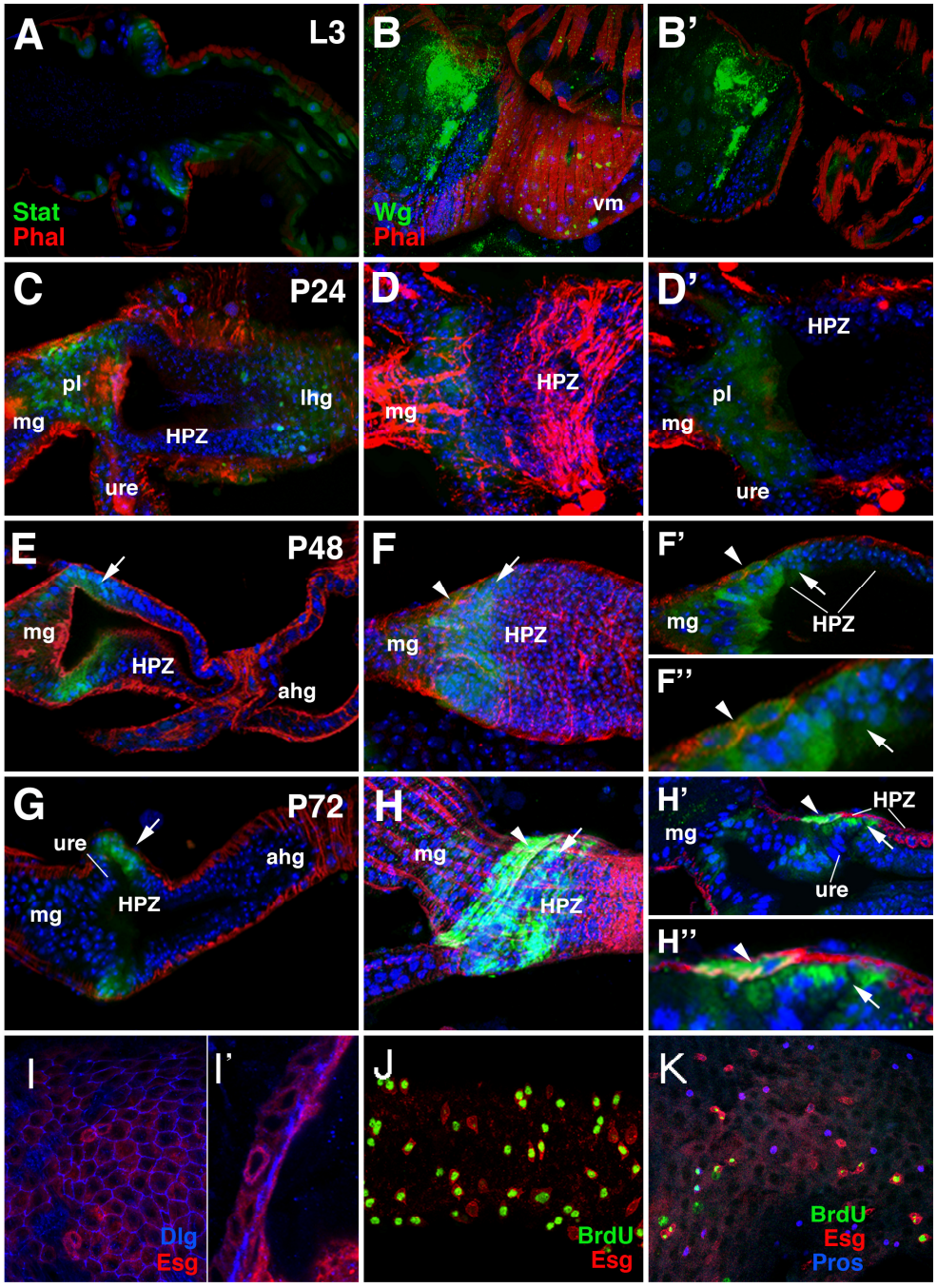
A
L3
Stat
Phal
B
Wg
Phal
vm
B'
C
P24
pl
lhg
mg
HPZ
ure
D
HPZ
mg
D'
HPZ
pl
mg
ure
E
P48
mg
HPZ
ahg
F
mg
HPZ
F'
mg
HPZ
F''
G
P72
ure
ahg
mg
HPZ
H
mg
HPZ
H'
HPZ
mg
ure
H''
I
Dlg
Esg
I'
J
BrdU
Esg
K
BrdU
Esg
Pros

Fig. 7. Zones of ISC maintenance and their signaling during metamorophosis (A, C, E, G) Confocal z-projections of the HPZ from L3 larva to P72 visualized with Stat92E-GFP expression (green). **(B, D, F, H)** Confocal z-projections of the HPZ from L3 larva to the P72 visualized with Wg-LacZ expression (green). **(A)** In the Late Larva Stat expression in the HPZ is restricted to the first few rows of cells near the midgut/hindgut boundary. **(B, B')** Wg signal in the HPZ is localized in a band of cells in the anterior hindgut. **(C)** By P24 cells of the HPZ expressing Stat have migrated past the midgut/hindgut boundary and compose many of the cells in the plug. **(D, D')** Wg is expressed in a weak and diffuse manner towards the anterior of the HPZ at P24. **(E, G)** At P48 and P72 respectively, Stat returns to the anterior HPZ (arrow). **(F, F', F'')** Wg expression can be detected in a diffuse manner in the anterior HPZ (arrow). In addition two rows of circular muscle at the midgut/hindgut boundary begin expression of wingless signal (arrowhead). **(H, H', H'')** At P72, Wg signal on the two rows or circular muscle becomes increased (arrowhead). Furthermore, Wg signal in the anterior HPZ epithelium increases and begins to form a sharper expression pattern (arrow). **(I, I')** Delta signal is still present in the pupa until after P6 when it shuts off. **(J)** pISCs undergo a cycle of proliferation at ~P24. **(K)** The first endocrine cells emerge from the pISC population at ~P48. **(', '')** Sagittal sections. Abbreviations: ahg, adult hindgut; HPZ, Hindgut Proliferative Zone; lhg, larval hindgut; mg, midgut; pl, plug; vm, visceral muscle; ure, ureter

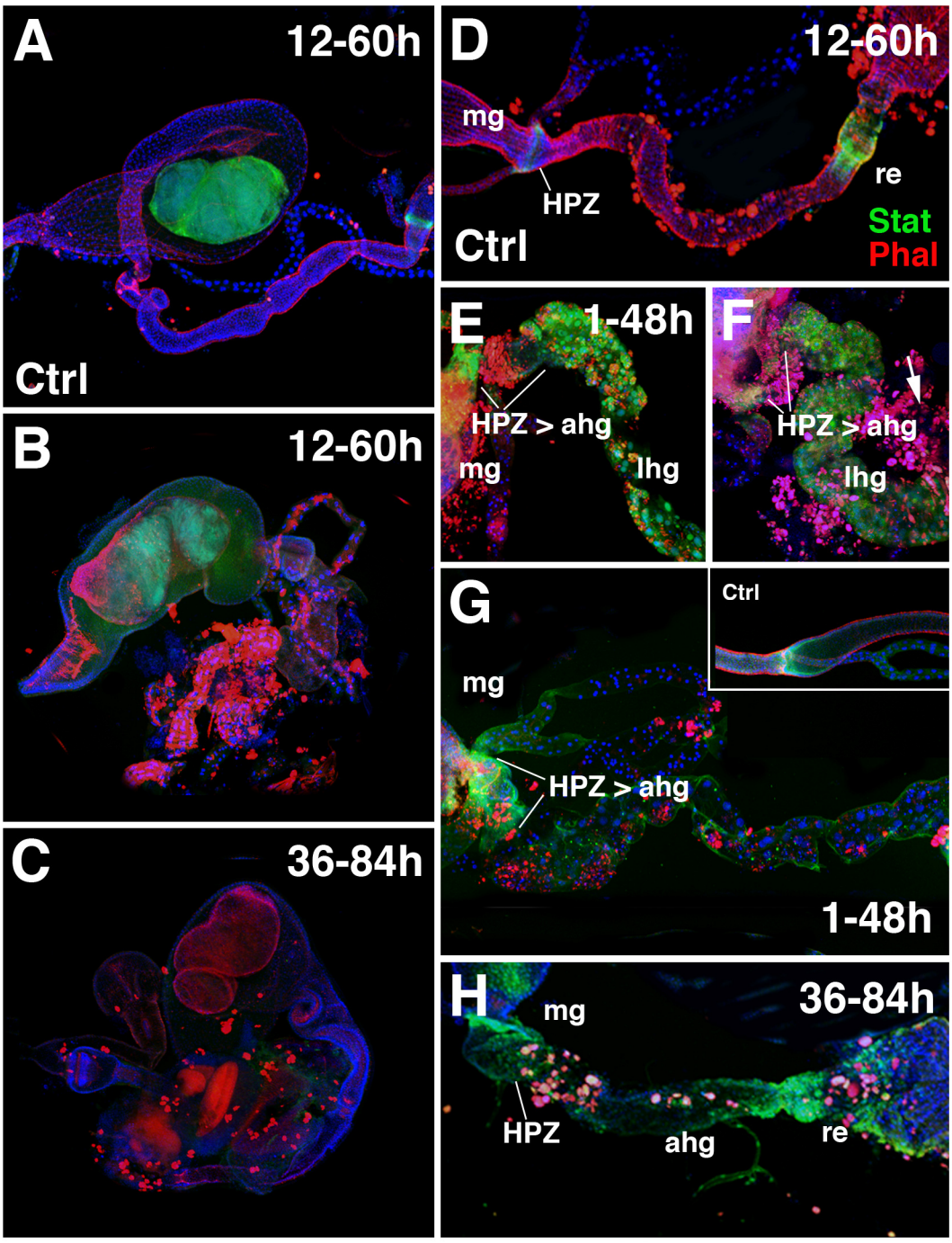
A
12-60h
Ctrl
B
12-60h
C
36-84h
D
12-60h
mg
HPZ
re
Ctrl
Stat
Phal
E
1-48h
HPZ > ahg
mg
lhg
F
HPZ > ahg
lhg
G
Ctrl
mg
HPZ > ahg
1-48h
H
mg
36-84h
HPZ
ahg
re

Fig. 8. The effect of muscle ablation on gut metamorphosis. (A-H) Confocal z-projections of muscle deletion experiments under the control of tub-Gal80^{ts}; 24B-Gal4; Uas-Hid, Uas-rpr of flies during multiple different stages of metamorphosis. All flies were incubated from white prepupa at 18C until reaching an age of ~P12**(A, B, D)**, ~P36 **(C, H)** or temperature shifted directly at puparium formation **(E-G)** , then shifted to 29C for 48 hr real time. Ctrl flies did not contain the Uas-hid, Uas-rpr. **(A-C)** Displays midgut morphology post muscle ablation during early stage **(B)** or late stage **(C)** knockdown. Both show a compressed phenotype compared to the ctrl. **(D-G)** Focus on hindgut morphology post muscle ablation. **(D)** shows normal elongation while at ~P48 **(E, G, F)** appear to have completely attached larval guts and muscle fibers are apoptosing (arrow). **(H)** shows a late stage muscle KO with stunted gut extension. All nuclei are stained with Topro (blue). Abbreviations: ahg, adult hindgut; HPZ, hindgut proliferative zone; lhg, larval hindgut; mg, midgut; re, rectum.

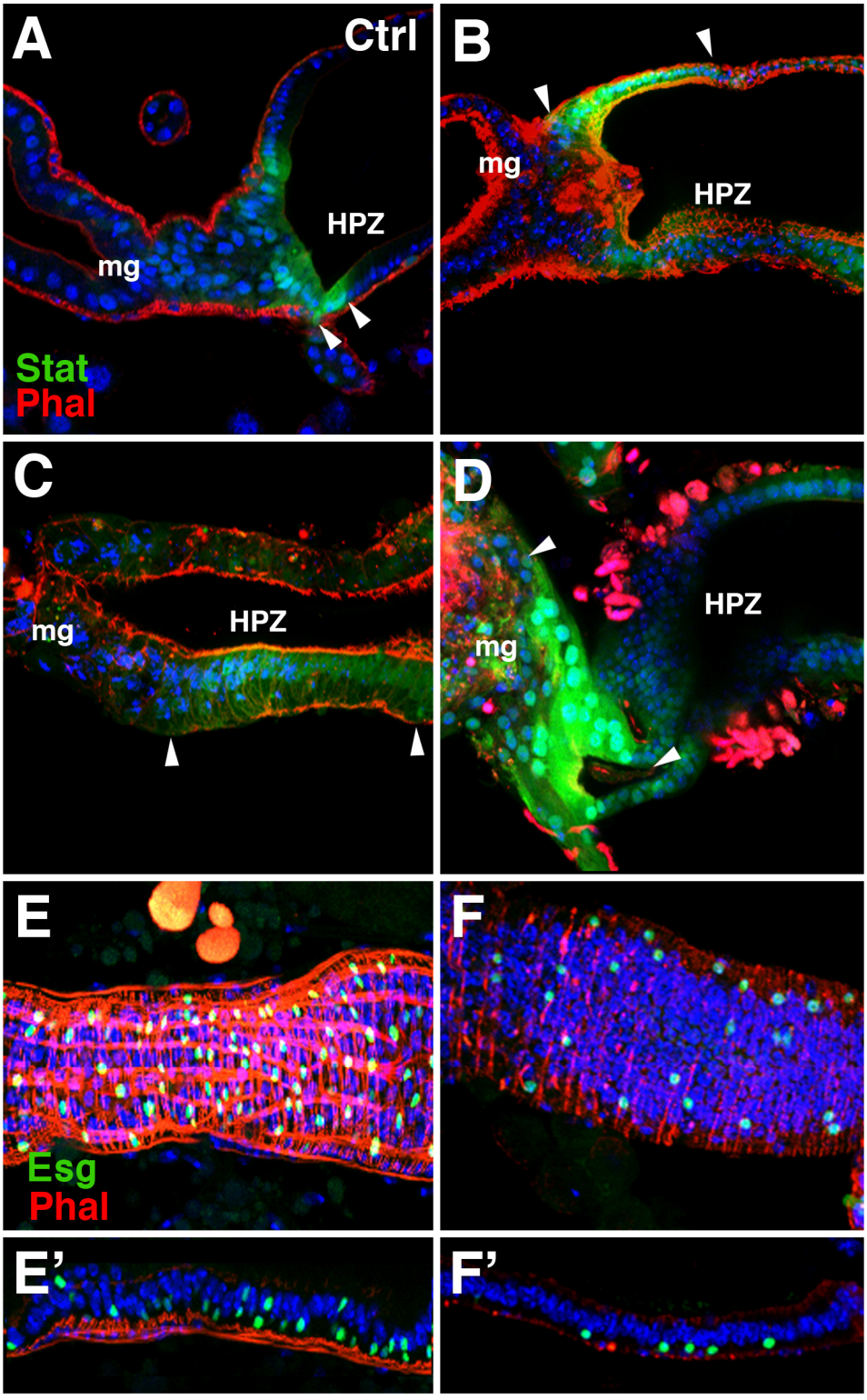
A
Ctrl
HPZ
mg
Stat
Phal
B
mg
HPZ
C
mg
HPZ
D
HPZ
mg
E
Esg
Phal
F
E'
F'

Fig. 9. Muscle ablation affects ISC populations. (A-F) Confocal Z-projections examining the effect of muscle ablation on the ISC progenitors of the Hindgut **(A-D)** and the Midgut **(E-F)**. Muscle ablation at early stages induces an elongated HPZ (arrowheads) and ectopic Stat expression **(A)** ctrl **(B-D)** KO. pISC numbers ate noticeably reduced in the absence of muscle **(E, E')** ctrl **(F, F')** KO. All nuclei are stained with Topro (blue). Abbreviations: HPZ, hindgut proliferative zone; mg, midgut.

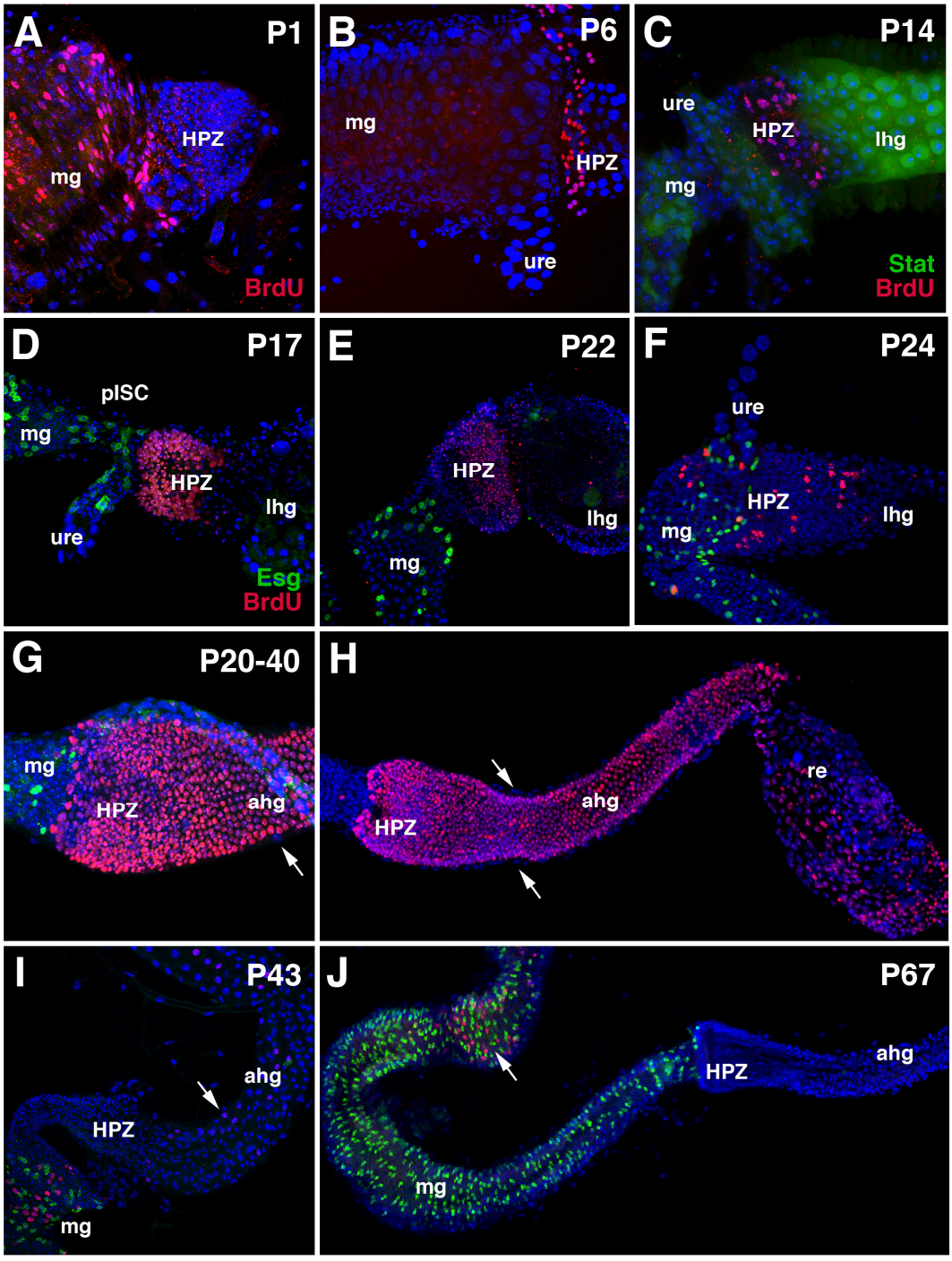
A
P1
HPZ
mg
BrdU
B
P6
mg
HPZ
ure
C
P14
ure
HPZ
lhg
mg
Stat
BrdU
D
P17
pISC
mg
HPZ
lhg
ure
Esg
BrdU
E
P22
HPZ
lhg
mg
F
P24
ure
HPZ
lhg
mg
G
P20-40
mg
HPZ
ahg
H
HPZ
ahg
re
I
P43
ahg
HPZ
mg
J
P67
HPZ
ahg
mg

Fig. S1. BrdU incorporation during hindgut extension. Confocal z-projections of BrdU incorpation in the hindgut at the given time points. **(A-C)** Early timepoint BrdU incorporation indicates a one or two rounds of cell division. While middle stages have large BrdU incorporation **(D, E)**. **(F)** Minimal BrdU incorporation at P24 and a long pulse from P20-P40 **(G, H)** suggests the mechanism for extension is convergent extension. BrdU incorporation at these times are likely due to endoreplication. Additionally no BrdU has been observed in the muscle nuclei (arrows). (I, J) After P40, the adult gut has already formed and very little proliferation occurs, though BrdU can be seen in the midgut **(J, arrow)**. . Abbreviations: ahg, adult hindgut; HPZ, Hindgut Proliferative Zone; lhg, larval hindgut; mg, midgut; pISC, presumptive intestinal stem cell; re, rectum; ure, ureter

References

Arango NA, Szotek PP, Manganaro TF, Oliva E, Donahoe PK, Teixeira J. (2005) Conditional deletion of beta-catenin in the mesenchyme of the developing mouse uterus results in a switch to adipogenesis in the myometrium. *Dev Biol*. 288(1):276-83

Beebe K, Lee WC, Micchelli CA. (2010) JAK/STAT signaling coordinates stem cell proliferation and multilineage differentiation in the Drosophila intestinal stem cell lineage. *Dev Biol*. 338(1):28-37

Bernick EP, Moffett SB, Moffett DF. (2007) Organization, ultrastructure, and development of midgut visceral muscle in larval *Aedes aegypti*. *Tissue Cell*. 39(4):277-92

Bourke LT, Knight RA, Latchman DS, Stephanou A, McCormick J. (2013) Signal transducer and activator of transcription-1 localizes to the mitochondria and modulates mitophagy. *JAKSTAT*. 2(4):e25666

Brand AH, Perrimon N. (1993) Targeted gene expression as a means of altering cell fates and generating dominant phenotypes. *Development*. 118(2):401-15.

Candelaria AG, Murray G, File SK, García-Arrarás JE. (2006) Contribution of mesenterial muscle dedifferentiation to intestine regeneration in the sea cucumber *Holothuria glaberrima*. *Cell Tissue Res*. 325(1):55-65

Denton D, Shravage B, Simin R, Mills K, Berry DL, Baehrecke EH, Kumar S. (2009) Autophagy, not apoptosis, is essential for midgut cell death in Drosophila. *Curr Biol*. 19(20):1741-6

Fox DT, Spradling AC. (2009) The Drosophila hindgut lacks constitutively active adult stem cells but proliferates in response to tissue damage. *Cell Stem Cell*. 5(3):290-7

García-Arrarás JE, Valentín-Tirado G, Flores JE, Rosa RJ, Rivera-Cruz A, San Miguel-Ruiz JE, Tossas K. (2011) Cell dedifferentiation and epithelial to mesenchymal transitions during intestinal regeneration in H. glaberrima. *BMC Dev Biol*. 11:61.

Grigorian M, Liu T, Banerjee U, Hartenstein V. (2013) The proteoglycan Trol controls the architecture of the extracellular matrix and balances proliferation and differentiation of blood progenitors in the Drosophila lymph gland. *Dev Biol*. 384(2):301-12

Jiang H, Edgar BA. (2009) EGFR signaling regulates the proliferation of Drosophila adult midgut progenitors. *Development*. 136(3):483-93

Klapper R. (2000) The longitudinal visceral musculature of Drosophila melanogaster persists through metamorphosis. *Mech Dev*. 95(1-2):47-54

Klapper R, Heuser S, Strasser T, Janning W. (2001) A new approach reveals syncytia within the visceral musculature of Drosophila melanogaster. *Development*. 128(13):2517-24.

Lee CY, Cooksey BA, Baehrecke EH. (2002) Steroid regulation of midgut cell death during Drosophila development. *Dev Biol.* 250(1):101-11

Lin G, Xu N, Xi R. (2008) Paracrine Wingless signalling controls self-renewal of Drosophila intestinal stem cells. *Nature*. 455(7216):1119-23.

Marianes A, Spradling AC. (2013) Physiological and stem cell compartmentalization within the Drosophila midgut. *Elife*. 2:e00886.

Mathur D, Bost A, Driver I, Ohlstein B. (2010) A transient niche regulates the specification of Drosophila intestinal stem cells. *Science*. 327(5962):210-3.

McLin VA, Henning SJ, Jamrich M. (2009) The role of the visceral mesoderm in the development of the gastrointestinal tract. *Gastroenterology*. 136(7):2074-91

Micchelli CA, Perrimon N. (2006) Evidence that stem cells reside in the adult Drosophila midgut epithelium. *Nature*. 439(7075):475-9

Mu X, Peng H, Pan H, Huard J, Li Y. (2011) Study of muscle cell dedifferentiation after skeletal muscle injury of mice with a Cre-Lox system. *PLoS One*. 6(2):e16699

Murray G, García-Arrarás JE. (2004) Myogenesis during holothurian intestinal regeneration. *Cell Tissue Res*. 318(3):515-24.

Ohlstein B, Spradling A. (2007) Multipotent Drosophila intestinal stem cells specify daughter cell fates by differential notch signaling. *Science*. 315(5814):988-92

Martin BS, Ruiz-Gómez M, Landgraf M, Bate M. (2001) A distinct set of founders and fusion-competent myoblasts make visceral muscles in the Drosophila embryo. *Development*. 128(17):3331-8

Quiñones JL, Rosa R, Ruiz DL, García-Arrarás JE. (2002) Extracellular matrix remodeling and metalloproteinase involvement during intestine regeneration in the sea cucumber Holothuria glaberrima. *Dev Biol*. 250(1):181-97.

Singh SR, Hou SX. (2009) Multipotent stem cells in the Malpighian tubules of adult Drosophila melanogaster. *J Exp Biol*. 212(Pt 3):413-23

Stephanou A, Latchman DS. (2003) STAT-1: a novel regulator of apoptosis. *Int J Exp Pathol*. 84(6):239-44

Takashima S, Paul M, Aghajanian P, Younossi-Hartenstein A, Hartenstein V. (2014) Changing lineage characteristics of developing Drosophila midgut stem cells depend on the control of prospero expression by the Wg and N signaling pathways. (unpublished)

Takashima S, Gold D, Hartenstein V. (2012) Stem cells and lineages of the intestine: a developmental and evolutionary perspective. *Dev Genes Evol*. 223(1-2):85-102

Takashima S, Mkrtchyan M, Younossi-Hartenstein A, Merriam JR, Hartenstein V. (2008) The behaviour of Drosophila adult hindgut stem cells is controlled by Wnt and Hh signalling. *Nature*. 454(7204):651-5.

Takashima S, Paul M, Aghajanian P, Younossi-Hartenstein A, Hartenstein V. (2013) Migration of Drosophila intestinal stem cells across organ boundaries. *Development*. 140(9):1903-11

Xu N, Wang SQ, Tan D, Gao Y, Lin G, Xi R. (2011) EGFR, Wingless and JAK/STAT signaling cooperatively maintain Drosophila intestinal stem cells. *Dev Biol*. 354(1):31-43

Zeng X, Chauhan C, Hou SX. (2013) Stem cells in the Drosophila digestive system. Adv *Exp Med Biol*. 786:63-78.

Chapter 5: Final Discussion

The metamorphosis of the stem cell populations

The *Drosophila* gut is such an attractive tissue to study because it is an easily manipulated model for stem cell/niche interactions. Indeed there are many studies highlighting tissue homeostasis in the hindgut (Fox et al., 2009; Takashima et al., 2008), midgut (Ohlstein et al., 2007; Micchelli et al., 2006) and the Malpighian tubules (Singh et al., 2009). Interestingly, though the origins of these stem cell populations differ, they are all under the control of at least one or most of these major signaling pathways (Wg, Notch/Delta, Stat, EGF, Hh) which are modulated by the visceral muscle in the larva and the adult. Our studies focus on how those stem cell populations manifest in the adult tissue through metamorphosis and how they are modulated through this process. First we will examine the development of the pISCs in the larval midgut, as well as the signaling molecules involved in their maintenance. This will be followed by a discussion of the pupal pISC development and pupal hindgut development. Finally we will explain the impact of the morphological changes of the visceral muscle and how it effects both of these metamorphosing tissues.

pISC Development and Maintenance in the Larva

We begin by explaining the midgut ISCs, which, in the adult, are under the control of Wg, Notch/Delta, Stat, and EGF. In the adult, Wg signaling promotes self-renewal and proliferation (Xu et al., 2011; Lin et al., 2009). Undifferentiated ISCs remain positive for Esg/Delta (Dl). Increased Notch (N) activity promotes the transition to post-mitotic enteroblasts (EBs), further high N expression leads to enterocyte cell differentiation (Ohlstein et al., 2007). N signaling acts downstream of Wg, both genes are epistatic to each other (Lin et al., 2009). In addition, we showed in chapter 3 that Wg plays an important role in the endocrine vs. enterocyte fate

decisions by regulating N expression starting from the late pupa through adulthood. Many of these signaling pathways are conserved in the vertebrate small intestine. The vertebrate Wg homologue, Wnt provides proliferation and self-renewal cues (Haegbarth et al., 2009) whereas Notch is involved in differentiation and mitotic arrest (van der Flier et al., 2008). In the larva, the ISCs begin as islands of 2 - 3 adult midgut progenitor (AMP) cells surrounded and maintained by a transient niche known as the peripheral cell. Larval AMPs are also under the control of Notch/Delta, in this case, overexpression of Notch leads to a peripheral cell phenotype (which will become the transient pupal midgut enterocytes), while a loss of function maintains an undifferentiated AMP phenotype (Mathur et al., 2010). In addition to the peripheral cells, the visceral muscles also play a role in larval AMP maintenance, as the circular muscle expresses EGF ligand Vein during larval development. Vein passively promotes proliferation, while overexpressing it does nothing to increase mitotic activity, EGFR loss of function leads to no proliferation.

Pupal pISC Development

In chapters 2 and 3, we examined the morphological changes inherent during midgut metamorphosis. The pISCs undergo three waves of parasynchronus division at ~P24, ~P48 and a final smaller wave at ~P72. We observed pISC motility, presumably to disperse the ISC population, though observations of the adult midgut suggest that populations of ISCs in the adult are specified to certain compartments. It would be a fair assumption that perhaps the pISCs are not yet specified to those compartments during metamorphosis (Marianes et al., 2013). Among these compartments are a copper rich region, an iron rich region, as well as other lipid rich compartments. In many cases, ISCs are segregated to their own compartments, however, in some

cases such as the LFC region and the iron rich region, ISCs are able to migrate freely past the boundaries between those specific regions. This is an indication that in such cases, the ISCs are not completely region specific.

Similar to the midgut ISCs that cross compartmental borders, in chapter 2 we revealed a population of pISCs in the posterior midgut which colonize the Malpighian tubules to form the adult stem cells of that region. This is a curious phenomenon as (1) the Malpighian tubules maintain their larval structures through adulthood (Singh et al., 2009) and (2) the Malpighian tubules are an ectodermally derived tissue (Lengyel et al., 2002; Lengyel et al., 1998) while the midgut has endodermal origins. This sort of transdifferentiation has only been observed at the midgut/hindgut boundary in *Drosophila*. This data suggests that specification of the pISCs must occur at some point during metamorphosis.

The Regulatory Signals of the Pupal pISCs

We observed few pISC differentiation events, however, a wave of differentiation does occur in the early pupa (enterocytes), ~P48 (endocrine) and at the onset of adulthood (enterocyte). PISCs do not have any Notch/Delta activity during much of midgut metamorphosis (P4-P60), however, they are still identifiable by their Esg signature. Much like the adult and larva, in the pupa, ectopic activation of N via its downstream effector suppressor of hairless (su(H)) leads to differentiation to the absorptive enterocyte phenotypes. Expression of N in Esg positive cells during early metamorphosis (P0-P4) may likely cause the formation of most of the adult enterocytes produced in the pupa as it plays this role in the adult and larval tissues. N does not become reactivated in Esg positive cells until P72, which preprograms a population pISCs as

enterocyte progenitors for eclosion. This may be due to regulation of N controlled by Wg which is expressed in the visceral muscle at various stages of metamorphosis.

Additionally, it is generally understood that low N activity is required for differentiation to endocrine fate in the adult (Ohlstein et al., 2007; Micchelli et al., 2006). Functionally, a lack of N activity during the pupal endocrine differentiation stage at P48 is a logical underpinning for this process to occur, as it is important for the activation of prospero itself, which is essential for endocrine fate determination. Prospero loss of function during metamorphosis prevents pISCs from differentiating and in fact leads to an increase in pISC number. We have determined, however, that cell division is not required for differentiation during metamorphosis. Increased pISC number in these scenarios may be a product of increased reception to Wg signal by cells that are no longer programmed to differentiate. This indicates that, the function of Notch, Prospero and Wingless in relation to midgut ISCs is conserved during multiple different stages of development including, now, metamorphosis. An interesting study would be to examine the effect of ectopic N before the migration of pISCs in the posterior midgut to the Malpighian tubules. This may shed light on possible mechanistic differences in posterior pISC programming. An increase of N signaling may prevent the formation of the renal stem cells by inducing an epithelial fate in the migrating pISCs.

Hindgut Morphology During Metamorphosis

Posterior to the midgut lies the hindgut. Few studies have fully examined the hindgut regenerative cell population. The general consensus is that the hindgut proliferative zone (HPZ) is fully active in the larval gut and is otherwise quiescent in the adult unless stimulated by tissue

damage (Fox et al., 2009; Takashima et al., 2008). This may be explained by indicating that these proliferating cells in the larva will become the extending pupal hindgut, which then becomes the adult hindgut. The HPZ contains three regions: the spindle cell zone (SCZ) which is Stat positive and mitotically active; the anterior region of the spindle cell zone (aSCZ) which contains a Wg positive set of cells that are very slow dividing; and the round cell zone (RCZ) which contains a rapidly proliferating population. These cells, when introduced to Hh signaling will differentiate into mature hindgut cells in the adult. Similar to the midgut and the vertebrate gut Wnt/Wg signal provides self renewal and proliferative cues and is present in both the larval and adult hindgut (Takashima et al., 2008). In addition, Hh signaling in vertebrate intestines has been suggested to play a role in villus differentiation, though its function has not been elucidated in fly intestinal tissues besides hindgut (Scoville et al., 2008).

In chapter 2 and chapter 4 we examined the transition of the hindgut from larval to adult in the pupa. We observed in chapter 2 in the early pupa, Wg controls which region of the HPZ migrates anteriorly to form part of the posterior midgut. By the time the cells have migrated (~P24), both Wg and Stat signal have reduced expression in the developing HPZ, however, they are still faintly expressed in the migrating plug. Before this migration occurs, there is a single round of cell division that occurs in the RCZ (or adult hindgut). After the larval cells begin their migration at ~P17 and at ~P22, the RCZ begins a large round of mitotic activity which continues until ~P30 when convergent extension of the adult hindgut begins. Peculiarly, there is no characteristic Stat or Wg signaling in the region where the HPZ would be located during these processes, though they have been associated with HPZ proliferation. This suggests that that must be another signal involved in HPZ proliferation. EGF may be a viable alternative pathway to

investigate for these proliferative events as it required for midgut ISC proliferation (Jiang et al., 2009; Xu et al., 2011).

Stat is, however, expressed in the dying larval hindgut and the leading edge of the extending adult gut. A possible function for its expression in the in the larval hindgut may be to induce apoptosis, this is an uncommon, but studied function of proteins such as Stat-1 in vertebrates and in some cases shown to mediate apoptosis through mitophagy (Stephanou et al., 2003; Bourke et al., 2013). Mitophagy is a case wherein mitochondria may overproduce reactive oxygen species and release prodeath proteins. Stat, however, is an antagonist of the JNK pathway, which was demonstrated to be activate in larval hindguts post p38b MAPK inactivation (Seisenbacher et al., 2011). The HPZ is reestablished at ~P72 with the return of normal Stat and Wg signals in the first 6-8 rows of cells in the anterior hindgut. After eclosion, the adult gut is maintained by this new adult HPZ (Takashima et al., 2008; Fox et al., 2009). While signaling molecules play a major role in the metamorphosis of the *Drosophila* gut, we have shown that the visceral muscle plays a major role as the source of that signal.

Visceral Muscle and its Regulatory Functions

The visceral muscle, along with Paneth cells, plays an important role in vertebrate ISC maintenance and development. Endothelial smooth muscle cells have had observed expression of Wnt, which as we described above has a large impact on the maintenance of ISCs in both the midgut and the hindgut (Gregorieff et al., 2005). Furthermore, myofibroblasts have been shown to express BMP (Kosinski et al., 2007) known to induce differentiation in the vertebrate ISCs, and have also been shown to prevent maintenance of ISCs when they are surgically removed

(Lahar et al., 2011). So too is the visceral muscle important for the ISCs in *Drosophila* (Jiang et al., 2012; Takashima et al., 2012). Our findings highlight the morphological changes undergone by the visceral muscle during metamorphosis and its effect on tissue development.

In the *Drosophila* larva and adult, the visceral muscle forms an orthogonal layer of circular and longitudinal syncytial muscle fibers that surround the midgut and a single layer of circular muscle fibers that surround the hindgut. Our studies in chapter 4 focused on the metamorphosis of the visceral muscle in depth. Previous studies by Klapper et al. have described the break down of longitudinal muscle fibers into 1-6 celled syncytia (Klapper, 2000; Klapper et al., 2001; Klapper et al., 2002). However, these studies did not provide a proper time course or mechanism for the syncytial breakdown. Furthermore, no investigation was done on the fate of circular muscle fibers during this period. In addition, often times in various vertebrate muscle tissues there is a population of muscle stem cells, known as satellite cells, that are present for tissue damage repair. They can be present in multiple smooth muscle tissues such as myometrial muscle or vascular smooth muscle (Szotek et al., 2007; Arango et al., 2005; Tang et al., 2012) or skeletal muscle (Lepper et al. 2011; Kadi et al. 2004). No such population of cells, however, has been observed in the *Drosophila* visceral muscle. Our studies in chapter 4 confirmed that during metamorphosis, the muscle nuclei themselves are retained during this breakdown period. Specifically, lineage tracing of muscle activated during the late larva and circular muscle clones could be observed in the pupa as well as the adult indicating cell survival. Moreover, BrdU incorporation confirmed no de novo formation of visceral muscle during metamorphosis.

We observed a dedifferentiation of the larval muscle fibers and a loss of the basement membrane beginning at ~P12 and reaching a climax between P24-P36. These results were coupled with myofibril depolymerization and the formation of mono-nucleated muscle cells or syncytia with weakened attachments. Previous studies in other organisms have described similar phenomena in dedifferentiating muscle. A similar process has been observed in *Aedes aegypti* during its metamorphosis. Though in that study, myofilamental breakdown was suggested to have occurred via proteosomal degradation (Bernick et al., 2007). In mice, dedifferentiating skeletal myotubes formed mononuclear myoblasts in response to injury (Mu et al., 2011). Even more striking are the studies in *Holothuria glaberrima* intestinal visceral muscle wherein damage induces depolymerization of myofilaments into spindle like structures. Subsequently, myofibers reform with a delayed myofilamental repolymerization much like that seen in our studies (Murray et al., 2004; García-Arrarás et al., 2011, Candelaria et al., 2006).

The dedifferentiation of muscle and subsequent redifferentiation coincides with widening and lengthening of the midgut epithelium respectively, indication that dedifferentiation may be required for this structural reorganization of the epithelium. Muscle dedifferentiation also occurs concurrently with one of the major waves of proliferation that we observed in pISCs in chapter 2, however, its exact role in this process is unclear. Subsequent redifferentiation of the muscle overlaps with pISC differentiation to endocrine fates and then enterocytes. Previously we mentioned that the muscle provides signals such as Wg and EGF for the purpose of maintaining pISCs (Jiang et al., 2009; Xu et al., 2011; Lin et al., 2009). Our studies also identified Wg signal in the boundary muscles directly adjacent to the HPZ that is maintained at least to the early adult. This signal is activated in the late pupa just as the muscle has reformed its connections and the

adult HPZ has reconstituted its Wg and Stat signal. A possible function of this Wg signal may be to induce quiescence in the adult HPZ during metamorphosis and during the adult lifecycle as the aSCZ in the larva is slowly dividing (Takashima et al., 2008), and in the adult is slowly dividing unless externally induced (Fox et al., 2009). It is, however, unknown whether or not this signal plays a funtional role in Stat or Wg expression in the HPZ. The muscle, though, does play a role in the maintenance of the metamorphosing gut in general.

Our muscle ablation experiments provided a unique opportunity to examine the functional relevance of muscle on the pupal development of the gut as well as its stem cell populations. Muscle ablation in the midgut led to wider, premature looking midguts when they should have lengthened. This could be due to the muscle's function as a scaffold for the intercalation of midgut enterocytes in the late pupa. Additionally, muscle ablation noticeably reduces the number of pISCs and endocrine cells present in the metamorphosing gut. This may be a function of a lack of Wg during later stages of metamorphosis, preventing later waves of proliferation. An abatement in the number of endocrine cells may also be a result of low pISC copy number. Alternatively, the muscle may have a direct role pertaining to endocrine differentiation via the loss of Wg signal which controls N expression preventing endocrine fate decision in favor of enterocyte differentiation. Muscle knockouts in the early pupa provided us with three interesting results regarding the hindgut: (1) larval hindgut apoptosis and detachment is mediated by the visceral muscle; (2) loss of the larval hindgut is necessary for the extension of the adult hindgut; (3) the muscle modulates Stat signaling in the HPZ as we observed a ubiquitous expression of Stat in a lengthened HPZ. Functionally, additional Stat may account for a longer HPZ as it is typically expressed in the posterior SCZ which is its proliferative region (Takashima et al., 2008)

while in the midgut it is required for ISC self-renewal (Beebe et al., 2010), though, the role of Stat in the hindgut has never been investigated. The ECM contains a variety of molecules that mediate interactions between the muscle the epithelium. Ablating the muscle also destroys the surrounding basement membrane. Among the proteins in the basement membrane, Trol has been implicated as a modulator of Hh signaling which is required in the hindgut to induce differentiation, which is not observed in muscle ablated hindguts (Park et al., 2003).

Concluding Remarks

Our studies have elucidated a dynamic niche that controls the early development of the adult intestinal epithelium. We have additionally shown that the progenitors of the adult midgut and hindgut undergo waves of division and differentiation that correspond to the presence and disappearance of mature muscle. Furthermore; N, Wg, and prospero signaling all play a role in pISC division and differentiation. ISCs of both the midgut and the hindgut have shown the propensity to migrate past tissue boundaries to form ISCs or epithelium of a new tissue type. Moreover, all of these processes may be under the control of the visceral muscle, which undergoes dedifferentiation and redifferentiation during crucial developmental stages in metamorphosis. These data taken together provide a descriptive stage by stage analysis of the metamorphosing gut, a phase often ignored for more stable environments of study.

References

Arango NA, Szotek PP, Manganaro TF, Oliva E, Donahoe PK, Teixeira J. (2005) Conditional deletion of beta-catenin in the mesenchyme of the developing mouse uterus results in a switch to adipogenesis in the myometrium. *Dev Biol*. 288(1):276-83

Beebe K, Lee WC, Micchelli CA. (2010) JAK/STAT signaling coordinates stem cell proliferation and multilineage differentiation in the Drosophila intestinal stem cell lineage. *Dev Biol*. 338(1):28-37

Bernick EP, Moffett SB, Moffett DF. (2007) Organization, ultrastructure, and development of midgut visceral muscle in larval *Aedes aegypti*. *Tissue Cell*. 39(4):277-92

Bourke LT, Knight RA, Latchman DS, Stephanou A, McCormick J. (2013) Signal transducer and activator of transcription-1 localizes to the mitochondria and modulates mitophagy. *JAKSTAT*. 2(4):e25666

Candelaria AG, Murray G, File SK, García-Arrarás JE. (2006) Contribution of mesenterial muscle dedifferentiation to intestine regeneration in the sea cucumber *Holothuria glaberrima*. *Cell Tissue Res*. 325(1):55-65

Fox DT, Spradling AC. (2009) The Drosophila hindgut lacks constitutively active adult stem cells but proliferates in response to tissue damage. *Cell Stem Cell*. 5(3):290-7

García-Arrarás JE, Valentín-Tirado G, Flores JE, Rosa RJ, Rivera-Cruz A, San Miguel-Ruiz JE, Tossas K. (2011) Cell dedifferentiation and epithelial to mesenchymal transitions during intestinal regeneration in H. glaberrima. *BMC Dev Biol*. 11:61.

Gregorieff A, Pinto D, Begthel H, Destrée O, Kielman M, Clevers H. (2005) Expression pattern of Wnt signaling components in the adult intestine. *Gastroenterology*. 129(2):626-38

Haegebarth A, Clevers H. (2009) Wnt signaling, lgr5, and stem cells in the intestine and skin. *Am J Pathol*. 174(3):715-21

Jiang H, Edgar BA. (2009) EGFR signaling regulates the proliferation of Drosophila adult midgut progenitors. *Development*. 136(3):483-93

Jiang H, Edgar BA. (2012) Intestinal stem cell function in Drosophila and mice. *Curr Opin Genet Dev*. 22(4):354-60

Kadi F, Schjerling P, Andersen LL, Charifi N, Madsen JL, Christensen LR, Andersen JL. (2004) The effects of heavy resistance training and detraining on satellite cells in human skeletal muscles. *J Physiol*. 558(Pt 3):1005-12

Klapper R. (2000) The longitudinal visceral musculature of Drosophila melanogaster persists through metamorphosis. *Mech Dev*. 95(1-2):47-54

Klapper R, Heuser S, Strasser T, Janning W. (2001) A new approach reveals syncytia within the visceral musculature of Drosophila melanogaster. *Development*. 128(13):2517-24.

Klapper R, Stute C, Schomaker O, Strasser T, Janning W, Renkawitz-Pohl R, Holz A. (2002) The formation of syncytia within the visceral musculature of the Drosophila midgut is dependent on duf, sns and mbc. *Mech Dev*. 110(1-2):85-96

Kosinski C, Li VS, Chan AS, Zhang J, Ho C, Tsui WY, Chan TL, Mifflin RC, Powell DW, Yuen ST, Leung SY, Chen X. (2007) Gene expression patterns of human colon tops and basal crypts and BMP antagonists as intestinal stem cell niche factors. *Proc Natl Acad Sci U S A*. 104(39):15418-23

Lahar N, Lei NY, Wang J, Jabaji Z, Tung SC, Joshi V, Lewis M, Stelzner M, Martín MG, Dunn JC. (2011) Intestinal subepithelial myofibroblasts support in vitro and in vivo growth of human small intestinal epithelium. *PLoS One*. 6(11):e26898.

Lengyel JA, Iwaki DD. (2002) It takes guts: the Drosophila hindgut as a model system for organogenesis. *Dev Biol*. 243(1):1-19

Lengyel JA, Liu XJ. (1998) Posterior gut development in Drosophila: a model system for identifying genes controlling epithelial morphogenesis. *Cell Res*. 8(4):273-84.

Lepper C, Partridge TA, Fan CM. (2011) An absolute requirement for Pax7-positive satellite cells in acute injury-induced skeletal muscle regeneration. *Development*. 138(17):3639-46

Lin G, Xu N, Xi R. (2008) Paracrine Wingless signalling controls self-renewal of Drosophila intestinal stem cells. *Nature*. 455(7216):1119-23.

Marianes A, Spradling AC. (2013) Physiological and stem cell compartmentalization within the Drosophila midgut. *Elife*. 2:e00886.

Mathur D, Bost A, Driver I, Ohlstein B. (2010) A transient niche regulates the specification of Drosophila intestinal stem cells. *Science*. 327(5962):210-3.

Micchelli CA, Perrimon N. (2006) Evidence that stem cells reside in the adult Drosophila midgut epithelium. *Nature*. 439(7075):475-9

Mu X, Peng H, Pan H, Huard J, Li Y. (2011) Study of muscle cell dedifferentiation after skeletal muscle injury of mice with a Cre-Lox system. *PLoS One*. 6(2):e16699

Murray G, García-Arrarás JE. (2004) Myogenesis during holothurian intestinal regeneration. *Cell Tissue Res*. 318(3):515-24.

Ohlstein B, Spradling A. (2007) Multipotent Drosophila intestinal stem cells specify daughter cell fates by differential notch signaling. *Science*. 315(5814):988-92

Park Y, Rangel C, Reynolds MM, Caldwell MC, Johns M, Nayak M, Welsh CJ, McDermott S, Datta S. (2003) Drosophila perlecan modulates FGF and hedgehog signals to activate neural stem cell division. *Dev Biol*. 253(2):247-57

Scoville, D. H., Sato, T., He, X. C. and Li, L. (2008). Current view: intestinal stem cells and signaling. Gastroenterology 134, 849-864.

Singh SR, Hou SX. (2009) Multipotent stem cells in the Malpighian tubules of adult Drosophila melanogaster. *J Exp Biol*. 212(Pt 3):413-23

Seisenbacher G, Hafen E, Stocker H. (2011) MK2-dependent p38b signalling protects Drosophila hindgut enterocytes against JNK-induced apoptosis under chronic stress. *PLoS Genet*. 7(8):e1002168

Stephanou A, Latchman DS. (2003) STAT-1: a novel regulator of apoptosis. *Int J Exp Pathol*. 84(6):239-44

Szotek PP, Chang HL, Zhang L, Preffer F, Dombkowski D, Donahoe PK, Teixeira J. (2007) Adult mouse myometrial label-retaining cells divide in response to gonadotropin stimulation. *Stem Cells*. 25(5):1317-25

Takashima S, Gold D, Hartenstein V. (2012) Stem cells and lineages of the intestine: a developmental and evolutionary perspective. *Dev Genes Evol*. 223(1-2):85-102

Takashima S, Mkrtchyan M, Younossi-Hartenstein A, Merriam JR, Hartenstein V. (2008) The behaviour of Drosophila adult hindgut stem cells is controlled by Wnt and Hh signalling. *Nature*. 454(7204):651-5.

Tang Z, Wang A, Yuan F, Yan Z, Liu B, Chu JS, Helms JA, Li S. (2012) Differentiation of multipotent vascular stem cells contributes to vascular diseases. *Nat Commun*. 3:875

van der Flier LG, Clevers H. (2009) Stem cells, self-renewal, and differentiation in the intestinal epithelium. *Annu Rev Physiol.* 71:241-60

Xu N, Wang SQ, Tan D, Gao Y, Lin G, Xi R. (2011) EGFR, Wingless and JAK/STAT signaling cooperatively maintain Drosophila intestinal stem cells. *Dev Biol*. 354(1):31-43